2009

Photoprotective strategies in overwintering rhododendrons

Xiang Wang
Iowa State University

Photoprotective strategies in overwintering rhododendrons

by

Xiang Wang

A dissertation submitted to the graduate faculty

in partial fulfillment of the requirements for the degree of

DOCTOR OF PHILOSOPHY

Major: Horticulture

Program of Study Committee:
Rajeev Arora, Major Professor
William R. Graves
Harry T. Horner
Allen D. Knapp
Stephen L. Krebs

Iowa State University

Ames, Iowa

2009

TABLE OF CONTENTS

ACKNOWLEDGEMENTS

I would like to thank my major professor, Dr. Rajeev Arora, for his guidance, encouragement, and financial support over the course of my study and work toward this degree. His long-term understanding and patience has been absolutely invaluable to me especially during the writing of the manuscripts and dissertation. His insights and words of encouragement have often inspired me and renewed my hopes for completing this degree. I have also benefited a lot from his expertise regarding designing and conducting experiments, analyzing the data, and thinking critically as a scientist. All this training in his lab has prepared me as a mature researcher for my future career.

I also want to thank my committee members: Drs. William R. Graves, Harry T. Horner, Allen D. Knapp, and Stephen L. Krebs. I thank Dr. Graves for his great suggestions and instructions on my manuscript writing. I thank Dr. Horner for his enormous contribution to the JASHS paper and my microscopy skills which I really enjoyed from the courses he taught. I thank Dr. Knapp for his generosity and technical assistance for using the fluorometer during the course of this study. I thank Dr. Krebs for his critical comments on the manuscripts and the long journey from Ohio to Ames each time I called for a committee meeting and for providing rhododendron plants for this study. I feel encouraged and helped every time when I think of the support from all of my committee members.

I would thank my former and present lab members of Plant Cold Hardiness Lab: Dr. Yanhui Peng, Wei Hao, Keting Chen, and fellow graduate students Chunzhen Zhang and Suqin Cai for their assistance in experiments and daily life for which I am very grateful. I

also owe very special thanks to Dr. Jeremy W. Singer (USDA-ARS National Soil Tilth Laboratory, Ames, IA) and Dr. Anania Fessehaie (Seed Science Center, ISU) for their selfless help with the equipment (LI-COR and Real time PCR, respectively).

I am forever indebted to my family for all of their help, support, and encouragement throughout my life. I would like to give my special thanks to my wife, Yanqin He, for her endless love, support, and encouragement through difficult times. Finally, I would like to thank my parents (Daian Wang and Aiping Xin), brothers (Fei Wang and Wei Wang) and sister (Na Wang) for being my strong support.

CHAPTER 1: GENERAL INTRODUCTION

Literature review

Rhododendron and cold acclimation

Rhododendron L. (from the Greek *rhodos*, "rose"; *dendron*, "tree") is a genus of flowering plants in the *Ericaceae* family, comprising over 1000 species with a wide distribution around the world (Chamberlain et al., 1996). The major origin center, with more than 300 species, occurs in the Sino-Himalayan Mountains from central Nepal and Sikkim east to Yunnan and Sichuan in Southwest China (Leach, 1961). Almost the same number of species is found in Southeast Asia from Thailand and Vietnam to Malaysia, Indonesia and New Guinea. Japan has more than 50, North America almost 30, and Europe seven native species (Chamberlain et al., 1996). The large, broad-leaved evergreen rhododendrons are important woody landscape plants, stretching from marginally freeze-tolerant species of Southeast Asia to 'super-hardy' ones inhabiting North America and circumpolar regions of Scandinavia (Sakai et al., 1986).

The genus *Rhododendron* can be divided into eight subgenera, and further to sections and subsections (Chamberlain et al., 1996). The large, broad-leaved evergreen shrubs or trees with large flowers comprise subgenus *Hymenanthes*, also termed the elepidotes. Lepidotes, subgenus *Rhododendron*, are usually lower bushes with smaller flowers and leaves, which are often aromatic, and scaly hair covers their above-ground parts. The plants belonging to the subgenera *Pentanthera* (deciduous), *Tsutsutsi* and *Azaleastrum* (evergreen) are called azaleas. In addition, there are four species that form three additional subgenera, *Candidastrum*, *Mumeazalea*, and *Therorhodion*. The two species (*R. catawbiense* and *R.*

ponticum) which were used in this dissertation belong to the subgenus *Hymenanthes*. In general, *Rhododendron* species exhibit an enormous diversity of size and shape in whole plants, leaves, and flowers. Their sizes range from tiny, mat-like plants to trees up to 30 m tall. Leaf size ranges from less than 6 mm to over 0.9 m long, and also appears in a variety of shapes: rounded, lance-shaped, and elliptical. The flowers may be white, red, pink, yellow, approximate blue, purple, magenta, orange, and in various shades and mixtures of most of these colors.

As one of the major environmental factors in nature, air temperature changes from season to season, and undergoes daily fluctuations. Many plants must be able to sense transient fluctuations as well as seasonal changes in temperature, and to respond to these changes by actively adjusting their biology to fit the subsequent temperature regime (Xin and Browse, 2000). Temperate-zone woody perennials typically experience substantial drops in average monthly minimum air temperatures ranging from ~ 20–30°C in the summer to several degrees below 0°C in the winter. They survive the harsh winter through cold acclimation (CA), a process which greatly increases plant freezing tolerance in response to shortening photoperiod, low non–freezing, and then subfreezing temperatures sequentially through early fall and winter (Weiser, 1970; Sakai and Larcher, 1987). Numerous changes are involved in CA such as gene expression, metabolism, and morphology. These changes include the increased expression of many genes, the reduction or cessation of growth, changes in membrane lipid composition, the accumulation of compatible osmolytes (proline, betaine, and soluble sugars), and increased levels of antioxidants (Guy, 1990; Thomashow, 1999; Xin and Browse, 2000; Öquist and Huner, 2003).

Within the genus *Rhododendron* the ability to withstand very cold temperatures

varies widely, and species from colder regions are hardier than those from warm regions (Kaku et al., 1980; Sakai et al., 1986; Kaku, 1993). The species from the Himalayas are only hardy to around –25°C (Sakai, 1982). Many species in the elepidote subsection *Pontica* are very hardy such as *R. catawbiense* and *R. maximum* (Sakai et al., 1986). Freezing tolerance of fully cold-acclimated leaves from *R. catawbiense* can be as low as –53°C (Wei et al., 2005). Soon after its introduction in North Carolina in 1809, *R. catawbiense* became the principal source of cold hardiness in *Rhododendron* breeding (Leach, 1961).

Challenges for winter survival of overwintering evergreens

Sunlight is not only the driving force for photosynthesis, but also presents a potential threat to photosynthetic apparatuses. When plants receive more light than they can utilize, the balance between the absorption and utilization of light energy is critical and necessary to minimize the potential for photo-oxidative damage. There are four possible fates of sunlight absorbed in the light-harvesting chlorophyll complexes (Demmig–Adams and Adams, 2000; Adams et al., 2004). When chlorophyll (Chl) absorbs light, it is excited from its ground state to its singlet excited state (^{1}Chl*). From there it has several ways to relax back to the ground state. First, it can relax by emitting light, seen as fluorescence. Second, the excitation energy is typically passed on from one Chl molecule to another, eventually reaching a photochemical reaction center where the energy is used to generate high-energy electrons for photosynthetic electron transport. Third, it can de-excite by dissipating as heat. Last, when ^{1}Chl* is not used for photochemistry, Chl may enter a triplet excited state (^{3}Chl*) that can pass the excitation energy on to oxygen, resulting in the formation of singlet excited oxygen ($^1O_2$*).

Cold temperature and high light are the two major environmental factors that challenge the overwintering evergreens under winter conditions. While cold temperatures have little direct effect on light collection in photosynthesis, they inhibit/decrease the enzymatic reactions of photosynthesis, which can potentially result in photon flux in excess of that required for photosynthetic evolution of O_2 (PSII reaction centers) or assimilation of CO_2 (Hopkins and Huner, 2003). This excess energy, if not dissipated as heat or fluorescence, may cause inhibition of PSII reaction centers (photoinhibition) (Öquist and Huner, 2003). Photoinhibition in evergreen leaves can be brought about through oxidative damage to PSII by reactive oxygen species (ROS) (Adams et al., 2004).

ROS are partially reduced forms of atmospheric oxygen. They typically result from the excitation of O_2 to form singlet oxygen ($^1O_2$) or from the transfer of one, two or three electrons to O_2 to form, respectively, a superoxide radical (O_2^-), hydrogen peroxide (H_2O_2) or a hydroxyl radical (HO^-). ROS are very toxic molecules that can cause oxidative damage to proteins, DNA, and lipids (Foyer et al., 1994; Rossini et al., 2006). Although they are rooted in one place, plants do not allow these ROS to accumulate to levels that could result in significant damage in the leaves until their life cycle is completed or until the extreme condition no longer allows the maintenance of green tissues (Adams et al., 2004).

As understory evergreens in deciduous forests or grown in the open, rhododendron leaves are commonly exposed to a combination of freezing temperatures and high irradiance in their natural habitats in winter. Previous work in our lab indicated that down-regulation of photosynthetic metabolism in overwintering leaves of *R. catawbiense* (Wei et al., 2005) could potentially render these plants vulnerable to photoinhibition.

Photoprotection mechanisms of overwintering evergreens

As described above, the potential for photodamage occurs when Chl absorbs a photon of light but is unable to pass this energy to photochemistry. Fortunately, higher plants have evolved several photoprotective mechanisms to avoid/reduce the damage, including morphological and anatomical adaptations (Mittler, 2002; Mullineaux and Karpinski, 2002), harmless dissipation of excess energy via xanthophyll cycle (Demmig–Adams and Adams, 1993; Verhoeven et al., 2005; Demmig–Adams and Adams, 2006), up-regulation of early light-induced proteins (ELIPs) (Hutin et al., 2003), and activation of antioxidant system (Niyogi, 1999).

Leaf morphological and anatomical adaptations to light stress

The quantity of light in natural environments can vary over several orders of magnitude and on a time scale that ranges from seconds to seasons. High light stress is very common to plants specially grown open in the field. A good way to avoid light stress is to avoid absorbing excess light in the first place. There are several means by which plants can reduce the level of radiation that reaches the leaf (Adams et al., 2004). One is the change of the leaf orientation relative to the direction of incident light (Björkman and Demmig-Adams, 1994). As temperatures fall below freezing, some members in the genus *Rhododendron* employ this strategy, with leaves moving from a relatively horizontal to a vertical position (thermonasty) (Nilsen, 1992). Another approach is to align the chloroplasts along the walls of the cells that are parallel with the incident radiation under low light, whereas the chloroplasts line up along the edges of the cell under high light. In addition, light can also be intercepted or reflected by deposits of waxes, salts, or pigments on or within the leaf hairs or the

epidermis surrounding the leaf mesophyll tissues (Adams et al., 2004).

Plants exhibit acclimated changes in response to light stress and many of these responses were described in the classic experiments - comparing 'sun' and 'shade' leaves (Björkman, 1981). Typically, 'sun' leaves are smaller, thicker, and heavier per unit area than 'shade' leaves, and have higher densities of leaf stomata. Increased leaf thickness, especially when brought about by the elongation or addition of palisade cells, has been linked to a reduction in mesophyll resistance to carbon dioxide (Nobel, 1977) and correlated with increases in factors potentially limiting photosynthesis. This sun/shade dichotomy has been evaluated for a large number of temperate species and related to shade tolerance and physiological performance. Research in beech found that 'sun' leaves possessed smaller leaf areas and higher stomata densities, and were thicker than the 'shade' leaves (Lichtenthaler et al., 1981). The chloroplast ultrastructure of 'shade' leaves was not only characterized by a much higher number of thylakoids per granum and a higher stacking degree of thylakoids, but also by broader grana than in sun leaves.

Dissipation of excess energy via xanthophyll cycle

All plants employ a form of photoprotection that safely dissipates excess energy as heat in a process involving carotenoid pigments in the xanthophyll cycle (Demmig-Adams et al., 1996) (**Figure 1**). Under excess light such as the midday in the field of open areas, the light-driven build-up of the trans-thylakoid pH gradient far exceeds the utilization of the gradient for ATP synthesis, and intra-thylakoid pH becomes more acidic. This pH change activates an enzyme, violaxanthin de-epoxidase (VDE; EC: 1.10.99.3), which rapidly converts violaxanthin (V) to antheraxanthin (A) and zeaxanthin (Z) (Yamamoto, 1979).

These latter two de-epoxidized components (A and Z) can accept excitation energy from chlorophyll and thereby facilitate energy dissipation (Demmig-Adams et al., 1996; Holt et al., 2005) by quenching the ^{1}Chl* directly (Müller et al., 2001). It also has been suggested that Z has the function of decreasing light-harvesting Chl antenna size and stability, and the excess light energy is therefore diminished (Havaux, 1998). In addition, Z may protect the thylakoid membrane against photooxidation by directly quenching $^1O_2$* and other ROS (Havaux and Niyogi, 1999). When light is not in excess such as early or late in the day, the xanthophyll cycle pigments are mainly present as V which is not capable of dissipating energy as heat (Adams and Demmig-Adams, 1992). Under this condition Z is epoxidized back to V by the catalyzation of an enzyme, zeaxanthin epoxidase (ZE; EC: 1.14.13.90).

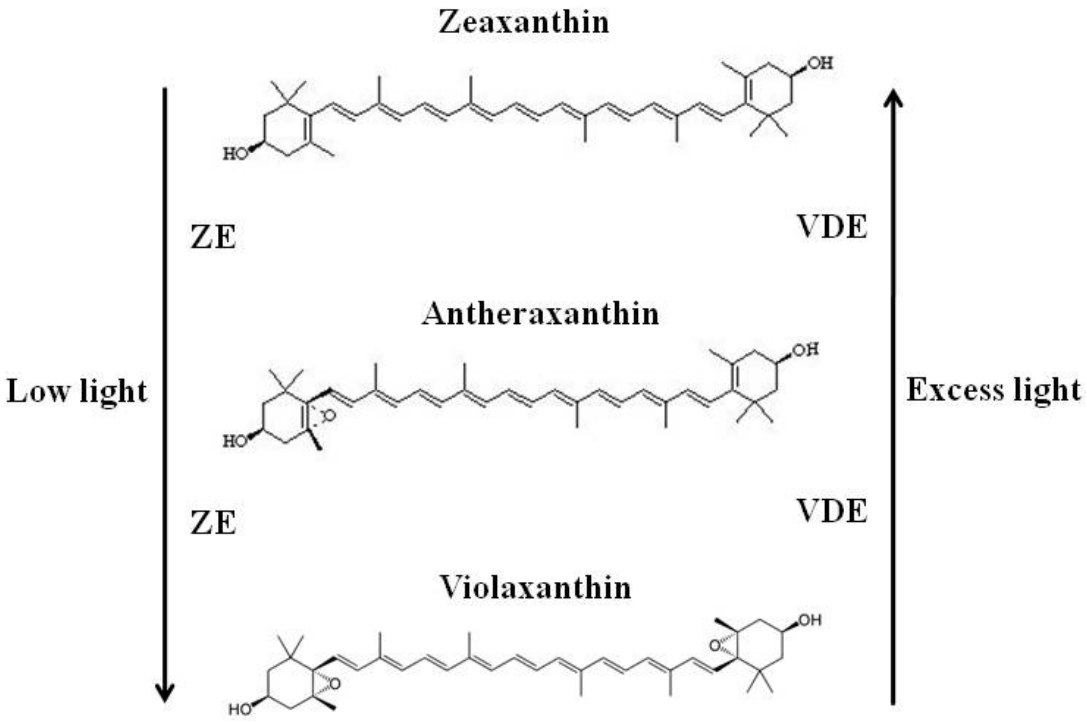

Figure 1. Xanthophyll cycle in plants

In higher plants, VDE is a 43-kDa nucleus-encoded protein that is localized in the thylakoid lumen (Bugos and Yamamoto, 1996). The purified VDE enzyme is activated by low pH (Eskling et al., 1997), and the cloning of the VDE gene revealed that the enzyme has a glutamate-rich region that may be protonated at low pH (Bugos and Yamamoto, 1996). Upon acidification of the lumen, VDE associates with the thylakoid membrane (Hager and Holocher, 1994), where it can interact with its substrate V. ZE is an O_2-dependent mono-oxygenase that uses reduced ferredoxin to first epoxidize Z and then A (Bouvier et al., 1996). Because of its optimum pH between 7 and 7.5 and the closeness to the pH of the stroma, ZE is thought to be located on the stromal side of the thylakoid membrane (Eskling et al., 1997; Siefermann and Yamamoto, 1975). Usually, it is thought that ZE catalyzes the epoxidation reaction under low light or darkness; however, some reports indicate that epoxidation can also be observed even under high light (Siefermann and Yamamoto, 1975; Frommolt et al., 2001). In addition, ZE and VDE are the first known plant members of the lipocalin family, a diverse group of proteins that bind small lipophilic molecules and share a conserved tertiary structure of eight β–strands in the barrel configuration (Bugos et al., 1998).

Early light-induced proteins (ELIPs) and photoprotection

In green plants, solar energy is collected by chlorophyll- and carotenoid-binding light-harvesting complexes (LHCs), which are encoded by a multigene family of *LHC* genes. The expression of these genes is tightly regulated by light (Hutin et al., 2003). High light intensities inhibit transcription of *LHC* genes and activate the synthesis of the early light-induced proteins (ELIPs), a class of proteins structurally related to the LHCs. As one of the first nuclear-encoded light-inducible proteins detectable within the thylakoid membrane

system, ELIPs contain three transmembrane helices and were first discovered to be transiently expressed during the greening of etiolated plants (Meyer and Kloppstech, 1984; Grimm et al., 1989; Heddad and Adamska, 2000).

It is proposed that ELIPs may transiently bind the released chlorophylls under high light stress and prevent the formation of free radicals and/or function in energy dissipation (Montané and Kloppstech 2000; Adamska 2001; Tzvetkova-Chevolleau et al., 2007). ELIPs accumulation, therefore, may constitute an adaptive response to winter conditions (cold and high light) in evergreens and play a key role in the protection of photosynthetic apparatuses from excess light. In support of their photoprotective role, an *Arabidopsis* mutant defective in targeting ELIPs to thylakoids was found to be sensitive to photo-oxidation while over-expression of *ELIPs* enhanced its light-tolerance (Hutin et al., 2003). A previous study in our lab showed that cDNAs encoding *ELIP* homologs were the most abundant class in an EST library generated from winter-collected leaf tissues of *R. catawbiense* (Wei et al., 2005). Recent studies, reporting ELIP proteins in several overwintering evergreens – subalpine firs and lodgepole pines (Zarter et al., 2006a) and bearberry (Zarter et al., 2006b), showed no accumulation of ELIPs in the summer-collected leaves but the distinct abundance occurred in the winter-collected samples. Collectively, these studies suggest that one possible mechanism by which overwintering evergreens might prevent photooxidative damage during winter is via accumulating ELIPs.

Antioxidant system and photoprotection

The generation of ROS is an inevitable consequence of oxygenic photosynthesis and respiration. Fortunately, higher plants have evolved multiple defense mechanisms to

minimize oxidative damage by chemical or enzymatic scavenging of ROS including antioxidant metabolites and enzymes. These metabolites include small molecules such as carotenoids, tocopherols, ascorbate and glutathione. As integral structural components of photosystems and light-harvesting complexes, carotenoids function as accessory light-harvesting and photoprotective pigments (Demmig-Adams et al., 1996). Tocopherols are major lipid-soluble antioxidants and are involved in scavenging $^1O_2$ and terminating lipid peroxidation chain reactions in thylakoid membranes (Fryer, 1992). As the main antioxidants in the chloroplast stroma, ascorbate and glutathione can scavenge ROS and provide reducing power for regenerating oxidized tocopherols and for ascorbate peroxidase (APX) and glutathione peroxidase (Noctor and Foyer, 1998).

Ascorbate is found in most plant tissues and cell compartments, with chloroplasts accumulating 25 to 30% of the total (Foyer, 1983; Horemans et al., 2000). There are about 30 to 40%, 20 to 30%, and 5 to 10% of the total ascorbate in the cytosol, vacuole, and apoplast, respectively (Horemans et al., 2000). Ascorbate is able to reduce O_2^- to H_2O_2 and also reacts with $^1O_2$ at a relatively fast rate. H_2O_2 is quenched by APX using ascorbate as a hydrogen donor. In addition, ascorbate is an essential co-substrate of the de-epoxidation of violaxanthin since it delivers hydrogen for this conversion. A previous report shows that the VDE activity is regulated by the luminal ascorbate concentration (Bratt et al., 1995).

Glutathione is found in most prokaryotes and eukaryotes. Reduced glutathione (GSH), a tripeptide thiol (γ-glutamine-cysteine-glycine), is the main form (accounting for about 90-99% of the total pool) under most conditions (Foyer et al., 1997). In the oxidized form two glutathione molecules are connected by a disulfide bond forming glutathione disulfide (GSSG). Glutathione is also a major water-soluble antioxidant in plants with

concentrations of about 5 mM in the chloroplast stroma (Noctor et al., 1998). It has several important roles: a) it directly reduces most ROS, but reacts rather slowly with H_2O_2; b) it is an important storage and transport form of reduced sulfur; c) it is important in heavy metal and xenobiotic detoxification.

Major ROS-scavenging enzymes in plants include superoxide dismutase (SOD), APX, and catalase (CAT). SOD is found in almost all cellular compartments, and acts as the first line of defense by dismutating O_2^- to H_2O_2. Then APX and CAT detoxify H_2O_2 (Mittler, 2002). The balance between SOD and APX or CAT activities in cells is crucial for determining the steady-state level of O_2^- and H_2O_2 (Bowler et al., 1991). This balance is thought to be important to prevent the formation of the highly toxic HO^- (Mittler, 2002). The different affinities of APX (μM range) and CAT (mM range) for H_2O_2 suggest that they belong to two different classes of H_2O_2-scavenging enzymes: APX might be responsible for the fine modulation of ROS for signaling, whereas CAT might be responsible for the removal of excess ROS. Since CAT does not require a supply of reducing equivalents for its function, it might be insensitive to the redox status of cells, and its function might not be affected during stress, unlike the other enzymes.

Thermonasty and aquaporins in *Rhododendron*

Thermonastic leaf movements are low temperature induced changes in leaf curling and orientation that occur in temperate forest species (Harshburger, 1899; Fukuda, 1933; Havis, 1964; Nilsen, 1992; Russell et al., 2009). The Ericaceae is the most dominant family of broad leaf, evergreen plants in temperate habitats, many species of which move their leaves to a more pendant position during the winter (Russell et al., 2009). Leaves of many

evergreen *Rhododendron* species exhibit thermonastic leaf movements (both leaf curling and drooping) under winter conditions when leaf temperature decreases below a critical low value (Nilsen, 1987). The physiological basis of the adaptive significance of thermonastic leaf movements to plants under cold winter conditions may be related to the combination of high light and low temperature that is characteristic of understory environments in temperate deciduous forests. It is likely that thermonastic leave movements help protect long lived evergreen leaves from photon-induced damage by reducing leaf exposure to light during freezing conditions in the winter. Therefore, thermonastic leaf movements may be a mechanism allowing the optimization of the effectiveness of the xanthophylls cycle and antioxidants in preventing photooxidative stress (Bao and Nilsen, 1988; Nilsen, 1992; Russell et al., 2009).

Water movement across the leaf cell membranes is important for water homeostasis in maintaining turgor and cell volume, and thus in controlling leaf movement. Although the physiological cause of leaf curling is not yet well understood, it is believed that leaf curling caused by subfreezing temperatures is a result of changes or redistribution of tissue water (Haupt and Feileib, 1979; Nilsen, 1992), which in turn could cause certain cells to selectively lose turgor leading to the leaf curling.

This redistribution of water is likely regulated by water channels, named aquaporins (AQPs) (Peng et al., 2008; Heinen et al., 2009). AQPs, which facilitate transport of water molecules across cell membranes, belong to the major intrinsic protein (MIP), and regulate hydraulic conductivity in response to changing environmental conditions (Agre et al., 1998; Kaldenhoff and Fischer, 2006). Evidence is accumulating that AQPs play an important role in plant hydraulic relations at the cell, tissue, organ, and whole plant level. They facilitate the

rapid, passive exchange of water across cell membranes and are responsible for up to 95% of the water permeability of plasma membranes (Henzler and Steudle, 2004; Heinen et al., 2009). Plant aquaporins can be sub-divided into four major groups, indicating different possible sub-cellular or plant organ localization: plasma membrane intrinsic proteins (PIPs); tonoplast intrinsic proteins (TIPs); NOD26-like intrinsic proteins (NIPs; where NOD26 is an aquaporin discovered in the peribacteroid membrane of nodulated soy bean roots); and small basic intrinsic proteins (SIPs) (Kaldenhoff and Fischer, 2006). As the largest number of AQP members in higher plants, plasma membrane intrinsic proteins (PIPs) can be divided into two phylogenetic groups, named PIP1 and PIP2. Previous reports showed that aquaporins of the PIP2 subfamily exhibited more efficient water channel activity than members of the PIP1 clusters (Daniels et al., 1994; Johansson et al., 1998; Kaldenhoff and Fischer, 2006).

Research objectives

The overall aim of the studies conducted in this dissertation was to investigate photoprotective strategies in overwintering rhododendrons. Two *Rhododendron* species (*R. catawbiense* Michx. and *R. ponticum* L.) were used across the studies which are divergent in their leaf freezing tolerance (superhardy *versus* less hardy, respectively) and in their thermonastic behavior (former shows thermonastic leaf movements, whereas the latter does not). More specific objectives of this research are as follows:

- Compare the leaf structural differences of the two *Rhododendron* species; to gain insight into how the specific leaf morphological and anatomical features (together with thermonasty or lack thereof) of the two species might be associated with

their ability to tolerate/avoid high irradiance and/or withstand dehydrative stresses during winter. (chapter 2)

- Compare and contrast photosynthesis, photoinhibition, and photoprotection response in the two species during seasonal cold acclimation; to gain insight into how photosynthetic behavior and specific photoprotective strategies (including photosynthesis adjustment, expression of *ELIPs* and accumulation / activity of antioxidant compounds / enzymes) might explain the mechanisms employed by these two species to tolerate / avoid high irradiance under low temperatures during winter. (chapter 3)
- To study whether *RcPIP2s* expression is associated with thermonasty in *Rododendron*. (chapter 4)

Organization of the remaining chapters

The rest of this dissertation is divided into four sections. Chapters two and three are complete articles already published in peer-reviewed journals. Chapter four is a manuscript submitted to the journal of *Plant Science* as a "short communication". Chapter five contains the overall conclusions from the three articles mentioned above.

References

Adams, W.W.III and B. Demmig-Adams. 1992. Operation of the xanthophyll cycle in higher plants in response to diurnal changes in incident sunlight. Planta 186: 390–398.

Adams, W.W.III., C.R. Zarter, V. Ebbert, and B. Demmig-Adams. 2004. Photoprotective strategies of overwintering evergreens. BioScience 54: 41–49.

Adamska, I. 2001. The Elip family of stress proteins in the thylakoid membranes of pro- and eukaryota. *In:* Aro, E.M., B. Andersson (eds), Advances in photosynthesis and respiration-regulation of photosynthesis. Kluwer Academic Publishers, Dordrecht, The Netherlands, pp 487–505.

Agre, P., M. Bonhivers, and M.J. Borgnia. 1998. The aquaporins, blueprints for cellular plumbing systems. J. Biol. Chem. 273: 14659–14662.

Asada, K. 1999. The water-water cycle in chloroplasts: scavenging of active oxygen and dissipation of excess photons. Annu. Rev. Plant Physiol. Plant Mol. Biol. 50: 601–639.

Bao, Y. and E.T. Nilsen. 1988. The ecophysiological significance of leaf movements in *Rhododendron maximum* L. Ecology 69: 1578–1587.

Björkman, O.B. 1981. Responses to different quantum flux densities. *In:* 0.L. Lange, P.S. Nobel, C.B. Osmond, H. Ziegler (eds), Encyclopedia of plant physiology new series, vol. 12 A, 57-107. Springer-Verlag, Berlin.

Björkman, O. and B. Demmig-Adams. 1994. Regulation of photosynthetic light energy capture, conversion and dissipation in leaves of higher plants. *In* E.D. Schulze, M.M. Caldwell (eds), Ecophysiology of Photosynthesis. Ecological Studies 100, Springer Verlag, Berlin, pp 1747.

Bouvier, F., A. d'Harlingues, P. Hugueney, E. Marin, A. Marion-Poll, and B. Camara. 1996. Xanthophyll biosynthesis: Cloning, expression, functional reconstitution, and regulation of b-cycloxenyl carotenoid expoxidase from pepper. J. Biol. Chem. 271: 28861–28867.

Bowler, C., L. Slooten, S. Vandenbranden, R. De Rycke, J. Botterman, C. Sybesma, M. Van Montagu, and D. Inze. 1991. Manganese superoxide dismutase can reduce cellular damage mediated by oxygen radicals in transgenic plants. EMBO J. 10: 1723–1732.

Bratt, C.E., P-O. Arvidsson, M. Carlsson, and H-E. Åkerlund. 1995. Regulation of violaxanthin de-epoxidase activity by pH and ascorbate concentration. Photosyn. Res. 45: 169-175.

Bugos, R.C. and H.Y. Yamamoto. 1996. Molecular cloning of violaxanthin de-epoxidase from romaine lettuce and expression in *Escherichia coli*. Proc. Natl. Acad. Sci. USA 93: 6320–6325.

Bugos, R.C., A.D. Hieber, and H.Y. Yamamoto. 1998. Xanthophyll cycle enzymes are members of the lipocalin family, the first identified from plants. J. Biol. Chem. 273: 15321–15324.

Chamberlain, D., R. Hyam, G. Argent, G. Fairweather, and K.S. Walter. 1996. The Genus *Rhododendron*. Its classification and synonymy. Royal Botanic Garden Edinburgh.

Daniels, M.J., T.E. Mirkov, and M.J. Chrispeels. 1994. The plasma membrane of *Arabidopsis thaliana* contains a mercury-insensitive aquaporin that is a homolog of the tonoplast water channel protein TIP. Plant Physiol. 106: 1325–1333.

Demmig–Adams, B. and W.W.III. Adams. 1993. The xanthophyll cycle, protein turnover, and the high light tolerance of sun-acclimated leaves. Plant Physiol. 103: 1413–1420.

Demmig-Adams, B., A.M. Gilmore, and W.W.III. Adams. 1996. In vivo functions of carotenoids in high plants. FASEB J. 10: 403–412.

Demmig-Adams, B. and W.W.III. Adams. 2000. Harvesting sunlight safely. Nature 403: 371–374.

Demmig–Adams, B. and W.W.III. Adams. 2006. Photoprotection in an ecological context: the remarkable complexity of thermal dissipation. New Phytol. 172: 11–21.

Eskling, M., P.O. Arvidsson, H.E. Åkerlund. 1997. The xanthophyll cycle, its regulation and components. Physiol. Plant. 100: 806–816.

Foyer, C.H., J. Rowell, and D. Walker. 1983. Measurement of ascorbate content of spinach leaf protoplasts and chloroplasts during illumination. Planta 157: 239-244.

Foyer, C.H., M. Lelandais, and K.J. Kunert. 1994. Photooxidative stress in plants. Physiol. Plant. 92: 696–717.

Foyer, C.H., H. Lopez-Delgado, J.F. Dat, and I.M. Scott. 1997. Hydrogen peroxide- and glutathione-associated mechanisms of acclamatory stress tolerance and signaling. Physiol. Plant. 100: 241–254.

Frommolt, R., R. Goss, and C. Wilhelm. 2001. The de-epoxidase and epoxidase reactions of *Mantoniella squamata (Prasinophyceae)* exhibit different substrate-specific reaction kinetics compared to spinach. Planta 213: 446–456.

Fryer, M.J. 1992. The antioxidant effects of thylakoid vitamin-E (alpha-tocopherol). Plant Cell Environ. 15: 385–392.

Fukuda, Y. 1933. Hygronastic leaf curling and uncurling movement of the leaves of *Rhododendron micranthum* Turcz. with respect to temperature and resistance to cold. Jap. J. Bot. 6: 191–224.

Grimm, B., E. Kruse, and K. Kloppstech. 1989. Transiently expressed early light-inducible proteins share transmembrane domains with light-harvesting chlorophyll-binding proteins. Plant Mol. Biol. 13: 583–593.

Guy, C.L. 1990. Cold acclimation and freezing stress tolerance: role of protein metabolism. Annu. Rev. Plant Physiol. Plant Mol. Biol. 41: 187–223.

Hager, A. and K. Holocher. 1994. Localization of the xanthophyll-cycle enzyme violaxanthin de-epoxidase within the thylakoid lumen and abolition of its mobility by a (light-depend) pH decrease. Planta 192: 581-589.

Harshburger, J.W. 1899. Thermotropic movement of leaves of *Rhododendron maximum*. Proc. Natl. Acad. Sci. USA 1899: 214–222.

Haupt, W. and M.E. Feileib. 1979. The physiology of movements. New York: Springer Verlag.

Havaux, M. 1998. Carotenoids as membrane stabilizers in chloroplasts. Trends Plant Sci. 3: 147-151.

Havaux, M. and K.K. Niyogi. 1999. The violaxanthin cycle protects plants from photooxidative damage by more than one mechanism. Proc. Natl. Acad. Sci. USA 96: 8762–8767.

Havis, J.R. 1964. Freezing of *Rhododendron* Leaves. Proc. Am. Soc. Hort. Sci. 84: 570–574.

Heddad, M. and I. Adamska. 2000. Light stress-regulated two-helix proteins in *Arabidopsis thaliana* related to the chlorophyll *a/b*-binding gene family. Proc. Natl. Acad. Sci. USA 97: 3741–3746.

Heinen, R.B., Q. Ye, and F. Chaumont. 2009. Role of aquaporins in leaf physiology. J. Exp. Bot. 60: 2971–2985.

Henzler, T., Q. Ye, and E. Steudle. 2004. Oxidative gating of water channels (aquaporins) in *Chara* by hydroxyl radicals. Plant Cell Environ. 27: 1184–1195.

Holt, N.E., G.R. Fleming, and K.K. Niyogi. 2004. Toward an understanding of the mechanism of nonphotochemical quenching in green plants. Biochemistry 43: 8281–8289.

Hopkins, W.G. and N.P.A. Huner. 2003. Introduction to Plant Physiology. Wiley, New York.

Horemans, N., C.H. Foyer, G. Potters, and H. Asard. 2000. Ascorbate function and associated transport systems in plants. Plant Physiol. Biochem. 38: 531–540.

Hutin, C., L. Nussaume, N. Moise, I. Moya, K. Kloppstech, and M. Havaux. 2003. Early light-induced proteins protect *Arabidopsis* from photooxidative stress. Proc. Natl. Acad. Sci. USA 1008: 4921–4926.

Johansson, I., M. Karlsson, V.K. Shukla, M.J. Chrispeels, C. Larsson, and P. Kjellbom. 1998. Water transport activity of the plasma membrane aquaporin PM28A is regulated by phosphorylation. Plant Cell 10: 451–459.

Kaku, S., M. Iwaya, and M. Kunishige. 1980. Supercooling ability of *Rhododendron* flower buds in relation to cooling rate and cold hardiness. Plant Cell Physiol. 21: 1205–1216.

Kaku, S. 1993. Monitoring stress sensitivity by water proton NMR relaxation times in leaves of azaleas that originated in different ecological habitats. Plant Cell Physiol. 34: 535–541.

Kaldenhoff, R. and M. Fischer. 2006. Aquaporins in plants. Acta Physiol. 187: 169–176.

Leach, D.G. 1961. *Rhododendrons* of the world and how to grow them. Charles Scribner's Sons, New York.

Lichtenthaler, H.K., C. Buschmann, M. Döll, H.-J. Fietz, T. Bach, U. Kozel, D. Meier, and U. Rahmsdorf. 1981. Photosynthetic activity, chloroplast ultrastructure, and leaf characteristics of high-light and low-light plants and of "sun" and "shade" leaves. Photosyn. Res. 2: 115–141.

Meyer, G. and K. Kloppstech. 1984. A rapidly light-induced chloroplast protein with a high turnover coded for by pea nuclear DNA. Eur. J. Biochem. 138: 201–207.

Mittler, R. 2002. Oxidative stress, antioxidants and stress tolerance. Trends Plant Sci. 7: 405–410.

Montané, M.H. and K. Kloppstech. 2000. The family of light harvesting-related proteins (LHCs, ELIPs, HLIPs): was the harvesting of light their primary function? Gene 258: 1–8.

Müller, P., X.P. Li, and K.K. Niyogi. 2001. Non-photochemical quenching: a response to excess light energy. Plant Physiol. 125: 1558–1566.

Mullineaux, P. and S. Karpinski. 2002. Signal transduction in response to excess light: getting out of the chloroplast. Curr. Opin. Plant Biol. 5: 43–48.

Nilsen, E.T. 1987. Influence of water relations and temperature on leaf movements of *Rhododendron* species. Plant Physiol. 83: 607–612.

Nilsen, E.T. and Y. Bao. 1988. The ecophysiological significance of leaf movements in *Rhododendron maximum*. Ecology 69: 1578–1587.

Nilsen, E.T. 1992. Thermonastic leaf movements: a synthesis of research with *Rhododendron*. Bot. J. Linnean Soc. 110: 205–233.

Niyogi, K.K. 1999. Photoprotection revisited: genetic and molecular approaches. Annu. Rev. Plant Physiol. Plant Mol. Biol. 50: 333–359.

Nobel, P.S. 1977. Internal leaf area and cellular CO_2 resistance: photosynthetic implications of variations with growth conditions and plant species. Physiol. Plant. 40: 137–144.

Noctor, G. and C.H. Foyer. 1998. Ascorbate and glutathione: keeping active oxygen under control. Annu. Rev. Plant Physiol. 49: 249–279.

Noctor, G., A-C.M. Arisi, L. Jouanin, K.J. Kunert, H. Rennenberg, and C.H. Foyer. 1998. Glutathione: Biosynthesis, metabolism and relationship to stress tolerance explored in transformed plants. J. Exp. Bot. 49: 623–647.

Öquist, G. and N.P.A. Huner. 2003. Photosynthesis of overwintering evergreen plants. Annu. Rev. Plant Biol. 54: 329–355.

Peng, Y., R. Arora, G. Li, X. Wang, and A. Fessehaie. 2008. *Rhododendron catawbiense* plasma membrane intrinsic proteins are aquaporins, and their over-expression compromises constitutive freezing tolerance and cold acclimation ability of transgenic *Arabidopsis* plants. Plant Cell Environ. 31: 1275–1289.

Rossini, S., A.P. Casazza, E.C.M. Engelmann, M. Havaux, R.C. Jennings, and C. Soave. 2006. Suppression of both ELIP1 and ELIP2 in *Arabidopsis thaliana* does not affect tolerance to photoinhibition and photooxidative stress. Plant Physiol. 141: 1264–1273.

Russell, R.B., T.T. Lei, and E.T. Nilsen. 2009. Freezing induced leaf movements and their potential implications to early spring carbon gain: *Rhododendron maximum* as exemplar. Funct. Ecol. 23: 463–471.

Sakai, A. 1982. Freezing resistance of ornamental trees and shrubs. J. Amer. Soc. Hort. Sci. 107: 572–581.

Sakai, A., L. Fuchigami, and C.J. Weiser. 1986. Cold hardiness in the genus *Rhododendron*. J. Amer. Soc. Hort. Sci. 111: 273–280.

Sakai, A. and W. Larcher. 1987. Frost survival of plants: responses and adaptation to freezing stress. Springer-Verlag, Berlin, Germany.

Siefermann, D. and H.Y. Yamamoto. 1975. Properties of NADPH and oxygen-dependent zeaxanthin epoxidation in isolated chloroplasts: a transmembrane model for the violaxanthin cycle. Biochim. Biophys. Acta 387: 149–158.

Thomashow, M.F. 1999. Plant cold acclimation: freezing tolerance genes and regulatory mechanisms. Annu. Rev. Plant Physiol. Plant Mol. Biol. 50: 571–599.

Tzvetkova-Chevolleau, T., F. Franck, A.E. Alawady, L. Dall'Osto, F. Carrière, R. Bassi, B. Grimm, L. Nussaume, and M. Havaux. 2007. The light stress-induced protein ELIP2 is a regulator of chlorophyll synthesis in *Arabidopsis thaliana*. Plant J. 50: 795–809.

Verhoeven, A.S., A. Swanberg, M. Thao, and J. Whiteman. 2005. Seasonal changes in leaf antioxidant systems and xanthophyll cycle characteristics in *Taxus x media* growing in sun and shade environments. Physiol. Plant. 123: 428–434.

Wei, H., A.L. Dhanaraj, L.J. Rowland, Y. Fu, S.L. Krebs, and R. Arora. 2005. Comparative analysis of expressed sequence tags (ESTs) from cold-acclimated and non-acclimated leaves of *Rhododendron catawbiense* Michx. Planta 221: 406–416.

Weiser, C.J. 1970. Cold resistance and injury in woody plants. Science 169: 1269–1278.

Xin, Z. and J. Browse. 2000. Cold comfort farm: the acclimation of plants to freezing temperatures, Plant Cell Environ. 23: 893–902.

Yamamoto, H.Y. 1979. Biochemistry of the violaxanthin cycle in higher plants. Pure Appl. Chem. 51: 639–648.

Zarter, C.R., W.W.III. Adams, V. Ebbert, D.J. Cuthbertson, I. Adamska, B. Demmig–Adams. 2006a. Winter down-regulation of intrinsic photosynthetic capacity coupled with up-regulation of Elip-like proteins and persistent energy dissipation in a subalpine forest, New Phytol. 172: 272–282.

Zarter, C.R., W.W.III. Adams, V. Ebbert, I. Adamska, S. Jansson, B. Demmig–Adams. 2006b. Winter acclimation of PsbS and related proteins in the evergreen *Arctostaphylos uva-ursi* as influenced by altitude and light environment, Plant Cell Environ. 29: 869–878.

CHAPTER 2. STRUCTURAL ADAPTATIONS IN OVERWINTERING LEAVES OF THERMONASTIC AND NON-THERMONASTIC *RHODODENDRON* SPECIES

A paper published in *Journal of the American Society for Horticultural Science*

(2008) **133** (6): 768–776

Xiang Wang and Rajeev Arora[1]

Department of Horticulture, Iowa State University, Ames, IA 50011-1100, USA

Harry T. Horner

Department of Genetics, Development and Cell Biology and Microscopy and NanoImaging Facility, Iowa State University, Ames, IA 50011-1020, USA

Stephen L. Krebs

David G. Leach Research Station of the Holden Arboretum, Kirtland, OH 44094, USA

[1]Corresponding author:

Rajeev Arora

Department of Horticulture,

Iowa State University,

Ames, IA 50011-1100, USA

E-mail: rarora@iastate.edu

Tel: 515-294-0031

Fax: 515-294-0730

ADDITIONAL INDEX WORDS. cold acclimation, leaf movement, photoinhibition, leaf anatomy

ABSTRACT. Evergreen rhododendrons (*Rhododendron* L.) are important woody landscape plants in many temperate zones. During winters, leaves of these plants frequently are exposed to a combination of cold temperatures, high radiation, and reduced photosynthetic activity, conditions that render them vulnerable to photooxidative damage. In addition, these plants are shallow-rooted and thus susceptible to leaf desiccation when soils are frozen. In this study, the potential adaptive significance of leaf morphology and anatomy in two contrasting *Rhododendron* species was investigated. *R. catawbiense* Michx. (native to eastern U.S.) exhibits thermonasty (leaf drooping and curling at subfreezing temperatures) and is more winter hardy (leaf freezing tolerance, LT_{50} of containerized plants ≈ –35 °C), while *R. ponticum* L. (native to central Asia) is less hardy (LT_{50} ≈ –16 °C), and non-thermonastic. Thermonasty may function as a light and/or desiccation avoidance strategy in rhododendrons. Microscopic results revealed that *R. ponticum* has significantly thicker leaf blades but thinner cuticle than *R. catawbiense*. There is one layer of upper epidermis and three layers of palisade mesophyll in *R. catawbiense* compared to two distinct layers of upper epidermis and two layers of palisade mesophyll in *R. ponticum*. We suggest that the additional layer of upper epidermis in *R. ponticum* and thicker cuticle and extra palisade layer in *R. catawbiense* represent structural adaptations for reducing light injury in leaves and could serve a photoprotective function in winter when leaf photochemistry is generally sluggish. Results also indicate that although stomatal density of *R. ponticum* is higher than that of *R. catawbiense* leaves, the overall opening of stomatal pores per unit leaf area (an integrated

value of stomatal density and pore-size) is higher by ~ two-fold in *R. catawbiense*, suggesting that *R. catawbiense* may be more prone to winter desiccation and that thermonasty may be a particularly beneficial trait in this species by serving as desiccation-avoidance strategy in addition to a photoprotection role.

Introduction

Rhododendrons are among the most widely grown woody ornamentals in the landscapes and public gardens with great horticultural interest. *Rhododendron* L. (Ericaceae) comprises almost 1000 species distributed worldwide (Chamberlain et al., 1996). Among them, over 800 species are distributed throughout the Northern Hemisphere, ranging from tropical to polar climates and varying widely in their cold hardiness (Leach, 1961; Sakai et al., 1986). Overwintering perennials in the temperate zone survive through harsh winters by an induced process termed cold acclimation (CA). This seasonal phenomenon greatly increases their cold hardiness in response to inductive short photoperiods, low non-freezing and then subfreezing temperatures sequentially through early fall and winter (Sakai and Larcher, 1987; Weiser, 1970). Evergreen rhododendrons are broad-leaved woody plants and the freezing tolerance of fully cold-acclimated leaves can be as low as –50 to –60 ^{o}C (Sakai et al., 1986; Wei et al., 2005).

As understory evergreen plants in the deciduous forests, leaves of most rhododendrons are commonly exposed to a combination of freezing temperatures and high light in their natural habitat during winter. Previous study in our laboratory indicated that downregulation of photosynthetic metabolism, [specifically five photosynthesis-related genes (light-

harvesting chlorophyll a/b-binding protein, RuBisCO small subunit precursor, RuBisCO activase, plastidic fructose bisphosphate aldolase, and chloroplast precursor of plastocyanin)] in overwintering leaves of *R. catawbiense* (Wei et al., 2005) could potentially result in light energy harvested by the leaves to be in excess of what can be processed by photosystems, thus making these plants particularly vulnerable to photoinhibition or photooxidative damage (Peng et al., 2008).

Many plants have evolved mechanisms to dissipate excess absorbed light safely as thermal energy through the xanthophyll cycle (Adams et al., 2004) and/or protect cells against the photooxidative damage via antioxidants such as tocopherols, ascorbate, and glutathione (Niyogi, 1999). Recent studies with several overwintering evergreens – rhododendron (*R. catawbiense*), subalpine firs [(*Abies lasiocarpa* (Hook.) Nutt.], and lodgepole pines (*Pinus contorta* Dougl. *ex* Loud.) - showed that the xanthophyll pool was significantly upregulated in sun-exposed winter leaves compared to the summer leaves and that it may play a key role in the prevention of photooxidative damage (Harris et al., 2006; Zarter et al., 2006a, 2006b).

The leaves of some evergreen *Rhododendron* species show thermonasty i.e., temperature-induced leaf movements, a phenomenon where leaves droop and curl at freezing temperatures in winter (Nilsen, 1987). Thermonasty or thermonasty-like responses have been observed on main stems of *Phryma leptostachya* L. (Endo and Miyauchi, 2006) and the petals of some flowers (*Tulipa* L. and *Crocus* L.) (Crombie, 1962); however, these movements occur at relatively warmer temperatures (~ 12 °C for *P. leptostachya*) while leaf thermonasty in rhododendrons typically occurs at subfreezing temperatures (Nilsen, 1987). Nilsen (1992) proposed several possible theories for thermonasty response in rhododendrons.

A hypothesized adaptive benefit of thermonastic leaf movement is avoidance of high light stress by reducing the leaf area and shading the leaf more. It has been suggested that without thermonasty, the leaves would be injured during bright, cold winter days, and as a consequence, the net photosynthesis rate in the following year would decrease and leaf mortality would increase (Bao and Nilsen, 1988). Another possible adaptive benefit of thermonasty is prevention of desiccation during cold periods (Nilsen, 1992). Rhododendrons are typically shallow-rooted plants and thus are susceptible to leaf desiccation under windy and/or freezing conditions in winter. Leaf curling could reduce transpiration by creating more humid microsites around the stomata of the lower leaf surface (Nilsen, 1992).

In addition to light avoidance and tolerance mechanisms, many plants exhibit photoacclimation in response to light stress that is manifested in the leaf morphological and anatomical adaptations (Anderson et al., 1995; Björkman, 1981; Walters et al., 2003). Photoacclimation can occur at two levels: 1) leaf level and 2) chloroplast level (Murchie and Horton, 1997). The different anatomy of "sun" and "shade" leaves is an example of leaf level acclimation (Björkman, 1981). For example, "sun" leaves are smaller and thicker with more columnar mesophyll cells than "shade" leaves and have a higher density of leaf stomata (Lichtenthaler et al., 1981; Nobel, 1977; Oguchi et al., 2003; Sims and Pearcy, 1992; Wentworth et al., 2006) as well as increased lengths of stomatal pores (Wild and Wolf, 1980). Since the leaves of overwintering rhododendrons are typically exposed to excess light in winter, they too are expected to have evolved leaf morphological and anatomical features to allow them to handle the high irradiance.

The objective of this study was to compare the leaf structural differences of the two *Rhododendron* species (*R. catawbiense* and *R. ponticum*) that are divergent in their leaf

freezing tolerance (super hardy vs less-hardy, respectively) and in their thermonastic behavior (former shows thermonasty while the latter does not). We hope to gain insight into how thermonasty (or lack thereof) together with the specific leaf morphological and anatomical features of the two species might be associated with their ability to tolerate/avoid high irradiance and/or withstand dehydrative stresses during winter.

Materials and Methods

PLANT MATERIAL AND GROWTH CONDITIONS. The plants from the two species of *Rhododendron* (*R. catawbiense* Michx. 'Catalgla' and *R. ponticum* L. 'RSBG 76/411'; RSBG is Rhododendron Species Foundation and Botanical Garden) were vegetatively propagated (semi-hardwood cuttings) and grown in the 19-L plastic pots at the David G. Leach Research Station of Holden Arboretum (Kirtland, OH). About 2-year-old containerized plants were sent to the Department of Horticulture at Iowa State University (ISU) in Ames, IA, USA, where they were maintained in Fafard mix 52 (Conrad Fafard, Inc., Agawam, MA) [pine bark (60%); peat, perlite and vermiculite (40%)] outside the ISU Horticulture greenhouse (lat. 42° 1' N, long. 93° 38' W). The granular slow-release fertilizer (5% N, 2% P, 2% K, 2% Ca, 2% S, and 2% Fe; Sustâne/Natural Fertilizer of America, Inc., Cannon Falls, MN, USA) was applied to the medium surface every three weeks during the growing season. The plants were allowed to acclimate naturally from Aug. to Dec. 2007. Average monthly minimum air temperatures from Aug. to Dec. 2007 at this location were 16.9, 11.1, 7.7, –2.8 and –10.8 °C, respectively. All the plants were partly shaded by placing the pots in the understory of a bald-cypress tree (*Taxodium distichum* L.). Daily changes of

irradiance on leaf surface on sunny days were quite stable and the irradiance ranged from 75 μmol m^{-2} s^{-1} (0800 HR) to 1300 μmol m^{-2} s^{-1} (1400 HR) with the average of ~ 350 μmol m^{-2} s^{-1}. The plants were watered as needed throughout the study.

FREEZING TOLERANCE (FT) TESTS. Leaf FT tests were performed by subjecting punched leaf discs (diameter = 1.27 cm) to a controlled freeze-thaw regime followed by the assessment of injury by measuring electrolyte leakage from freeze-thaw injured tissues as described by Lim et al. (1998). The discs were cooled in a temperature-controlled glycol bath (Isotemp 3028; Fisher Scientific, Pittsburgh, PA) for nonacclimated (NA) leaves sampled in Aug. 2007 or in a programmable freezer (model 85-3.1; ScienTemp, Adrian, MI) for CA leaves sampled in Dec. 2007. The lowest treatment temperatures for NA samples (in the glycol bath) and CA samples (in the programmable freezer) were –20 and –50 °C, respectively. Two separate cooling devices were used in this study because the former's cooling limit is only up to –22 °C, however, ice nucleation (at about –1 and –3 °C for the glycol bath and programmable freezer, respectively) was ensured in all the freezing tests and tissues were cooled at relatively slow cooling rates (–1 to –2 °C/h). The treatment temperatures at which NA or CA samples were removed from the cooling bath or the programmable freezer were at –2 to –3 °C and -5 °C increments, respectively and included an unfrozen control. Fully expanded leaves from current year growth were collected to conduct the tests. Three replications were made at each treatment temperature from three individual leaves (one leaf from each of three plants per species).

For NA leaves, punched leaf discs were placed in test tubes with 80 μL demineralised water; the tubes were placed in the glycol bath for 1 h at –1 °C and ice chips were added to initiate ice-nucleation. After an additional hour at –1 °C, the temperature was cooled at a rate

of 1 °C per hour. Frozen samples at each treatment temperature were removed from the glycol bath and thawed on ice overnight. Samples were removed from ice and thawed at 4 °C for 1 h and then at room temperature for another hour. Ions were extracted with 20 mL demineralised water followed by vacuum infiltration (three times for 3 min each at ~100 kPa) and shaking for 3 h at 250 rpm. Initial electrical conductivity was measured for each sample with a conductivity meter (model 3100; YSI Inc, Yellow Spring, OH). Final electrolyte leakage for each sample was determined after autoclaving the samples at 121 °C for 20 min. Percent ion leakage at each temperature was calculated and converted to percentage injury, and then LT_{50} (the temperature, at which 50% injury occurred and defined as FT) was calculated according to Lim et al. (1998). For cold-acclimated samples, leaf discs were cooled in the programmable freezer with ice nucleation occurring at about –2 to –3 °C with the cooling rate of ~ 1 °C per hour during the first 4 hours (up to –3 °C) and ~ 4 °C per hour until the lowest treatment temperature was reached. All the remaining processes were the same as those conducted for NA samples.

CHLOROPHYLL FLUORESCENCE MEASUREMENTS. Modulated chlorophyll fluorescence was measured with a fluorometer (PAM-2000; Waltz, Effetrich, Germany) and analyzed by Data Acquisition Software DA-2000 (Waltz). Both NA (August) and CA (November) current year leaves from the two species were used. Intact leaves were dark-adapted for 30 min to measure the maximal quantum yield of photosystem II (F_v/F_m) according to Heddad et al. (2006). This parameter reflects the maximal efficiency of photosystem II that is measured in dark-adapted tissues. Three leaves from three different plants were used for all measurements (one leaf from each of the three plants per species). All measurements were made between 1000 and 1200 HR on sunny days.

LIGHT AND SCANNING ELECTRON MICROSCOPY. Punches (diameter = 1 mm) were made from fully expanded leaves at room temperature (NA leaves) or in the cold room (CA leaves) to be used for microscopy analysis. Punches from three separate leaves (one leaf from each of three plants / species and several punches / leaf) were made from the mid-length along mid ribs and three punches / species (one punch / leaf) were randomly selected for microscopy.

For LM, leaf discs were fixed in 2% paraformaldehyde / 2% glutaraldehyde in 0.1 M cacodylate buffer (pH 7.2) under low vacuum for at least 2 h and then stored at 4 °C overnight. The fixed tissues were washed in the cacodylate buffer, dehydrated in a graded ethanol series (25%, 50%, 70%, 95%, 100%) and then transferred to 100% acetone. Each wash lasted for 30 min. The dehydrated discs were gradually infiltrated with a low-viscosity epoxy resin (Spurr, 1969) and embedded, and polymerized at 60 °C for 48 h. Three thin transverse sections (0.5 μm) from each species were made with an ultramicrotome using glass knives, mounted on microscope slides, and stained with toluidine blue O. The LM images were taken on a light microscope (Olympus BH10; Olympus Imaging America Inc., Center Valley, PA) with bright-field optics.

For SEM, the tissues fixed for LM study were post-fixed with 1% osmium tetroxide (OsO_4), dehydrated in a graded ethanol series, and critical point dried using liquid CO_2 (DCP-1; Denton Vacuum Inc., Moorestown, NJ). Samples were then attached to aluminium stubs using adhesive tabs, and silver painted around their edges. The mounted samples were sputter-coated with gold/palladium (20:80) and viewed with a JEOL JSM-5800 LV scanning electron microscope (JEOL Ltd., Tokyo, Japan) at 10 kV. Images were digitally captured.

All anatomical data were obtained using SEM images from NA and CA samples with at least three replications. These parameters included thickness of leaf blades and adaxial epidermis, depth of palisade parenchyma, thickness of leaf adaxial cuticle, stomatal density, length and width of stomatal pores. Total opening area of stomatal pores per unit leaf area was calculated by integrating stomatal density (number of stomata / unit leaf area) and average stomatal pore-size (width and length).

STATISTICAL ANALYSIS. Statistical significance of differences between the two species in measured parameters was tested by Student's t-test. Means were considered to be significantly different when $P \leq 0.05$.

Results

THERMONASTY, LEAF FREEZING TOLERANCE, AND MAXIMAL QUANTUM YIELD OF PHOTOSYSTEM II (F_v/F_m). Thermonastic leaf movement at subfreezing temperatures (–5.5 °C) clearly appeared in CA leaves of *R. catawbiense*, but not in *R. ponticum* (Fig. 1). Leaf freezing tolerance (LT_{50}) of *R. ponticum* and *R. catawbiense* was –4.7 °C and –7.1 °C for NA plants, and –15.6 °C and –34.5 °C for CA plants, respectively. Compared with *R. ponticum*, the LT_{50} of *R. catawbiense* was 58% and 121% lower (more negative) in NA and CA plants, respectively. Both species showed photoinhibition in November (lower values of F_v/F_m) compared to the measurements in August (Table 1). *R. catawbiense* showed greater photoinhibition than *R. ponticum* especially in CA leaves (20% vs 13% reduction in F_v/F_m; Table 1).

LEAF ANATOMY OF *R. ponticum* AND *R. catawbiense*

LEAF BLADES. LM and SEM images of anatomical features of NA and CA leaf blades are shown with (Figs. 2 and 3). There were two distinct layers of upper (adaxial) epidermis and two to three layers of palisade mesophyll in *R. ponticum* (Figs. 2A, 2C, 3A, and 3C); however, there were one layer of adaxial epidermis and three to four layers of palisade mesophyll in *R. catawbiense* (Figs. 2B, 2D, 3B, and 3D).

Thickness of leaf blades of *R. ponticum* was greater than that of *R. catawbiense* in both NA and CA leaves (Fig. 4A). Moreover, compared with NA leaves, thickness of leaf blades from CA plants increased significantly (by ~ 17%) in *R. ponticum*; however, no such change was observed in *R. catawbiense*. Thickness of adaxial epidermis of *R. ponticum* was also greater by ~ two-fold than that of *R. catawbiense* in both NA (~ 25.7 vs ~ 14.6 μm) and CA (~ 28.6 vs ~ 14.6 μm) leaves (Fig. 4B). Compared with NA leaves, thickness of adaxial epidermis from CA plants was significantly greater (by ~ 12%) in *R. ponticum*; however, no such change was observed in *R. catawbiense*. Depth of the palisade parenchyma of *R. ponticum* was relatively smaller (by ~ 14%) than that of *R. catawbiense* in NA leaves, but somewhat greater (by ~ 4%) than that of *R. catawbiense* in CA leaves (Fig. 4C). Consequently, depth of the palisade parenchyma in CA plants increased ~ 26% compared to NA leaves in *R. ponticum*; however, there was no change in *R. catawbiense* (Fig. 4C).

Thickness of adaxial cuticle from NA and CA leaves are shown in Fig. 5 A-E. Compared with *R. ponticum*, cuticle thickness in *R. catawbiense* was ~ 16% and ~ 7% greater in NA (5.1 vs 4.4 μm) and CA (6.3 vs 5.9 μm) leaves, respectively (Fig. 5E). Also, CA leaves exhibited significantly greater cuticle thickness than NA leaves in both species with an increase of ~ 34% and ~ 24% for *R. ponticum* and *R. catawbiense*, respectively (Fig. 5E).

DIFFERENCES IN ABAXIAL STOMATA PROPERTIES. No wax could be observed around the stomata in *R. ponticum* (Figs. 6A and 6C), while a substantial amount of wax was noted in *R. catawbiense* (Figs. 6B and 6D). Stomatal density of *R. ponticum* was significantly higher than that of *R. catawbiense* in both NA (~ 335 vs ~ 222 stomata mm^{-2}) and CA (~ 306 vs ~ 128 stomata mm^{-2}) leaves (Fig. 6E). Compared with NA leaves, both species showed a significant decrease in stomatal density in CA leaves – by ~ 41.9% and ~ 8.6% for *R. catawbiense* and *R. ponticum,* respectively (Fig. 6E). The two species showed different size (length, width and opening area of pores) and shape of stomatal pores (Figs. 7A, 7B, 7C, and 7D). Compared with *R. ponticum*, *R. catawbiense* showed significantly greater values (averaged over NA and CA samples) for the length (~ 13.4 vs ~ 7.1 μm) and width (~ 6.3 vs ~ 2.7 μm) (Figs. 7E and 7F, respectively). The opening area of stomatal pores / leaf area for *R. catawbiense* leaves was 2.9-fold that of *R. ponticum* (~ 17970 vs ~ 6081 $\mu m^2/mm^2$) in NA leaves, while it was 1.9-fold (~ 11807 vs ~ 6277 $\mu m^2/mm^2$) (Fig. 7G) that of *R. ponticum* in CA leaves.

Discussion

The relationships between thermonastic leaf movements, leaf freezing tolerance, and photoinhibition (F_v/F_m) in rhododendron are not well understood. Our results showed that the thermonastic species (*R. catawbiense*) (Fig. 1) had higher leaf freezing tolerance than the non-thermonastic species (*R. ponticum*) in both NA and CA leaves (Table 1). A previous study of 32 *Rhododendron* species exhibited a strong positive correlation between the degree of leaf curling and freezing tolerance (Nilsen and Tolbert, 1993), suggesting that

thermonastic leaf movements may play a functional role in freezing tolerance in some *Rhododendron* species.

Our results showed that *R. catawbiense* leaves were more photoinhibited than *R. ponticum* leaves in both NA and CA samples, but particularly more pronounced in winter (Table 1), indicating that *R. catawbiense* is more photosensitive than *R. ponticum* under comparable conditions. It is known that rhododendron plants, most of which belong to shade-loving species, experience the largest radiation of the year in winter because irradiance under a canopy of deciduous trees is higher in winter than in the summer. Thermonastic leaf movements of rhododendron plants at subfreezing temperatures were thought to alleviate photoinhibition (Nilsen, 1992) by reducing the quantity of light impinging on the leaf, thereby preventing or limiting photoinhibition. Thus, we suggest that leaf movements in *R. catawbiense* together with other leaf adaptations may help reduce photoinhibition in winter in this species which often grows in the open, e.g. the so-called "balds" above tree line in the Appalachian Mountains and hence more prone to light stress. The non-thermonastic species (*R. ponticum*); however, may have evolved other avoidance or tolerance mechanisms for maintaining photosystem II photochemical efficiency under winter conditions.

Significantly different anatomy between "sun" and "shade" leaves is a good example of photoacclimation (Björkman, 1981). Our results showed that both species had some characteristics of "sun" leaves. For example, *R. ponticum* had thicker leaf blades (Fig. 4A) and higher density of leaf stomata (Fig. 6E), the characteristics typically observed in "sun" leaves (Oguchi et al., 2003; Sims and Pearcy, 1992; Wentworth et al., 2006). Two-layered adaxial epidermis in *R. ponticum* leaves is a rather special feature and contributes to thicker leaf blades in this species. Our data indicated that, in this species, leaf thickness further

increased in cold acclimated tissues. Similar cold acclimation induced leaf thickness has been previously reported in other species, such as rye and winter oilseed rape, and attributed to either increased mesophyll cell size or cell wall thickness (Huner et al., 1981; Stefanowska et al., 1999). Leaf epidermal cells are thought to protect leaves against high irradiance (Martin and Juniper, 1970) and / or ultraviolet radiation (Liakoura et al., 2003). The additional layer of upper epidermis and thicker adaxial epidermal cells in *R. ponticum* (Figs. 2A, 2C, and 4B) could be structural adaptations presumably associated with the photoprotection (from total light and / or specifically UV) during winter in this species.

Our results also showed that although *R. catawbiense* leaves had only one layer of upper epidermis, they contained extra palisade layer compared to *R. ponticum* (Figs. 2B, 2D, 3B, and 3D). Previous research shows that "sun" leaves are more likely to contain multiple layers of palisade cells (Osborn and Taylor, 1990) which may take advantage of the extra layers of photosynthetic cells to increase photosynthetic efficiency under high sunlight. We speculate that the extra palisade layer in *R. catawbiense,* the hardier species, may be associated with more efficient light use and thus reducing light injury under winter conditions. It is noteworthy that multiple palisade (as opposed to single layer) has been associated with greater leaf freezing tolerance in some species, such as *Solanum tuberosum* L. (Palta and Li, 1979; Pino et al., 2008). Combined with thermonastic leaf movements, the extra palisade layer in this species may constitute a component of photoprotective strategy in winter. In short, these structural and leaf movement differences between these two species indicate that both species have evolved different mechanisms or adaptive structures to tolerate / avoid high irradiance in winter. However, data from future studies on potential differences in the

light absorptivity and light-induced injury in these two species should be useful in supporting this observation.

Cuticles, as the primary interface between the plant and its environment, receive a significant amount of solar radiation (Osborn and Taylor, 1990). They play a key role in maintaining the plant's integrity within an inherently hostile environment and provide a protective barrier to unfavourable light or water. Typically cuticles of "sun" leaves are thicker (Martin and Juniper 1970). Also an increase in accumulating cuticle wax is a response of many plants to higher irradiance (Reed and Tukey, 1982; Sheperd et al., 1995) and cuticle wax is considered as a photoprotective layer (Shepherd and Griffiths, 2006) by reflecting and diffusing light. In our study, *R. catawbiense* had thicker cuticles (Fig. 5) with a large accumulation of cuticle wax (Fig. 6) on the surface of the abaxial epidermis cells compared to *R. ponticum* in both NA and CA leaves, rendering *R. catawbiense* leaves to be more like "sun" leaves. Thus, we suggest that the thicker cuticles together with the accumulation of cuticle wax in the leaves of *R. catawbiense* may have adaptive significance *vis-a-vis* photoprotection in this species.

Epidermal cells have two features that are the key to preventing evaporative water loss: dense packing and coverage by cuticles. Cuticle wax in the abaxial and adaxial surface of the epidermis cells is considered to prevent water loss (Shepherd and Griffiths, 2006). Since rhododendron plants are shallow-rooted, they are particularly susceptible to leaf desiccation under windy and/or freezing conditions in winter. Our results showed that although the stomatal density of *R. ponticum* was much higher than that of *R. catawbiense* in both NA and CA plants (Fig. 6E), the "overall opening" of stomatal pores per unit leaf area (an integrated value of stomatal density and pore-size) was much greater in *R. catawbiense* than that in *R.*

ponticum (Fig. 7G); it is noteworthy, however, that this conclusion has an underlying assumption that stomata have similar degree of "openness" (or similar pore size) in NA and CA leaves. This feature indicates that the leaves of *R. catawbiense* may be more prone to winter desiccation than *R. ponticum* when soils are frozen, especially since this species frequently grows on open "balds". Thus, we suggest that accumulation of a relatively large amount of cuticle wax in the abaxial leaf surface (Fig. 6B and 6D) in *R. catawbiense* as well as thicker cuticles in the adaxial leaf surface of this species may help them reduce water loss in winter; a recent study of the relationship between leaf wax deposition and drought tolerance in tobacco demonstrated that leaf cuticular wax load increased significantly when plants were subjected to a periodic drought (Cameron et al., 2006).

We observed a reduction in stomatal density of the winter leaves relative to summer ones in the two *Rhododendron* species included in this study (Fig. 6E). This is a rather unexpected result since stomata are believed to be formed from initials early in leaf development and, therefore, stomatal density is not expected to change over time in mature, fully expanded leaves, the ones used here. Future studies focused at investigating temporal changes in the stomatal density (between seasons or even years since leaves last several years in this evergreen species) should provide further insight in to this rather intriguing phenomenon.

In conclusion, the two species have evolved distinct leaf structural adaptations to winter conditions. The additional layer of upper epidermis and multiple palisade layers in *R. ponticum* leaves, and thicker cuticle with wax and extra palisade layer in *R. catawbiense* may constitute structural adaptations involved in reducing light stress during winter when photosynthesis is generally downregulated. Our results also indicated that whereas stomatal density of *R. ponticum* was higher than that of *R. catawbiense* leaves, the remarkably higher

overall opening of stomatal pores per unit leaf area (an integrated value of stomatal density and pore-size) in *R. catawbiense* might render this species more prone to winter desiccation and thus thermonasty may serve as desiccation-avoidance strategy in this species perhaps in addition to serving a light-avoidance role.

Acknowledgements

This journal paper of the Iowa Agriculture and Home Economics Experiment Station, Ames, Iowa (Project 3601) was supported by Hatch Act and State of Iowa funds. We thank Tracey Pepper and Randall Den Adel of Microscopy and NanoImaging Facility (Department of Genetics, Development and Cell Biology, Iowa State University) for helpful assistance and advice for the microscopy work. We thank Dr. Allen D. Knapp for providing the fluorometer and Ms. Maria M. Hartt (Department of Agronomy, Iowa State University) for technical advice and assistance with F_v/F_m measurements. We also thank Arlen Patrick (greenhouse manager, Department of Horticulture, Iowa State University) for assisting with plant care throughout this study.

Literature Cited

Adams III., W.W., C.R. Zarter, V. Ebbert, and B. Demmig-Adams. 2004. Photoprotective strategies of overwintering evergreens. BioScience 54:41–49.

Anderson, J.M., W.S. Chow, and Y.I. Park. 1995. The grand design of photosynthesis:

Acclimation of the photosynthetic apparatus to environmental cues. Photosyn. Res. 46:129–139.

Bao, Y. and E.T. Nilsen. 1988. The ecophysiological significance of leaf movements in *Rhododendron maximum* L. Ecology 69:1578–1587.

Björkman, O.B. 1981. Responses to different quantum flux densities, p. 57–107. In: O.L. Lange, P.S. Nobel, C.B. Osmond, and H. Ziegler (eds.). Encyclopedia of plant physiology, new series, vol. 12 A. Springer-Verlag, Berlin.

Cameron, K.D., M.A. Teece, and L.B. Smart. 2006. Increased accumulation of cuticular wax and expression of lipid transfer protein in response to periodic drying events in leaves of tree tobacco. Plant Physiol. 140:176–183.

Chamberlain, D., R. Hyam, G. Argent, G. Fairweather, and K.S. Walter. 1996. The Genus *Rhododendron*. Its classification and synonymy. Royal Botanic Garden Edinburgh.

Crombie, W.M.L. 1962. Thermonasty, p. 15–28. In: W. Ruhland and E. Bünning (eds.). Encyclopedia of Plant Physiology, Vol. 17, Physiology of movements 2. Springer-Verlag, Berlin.

Endo, Y. and T. Miyauchi. 2006. Thermonasty of young main stems of *Phryma leptostachya* (Phrymaceae). J. Plant Res. 119:449–457.

Harris, G.C., V. Antoine, M. Chan, D. Nevidomskyte, and M. Königer. 2006. Seasonal changes in photosynthesis, protein composition and mineral content in *Rhododendron* leaves. Plant Sci. 170:314–325.

Heddad, M., H. Norén, V. Reiser, M. Dunaeva, B. Andersson, and I. Adamska. 2006. Differential expression and localization of early light-induced proteins in *Arabidopsis*. Plant Physiol. 142:75–87.

Huner, N.P.A., J.P. Palta, P.H. Li, and J.V. Carter. 1981. Anatomical changes in leaves of Puma rye in response to growth at cold-hardening temperatures. Bot. Gaz. 142:55–62.

Leach, D.G. 1961. *Rhododendrons* of the world and how to grow them. Charles Scribner's Sons, New York.

Liakoura, V., J.E. Bornman, and G. Karabourniotis. 2003. The ability of abaxial and adaxial epidermis of sun and shade leaves to attenuate UV-A and UV-B radiation in relation to the UV absorbing capacity of the whole leaf methanolic extracts. Physiol. Plant. 117:33–43.

Lichtenthaler, H.K., C. Buschmann, M. Döll, H.-J. Fietz, T. Bach, U. Kozel, D. Meier, and U. Rahmsdorf. 1981. Photosynthetic activity, chloroplast ultrastructure, and leaf characteristics of high-light and low-light plants and of "sun" and "shade" leaves. Photosyn. Res. 2:115–141.

Lim, C.C., R. Arora, and E.D. Townsend. 1998. Comparing Gompertz and Richards functions to estimate freezing injury in *Rhododendron* using electrolyte leakage. J. Amer. Soc. Hort. Sci. 123:246–252.

Martin, J.T. and B.E. Juniper. 1970. The cuticles of plants. Edward Arnold, London. 347 pp.

Murchie, E.H. and P. Horton. 1997. Acclimation of photosynthesis to irradiance and spectral quality in British plant species: chlorophyll content, photosynthetic capacity and habitat preference. Plant Cell Environ. 20:438–448.

Nilsen, E.T. 1987. Influence of water relations and temperature on leaf movements of *Rhododendron* species. Plant Physiol. 83:607–612.

Nilsen, E.T. 1992. Thermonastic leaf movements: a synthesis of research with *Rhododendron*. Bot. J. Linnean Soc. 110:205–233.

Nilsen, E.T. and A. Tolbert. 1993. Does winter leaf curling confer cold stress tolerance in *Rhododendron*? J. Amer. Rhododendron Soc. 47:98–104.

Niyogi, K.K. 1999. Photoprotection revisited: genetic and molecular approaches. Annu. Rev. Plant Physiol. Plant Mol. Biol. 50:333–359.

Nobel, P.S. 1977. Internal leaf area and cellular CO_2 resistance: photosynthetic implications of variations with growth conditions and plant species. Physiol. Plant. 40:137–144.

Oguchi, R., K. Hikosaka, and T. Hirose. 2003. Does the change in light acclimation need leaf anatomy? Plant Cell Environ. 26:505–512.

Osborn, J.F. and T.N. Taylor. 1990. Morphological and ultrastructural studies of plant cuticular membranes. I. Sun and shade leaves of *Quercus velutina* (Fagaceae). Bot. Gaz. 151:465–476.

Palta, J.P. and P.H. Li. 1979. Frost-hardiness in relation to leaf anatomy and natural distribution of several *Solanum* species. Crop Sci. 19:665–671.

Peng, Y., W. Lin, H. Wei, S.L. Krebs, and R. Arora. 2008. Phylogenetic analysis and seasonal cold acclimation-associated expression of early light-induced protein genes of *Rhododendron catawbiense*. Physiol. Plant. 132:44–52.

Pino, M.T., J.S. Skinner, Z. Jeknic, P.M. Hayes, A.H. Soeldner, M.F. Thomashow, and T.H. Chen. 2008. Ectopic *AtCBF1* over-expression enhances freezing tolerance and induces cold acclimation-associated physiological modifications in potato. Plant Cell Environ. 31:393–406.

Reed, D.W. and H.B. Jr. Tukey. 1982. Light intensity and temperature effects on epicuticular wax morphology and internal cuticle ultrastructure of carnation and brussels sprouts leaf cuticles. J. Amer. Hort. Sci. 107:417–420.

Sakai, A., L. Fuchigami, and C.J. Weiser. 1986. Cold hardiness in the genus *Rhododendron*. J. Amer. Soc. Hort. Sci. 111:273–280.

Sakai, A. and W. Larcher. 1987. Frost survival of plants: responses and adaptation to freezing stress. Springer-Verlag, Berlin, Germany.

Shepherd, T., G.W. Robertson, D.W. Griffiths, A.N.E. Birch, and G. Duncan. 1995. Effects of environment on the composition of epicuticular wax from kale and swede. Phytochemistry. 40:407–417.

Shepherd, T. and D.W. Griffiths. 2006. The effects of stress on plant cuticular waxes. New Phytol. 171:469–499.

Sims, D.A. and R.W. Pearcy. 1992. Response of leaf anatomy and photosynthetic capacity in *Alocasia macrorrhiza* (Araceae) to a transfer from low to high light. Amer. J. Bot. 79:449–455.

Spurr, A.R.1969. A low-viscosity epoxy resin embedding medium for electron microscopy. J. Ultrastructure Res. 26:31–43.

Stefanowska, M., M. Kuraś, M. Kubacka-Zębalska, and A. Kacperska. 1999. Low temperature affects pattern of leaf growth and structure of cell walls in winter oilseed rape. Ann. Bot. 84:313–319.

Walters, R.G., F. Shephard, J.J.M. Rogers, S.A. Rolfe, and P. Horton. 2003. Identification of mutants of *Arabidopsis* defective in acclimation of photosynthesis to the light environment. Plant Physiol. 131:472–481.

Wei, H., A.L. Dhanaraj, L.J. Rowland, Y. Fu, S.L. Krebs, and R. Arora. 2005. Comparative analysis of expressed sequence tags (ESTs) from cold-acclimated and non-acclimated leaves of *Rhododendron catawbiense* Michx. Planta 221:406–416.

Weiser, C.J. 1970. Cold resistance and injury in woody plants. Science 169:1269–1278.

Wentworth, M., E.H. Murchie, J.E. Gray, D. Villegas, C. Pastenes, M. Pinto, and P. Horton. 2006. Differential adaptation of two varieties of common bean to abiotic stress - II. acclimation of photosynthesis. J. Expt. Bot. 57:699–709.

Wild, A. and G. Wolf. 1980. The effect of different light intensities on the frequency and size of stomata, the size of cells, the number, size and chlorophyll content of chloroplasts in the mesophyll and the guard cells during the ontogeny of primary leaves of *Sinapis alba.* Zeitschrift Für Pflanzenphysiologie. 97:325–342.

Zarter, C.R, B. Demmig-Adams, V. Ebbert, I. Adamska, and W.W. Adams III. 2006a. Photosynthetic capacity and light harvesting efficiency during the winter-to-spring transition in subalpine conifers. New Phytol. 172:283–292.

Zarter, C.R., W.W. Adams III, V. Ebbert, D.J. Cuthbertson, I. Adamska, and B. Demmig-Adams. 2006b. Winter down-regulation of intrinsic photosynthetic capacity coupled with up-regulation of Elip-like proteins and persistent energy dissipation in a subalpine forest. New Phytol. 172:272–282.

Table 1. Leaf freezing tolerance (LT_{50}) and maximal quantum yield of photosystem II (F_v/F_m) of *Rhododendron ponticum* and *Rhododendron catawbiense* from nonacclimated (NA) and cold-accimated (CA) leaves in 2007. Data presented are mean +_ SE (n = 3). Different letters indicate significant differences between species and sampling dates ($P \leq 0.05$).

Species	LT_{50} (°C)		F_v/F_m	
	NA (August)	CA (December)	NA (August)	CA (December)
R. ponticum	–4.7a ± 0.2	–15.6c ± 1.0	0.76a ± 0.01	0.66b ± 0.01
R catawbiense	–7.1b ± 0.4	–34.5d ± 1.8	0.74a ± 0.02	0.59c ± 0.03

Figure captions

Fig. 1. The photograph showing no leaf movement and thermonastic leaf movement (see arrows) in *Rhododendron ponticum* and *Rhododendron catawbiense*, respectively. The picture was taken on a sunny day while the ambient temperature was –5.5 ºC in Dec. 2006.

Fig. 2. Light micrographs of laminal anatomy of nonacclimated (NA) (**A** and **B**) and cold-acclimated (CA) (**C** and **D**) leaves from *Rhododendron ponticum* and *R. catawbiense*. (**A** and **C**): Transverse sections of NA and CA leaves from *R. ponticum*, respectively. (**B** and **D**): Transverse sections of NA and CA leaves from *R. catawbiense*, respectively. Bars = 100 µm. **pp**, palisade parenchyma; **sp**, spongy parenchyma; **ue**, upper (adaxial) epidermis.

Fig. 3. Scanning electron micrographs of laminal anatomy of nonacclimated (NA) (**A** and **B**) and cold-acclimated (CA) (**C** and **D**) leaves from *Rhododendron ponticum* and *R. catawbiense*. (**A** and **C**): Leaf-fracture images of NA and CA plants from *R. ponticum*, respectively. Bars = 100 µm. (**B** and **D**): Leaf-fracture images of NA and CA plants from *R. catawbiense*, respectively. Bars = 100 µm. **pp**, palisade parenchyma; **sp**, spongy parenchyma; **ue**, upper (adaxial) epidermis.

Fig. 4. Comparison of thickness of leaf blades (**A**), thickness of adaxial epidermis (**B**), and depth of palisade parenchyma (**C**) from nonacclimated (NA) and cold-acclimated (CA) leaves of *Rhododendron ponticum* and *R. catawbiense.* Data presented are mean +_ SE (n =

10 independent measurements from three sections per species; 3+3+4). Leaf samples were fixed and treated with the same way as described in Fig. 3.

Fig. 5. Scanning electron micrographs showing thickness of adaxial cuticles of nonacclimated (NA) (**A** and **B**) and cold-acclimated (CA) (**C** and **D**) leaves from *Rhododendron ponticum* and *R. catawbiense.* (**A** and **C**): Images showing cuticle thickness of NA and CA leaves from *R. ponticum*, respectively. Bars = 5 µm. (**B** and **D**): Images showing cuticle thickness of NA and CA plants from *R. catawbiense*, respectively. Bars = 5 µm. (**E**) Comparison of thickness of adaxial cuticle from nonacclimated (NA) and cold-acclimated (CA) leaves of *R. ponticum* and *R. catawbiense*. Note that cuticle thickness is marked by arrows. Data presented are mean +_ SE (n = 10 independent measurements from three sections per species; 3+3+4). Leaf samples were fixed and treated with the same way as described in Fig. 3.

Fig. 6. Scanning electron micrographs showing the abaxial stomatal density of nonacclimated (NA) (**A** and **B**) and cold-acclimated (CA) (**C** and **D**) leaves from *Rhododendron ponticum* and *R. catawbiense*. (**A** and **C**): Images showing stomatal density of NA and CA leaves from *R. ponticum*, respectively. Note that there was no wax accumulated around the stomata. Bars = 100 µm. (**B** and **D**): Images showing stomatal density of NA and CA plants from *R. catawbiense*, respectively. Note the wax accumulated around the stomata (arrows). Bars = 100 µm. (**E**) Comparison of stomata density from nonacclimated (NA) and cold-acclimated (CA) leaves of *R. ponticum* and *R. catawbiense*. Data presented are mean +_ SE (n = 5

independent measurements from three leaf discs per species; 2+2+1). Leaf samples were fixed and treated with the same way as described in Fig. 3.

Fig. 7. Scanning electron micrographs showing the size (μm) and opening area (an integrated value of stomatal density and pore-size calculated as μm^2 per mm^2 leaf area) of stomata pores of nonacclimated (NA) (**A** and **B**) and cold-acclimated (CA) (**C** and **D**) leaves from *Rhododendron ponticum* and *R. catawbiense*, respectively. (**A** and **C**): Images showing stomatal pores of NA and CA leaves from *R. ponticum*, respectively. Bars = 5 μm. (**B** and **D**): Images showing stomatal pores of NA and CA plants from *R. catawbiense*, respectively. Bars = 5 μm. (**E, F and G**): Comparison of the length, width and opening area of stomata pores from nonacclimated (NA) and cold-acclimated (CA) leaves of *R. ponticum* and *R. catawbiense*, respectively. Data presented are mean +_ SE (n = 5 independent measurements from three leaf discs per species; 2+2+1). Leaf samples were fixed and treated with the same way as described in Fig. 3.

Fig. 1

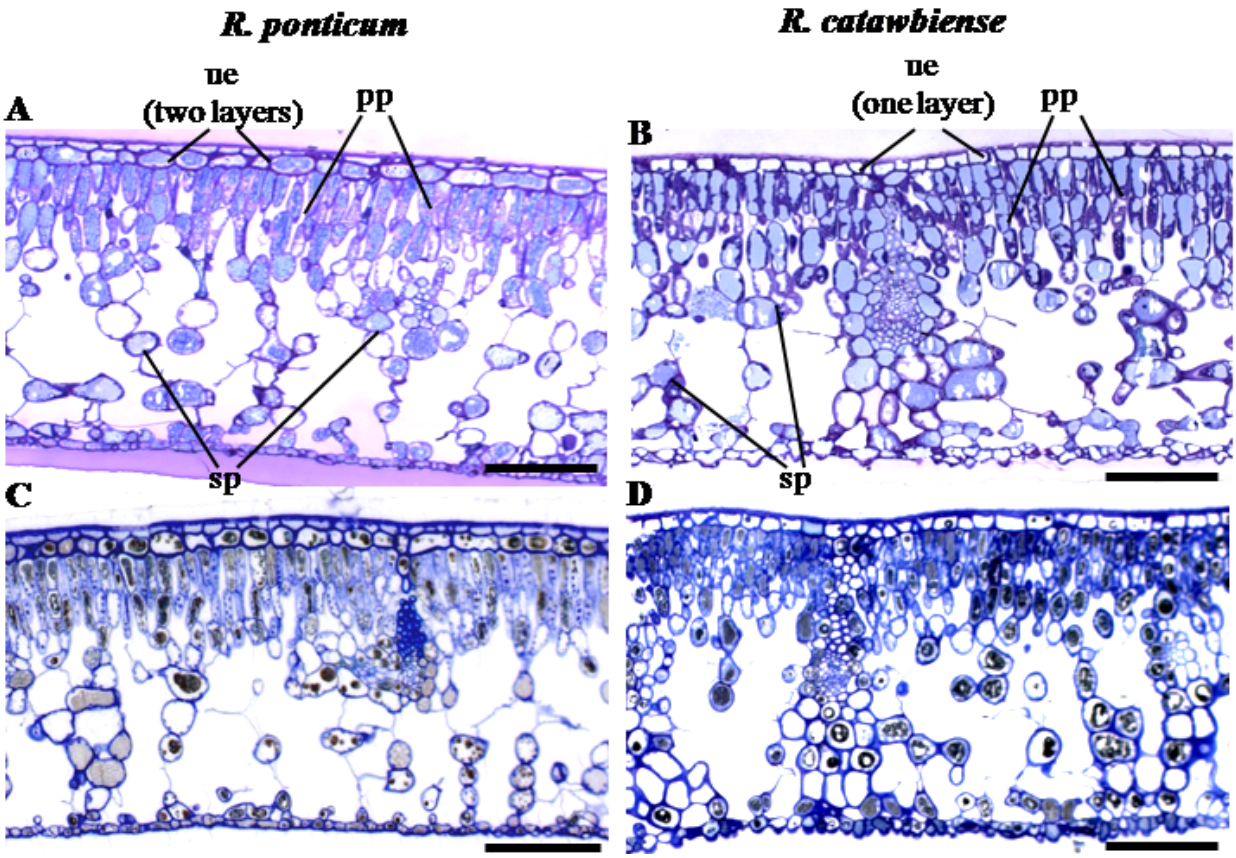
R. ponticum
R. catawbiense
A
ue
(two layers)
pp
sp
B
ue
(one layer)
pp
sp
C
D

Fig. 2

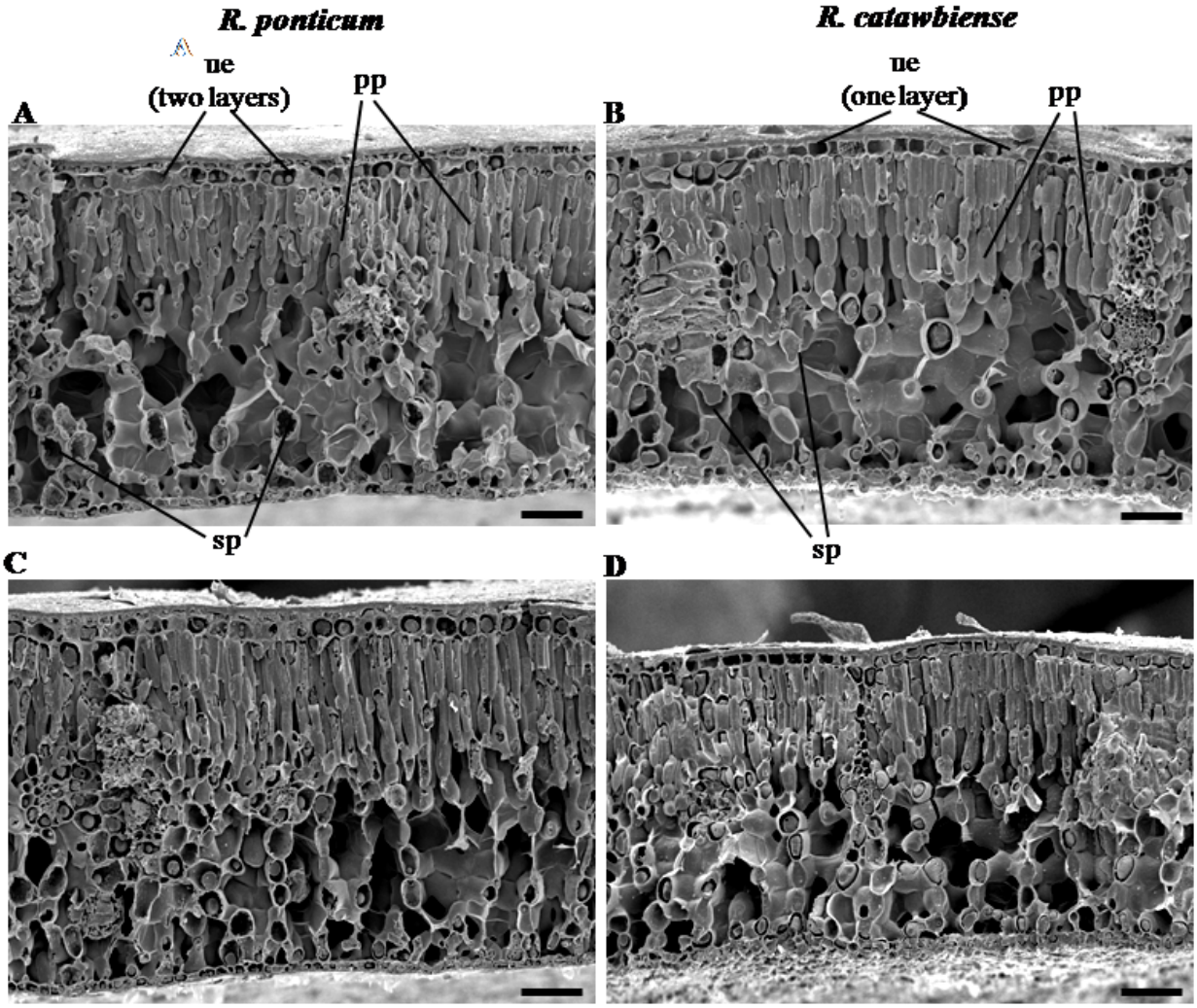
R. ponticum
ue
(two layers)
pp
A
sp
R. catawbiense
ue
(one layer)
pp
B
sp
C
D

Fig. 3

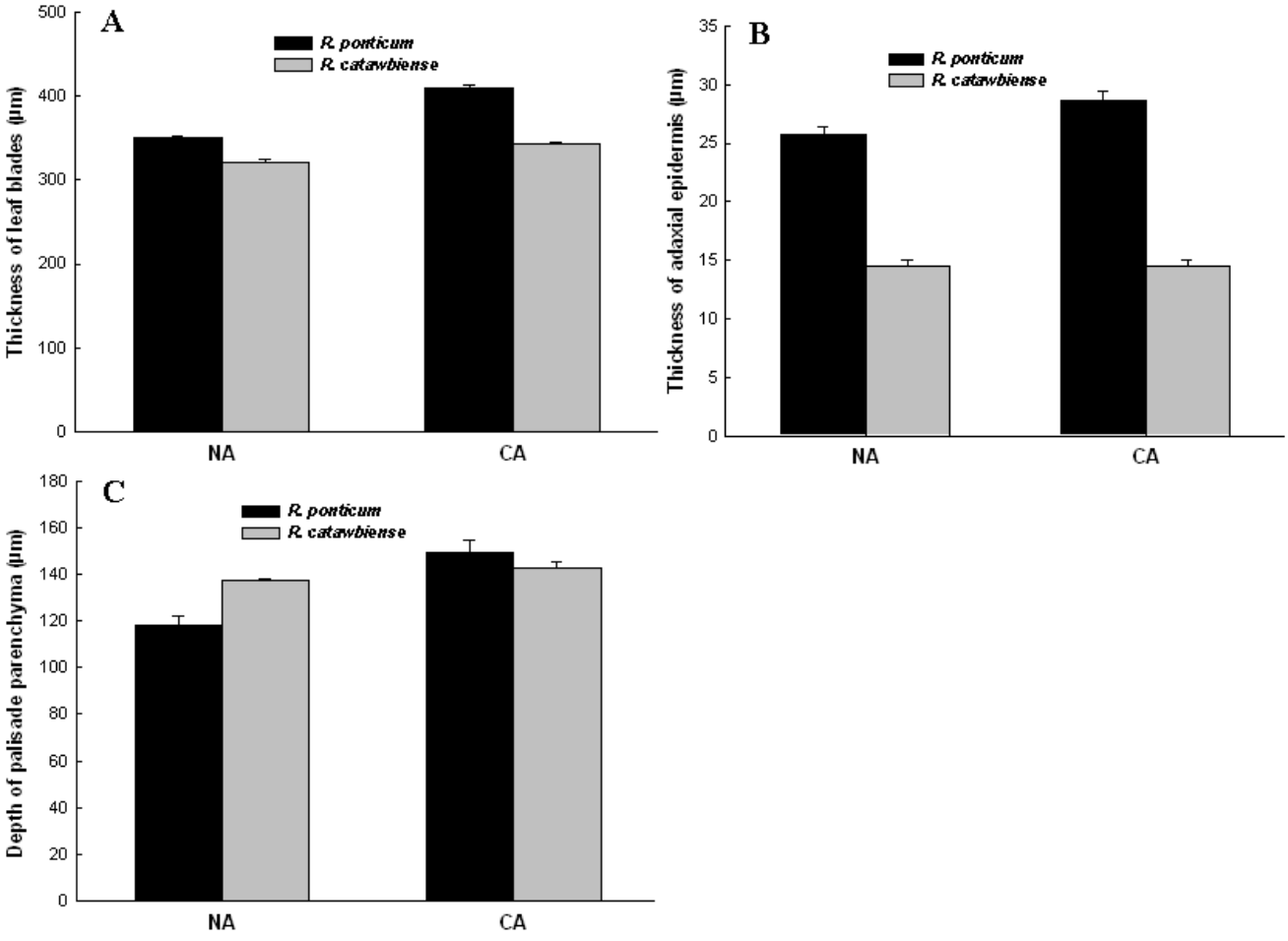
A
R. ponticum
R. catawbiense
Thickness of leaf blades (μm)
500
400
300
200
100
0
NA
CA
B
R. ponticum
R. catawbiense
Thickness of adaxial epidermis (μm)
35
30
25
20
15
10
5
0
NA
CA
C
R. ponticum
R. catawbiense
Depth of palisade parenchyma (μm)
180
160
140
120
100
80
60
40
20
0
NA
CA

Fig. 4

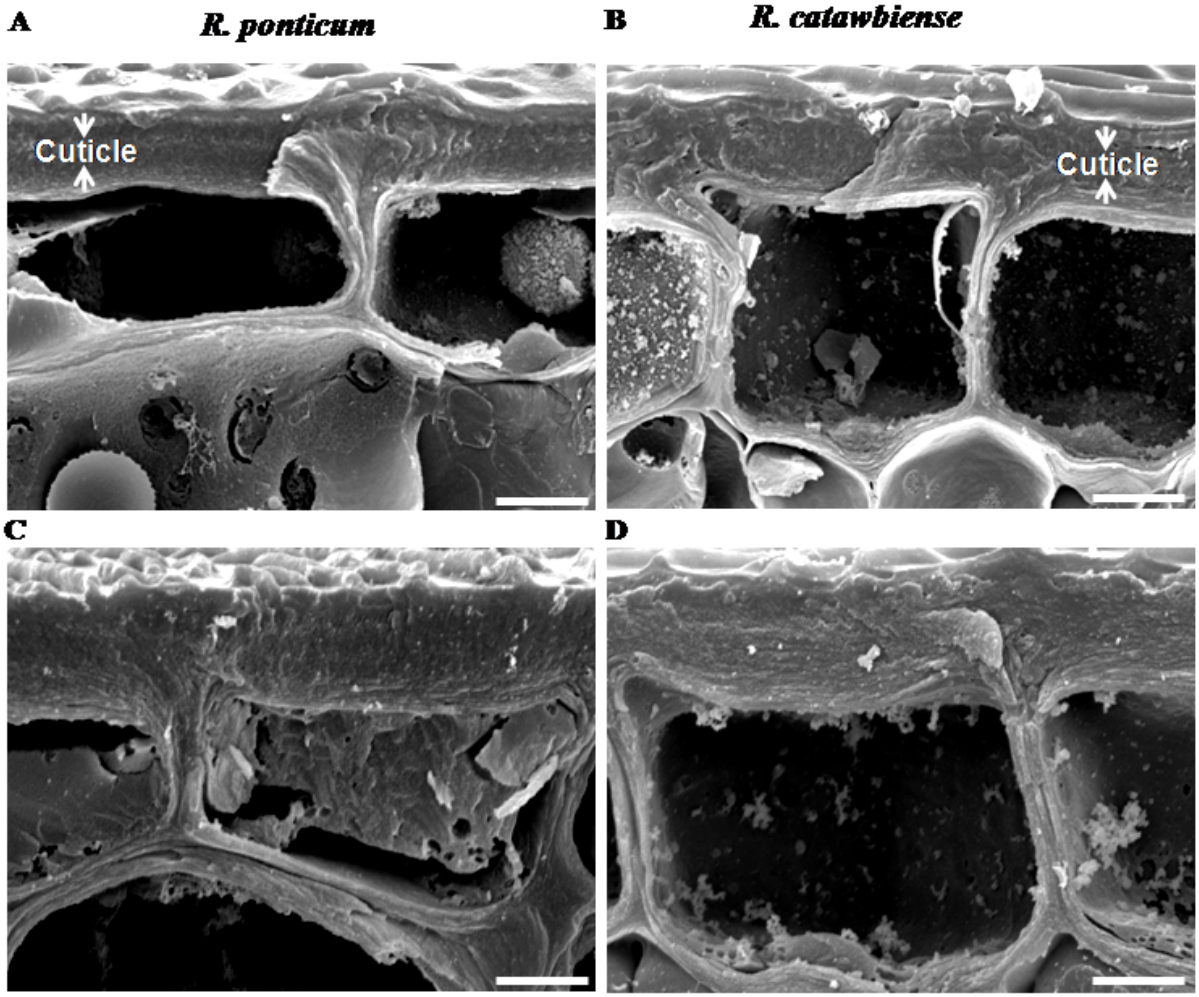
A
R. ponticum
B
R. catawbiense
Cuticle
Cuticle
C
D

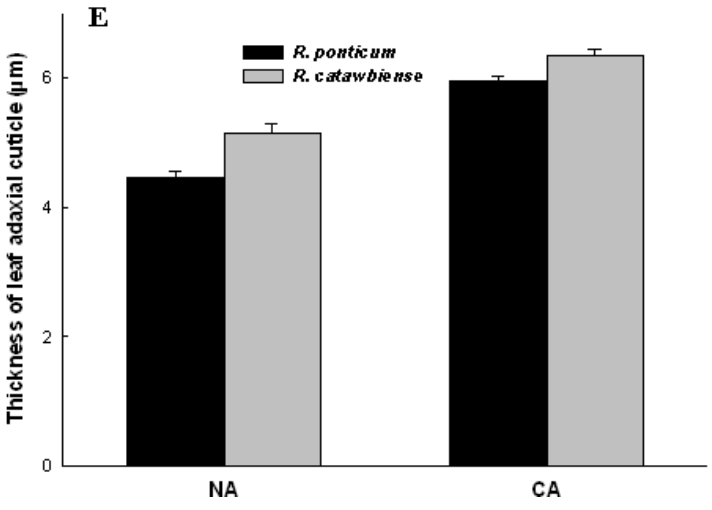
E
R. ponticum
R. catawbiense
Thickness of leaf adaxial cuticle (μm)
0
2
4
6
NA
CA

Fig. 5

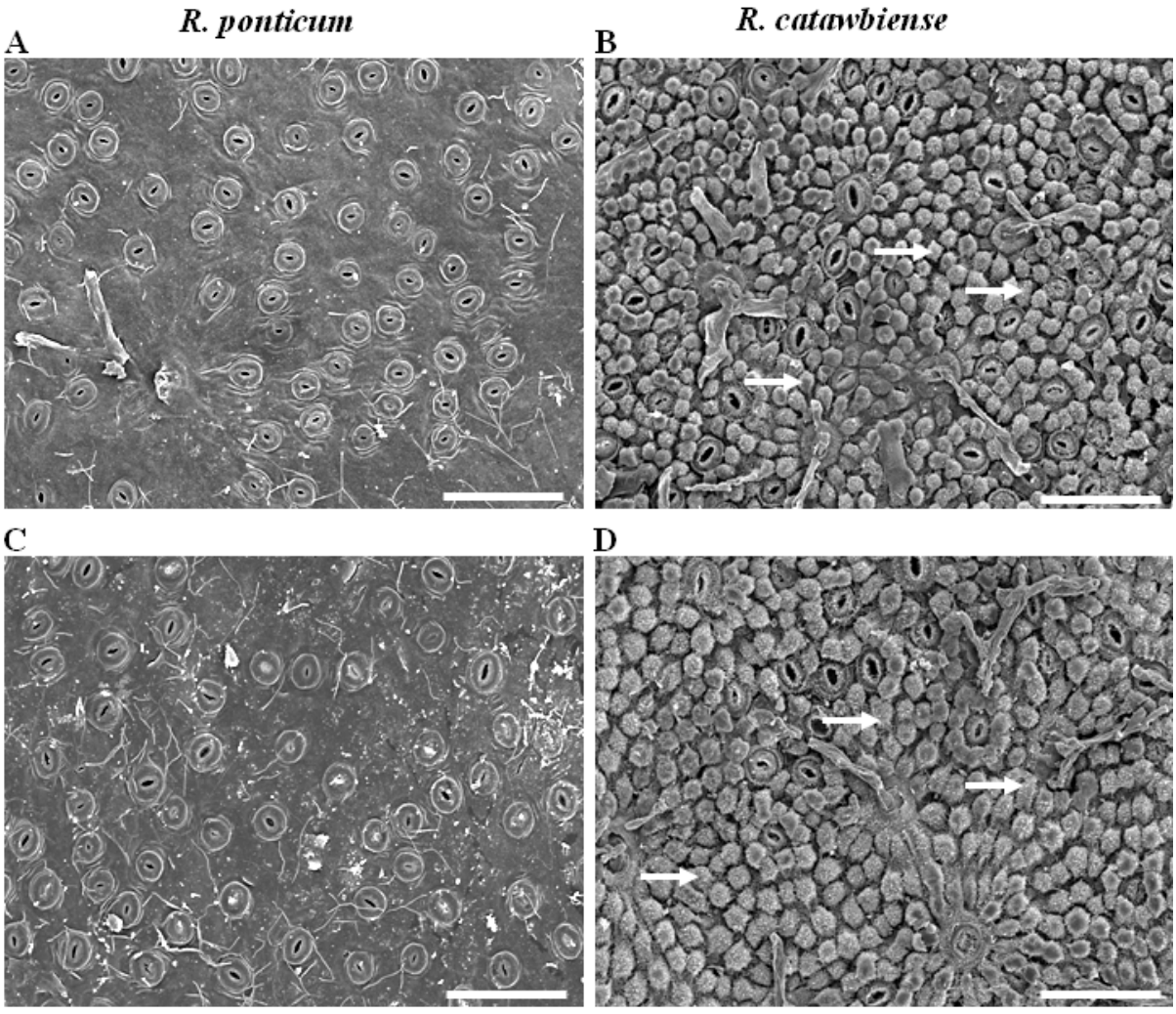
R. ponticum
R. catawbiense
A
B
C
D
E
R. ponticum
R. catawbiense
Stomatal density (stomata/mm2)
400
350
300
250
200
150
100
50
0
NA
CA

Fig. 6

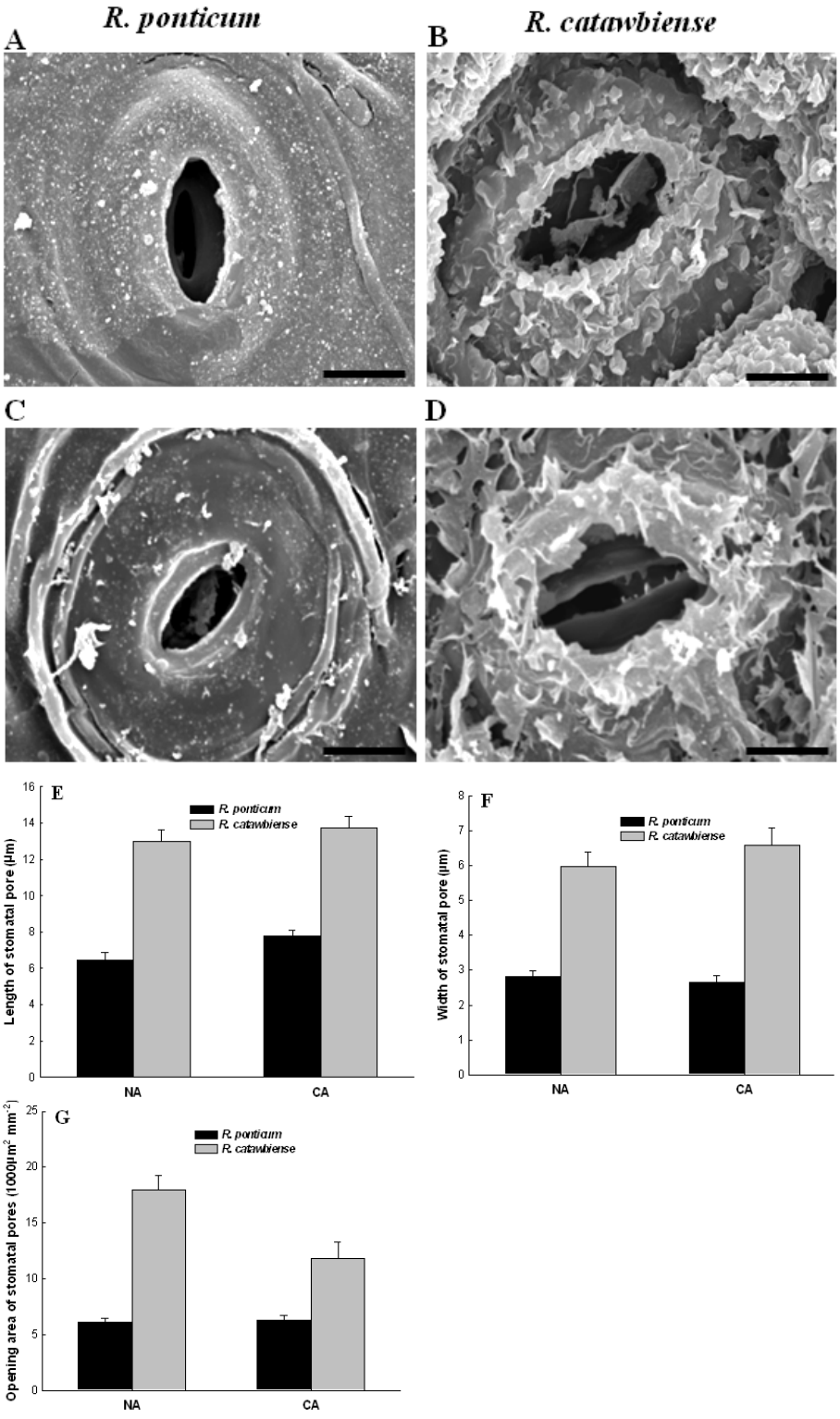
R. ponticum
R. catawbiense
A
B
C
D
E
F
G
R. ponticum
R. catawbiense
Length of stomatal pore (μm)
Width of stomatal pore (μm)
Opening area of stomatal pores (1000μm² mm⁻²)
NA
CA

Fig. 7

CHAPTER 3. SEASONAL CHANGES IN PHOTOSYNTHESIS, ANTIOXIDANT SYSTEMS AND ELIP EXPRESSION IN A THERMONASTIC AND NON-THERMONASTIC RHODODENDRON SPECIES: A COMPARISON OF PHOTOPROTECTIVE STRATEGIES IN OVERWINTERING PLANTS

A paper published in *Plant Science* (2009) **177** (6): 607–617

Xiang Wang [a], Yanhui Peng [a], Jeremy W. Singer [b], Anania Fessehaie [c], Stephen L. Krebs [d], Rajeev Arora [a, *]

[a] *Department of Horticulture, Iowa State University, Ames, IA 50011, USA*

[b] *U.S. Department of Agriculture, Agricultural Research Service, National Soil Tilth Laboratory, Ames, IA 50011, USA*

[c] *Seed Science Center, Iowa State University, Ames, IA 50011, USA*

[d] *The Holden Arboretum, 9500 Sperry Road, Kirtland, OH 44094, USA*

Corresponding author:

Rajeev Arora

Department of Horticulture, Iowa State University

Ames, IA 50011, USA

E-mail: rarora@iastate.edu

Tel: 515-294-0031; Fax: 515-294-0730

ABSTRACT

Leaves of overwintering evergreen rhododendrons are typically exposed to freezing temperatures and high light during winters which can potentially result in photon flux exceeding that required for photochemistry. This excess energy, if not dissipated as heat or fluorescence, may cause photo-oxidative damage to PSII. The goal of this study is to compare the photoprotection strategies during seasonal cold acclimation (CA) in two *Rhododendron* species (*R. catawbiense* Michx. and *R. ponticum* L.) that are divergent in their leaf freezing tolerance and thermonastic behaviour (temperature-induced leaf movement). *R. catawbiense* exhibits thermonasty while *R. ponticum* does not. Differences in leaf freezing tolerance (LT_{50}), photosynthesis, photoinhibition, early light-induced proteins (*ELIPs*) gene expression, and accumulation of antioxidant metabolites and enzymes during seasonal CA were investigated. During seasonal CA, maximum photosynthetic rate (P_{max}) and maximum quantum efficiency of PSII (F_v/F_m) were significantly down-regulated. Compared with *R. catawbiense*, *R. ponticum* showed less photoinhibition and higher accumulation of antioxidant systems while *R. catawbiense* exhibited more efficient up-regulation of *ELIP* expression and antioxidant system. The two species respond differently to winter conditions and have evolved strategies to avoid, reduce and / or tolerate photooxidative stress in winter. These include down-regulation of photosynthesis and up-regulation of *ELIPs* and antioxidant systems, together with specialized leaf anatomy and thermonasty behaviour.

Keywords: Antioxidant system, Cold acclimation, Early light-induced proteins, Photoprotection, *Rhododendron*

Abbreviations: APX, ascorbate peroxidase; CAT, catalase; CA, cold acclimation; ELIP, early light-induced protein; F_v/F_m, maximum quantum efficiency of PSII photochemistry; LSP, light saturation point; LFT, leaf freezing tolerance; MDA, malondialdehyde; NA, non-acclimation; PAR, photosynthetically active radiation; P_{max}, maximum photosynthetic rate; Pn, net photosynthetic rate; PCR, polymerase chain reaction; POD, peroxidise; PPFD, photosynthetic photon flux density; PSII, photosystem II; ROS, reactive oxygen species; RT, reverse transcriptase; SOD, superoxide dismutase; AsA, ascorbate acid; GSH, glutathione

1. Introduction

Temperate-zone woody perennials typically experience substantial drops in average monthly minimum air temperatures ranging from ~ 20–30°C in the summer to several degrees <0°C in the winter, which they can survive by a process called cold acclimation (CA). This process greatly increases plant freezing tolerance in response to shortening photoperiod, low non–freezing, and then subfreezing temperatures sequentially through early fall and winter [1, 2]. CA involves changes in gene expression as well as many cellular processes that result in modified metabolic and biosynthetic pathways and storage patterns enabling tissues to survive cold /freezing conditions [3–6]. Broad-leaved, evergreen rhododendrons are important woody landscape plants. They belong to genus *Rhododendron* that comprises ~ 1000 species with a wide distribution throughout the world, stretching from marginally freeze-tolerant species of Southeast Asia to ‘super-hardy’ ones inhabiting North America and circumpolar regions of Scandinavia [7].

Sunlight is the driving force for photosynthesis, and the balance between light absorption and utilization is important for plant’s normal life. Cold temperatures during

winter can inhibit the enzymatic reactions of photosynthesis, while they do not affect the light absorption ability of overwintering evergreens. This can potentially result in photon flux in excess of that required for photosynthetic evolution of O_2 (PSII reaction centers) or assimilation of CO_2 [8]. This excess energy, if not dissipated as heat or fluorescence, may cause inhibition of PSII reaction centers (photoinhibition) [4].

Photoinhibition in evergreen leaves can be brought about by oxidative damage to PSII by reactive oxygen species (ROS) [9]. ROS, such as $^1O_2$, H_2O_2, O_2^-, and $HO^{\cdot}$, are toxic molecules that can cause oxidative damage to proteins, DNA, and lipids [10, 11]. As understory evergreens in deciduous forests or grown in the open, rhododendron leaves are commonly exposed to a combination of freezing temperatures and high irradiance in their natural habitats in winter. Previous work in our lab indicated that down-regulation of photosynthetic metabolism in overwintering leaves of *R. catawbiense* [12] could potentially render these plants vulnerable to photoinhibition.

Higher plants have, supposedly, evolved several mechanisms to avoid photoinhibition, such as activation of antioxidant system, up-regulation of early-light-induced (ELIP) proteins, and xanthophyll-cycle-dependent heat energy dissipation, among others [13–17]. Leaf antioxidant systems can prevent or alleviate the damage caused by ROS under stress conditions, and include enzymes such as superoxide dismutase (SOD), catalase (CAT), peroxidase (POD), ascorbate peroxidase (APX), and metabolites including ascorbic acid (AsA) and glutathione (GSH) [16, 18, 19].

ELIPs are nuclear–encoded, light stress induced proteins located in thylakoid membranes and belong to the chlorophyll *a/b*-binding protein family with a wide distribution among plant species [20]. It is proposed that ELIPs may transiently bind the released

chlorophylls under high light stress and prevent the formation of free radicals and/or function in energy dissipation [20, 21]. ELIP accumulation, therefore, may constitute an adaptive response to winter conditions (cold and high light) in evergreens and play a key role in the protection of photosynthetic apparatus from excess light.

Leaves of many evergreen *Rhododendron* species exhibit thermonasty - leaf drooping and curling phenomenon induced by freezing temperatures [22]. Several theories have been proposed for adaptive benefit of thermonasty in rhododendrons [23]. Nilsen's group has been pursuing a hypothesis that thermonasty reduces leaf exposure to light during freezing conditions in the winter allowing optimization of the effectiveness of antioxidant and xanthophyll cycle systems in preventing photooxidative stress [23–25]. Interestingly, however, some large leaf rhododendrons do not exhibit leaf curling but undergo only marginal drooping during cold winters. But a comparison of photoprotective strategies in overwintering leaves of thermonastic and non-thermonastic *Rhododendron* species has not been addressed before.

In this study, two *Rhododendron* species (*R. catawbiense* and *R. ponticum*) that are highly divergent in their leaf freezing tolerance (super hardy *vs* less-hardy, respectively) and thermonastic behaviour (former shows typical thermonasty while the latter exhibits no curling but marginal drooping; Fig. 1) were used to characterize their photosynthesis and photoinhibition, photoprotection responses, such as changes in antioxidant systems and ELIPs expression, during seasonal CA; due to their above mentioned differences in leaf movement behaviour, we have categorized *R. catawbience* and *R. ponticum* as thermonastic and non-thermonastic species, respectively. Our overall objective is to gain insight into how photosynthetic behaviour and specific photoprotective strategies together with the

thermonasty (or lack thereof) and leaf anatomical characteristics (previously studied in our lab [26]) might explain the mechanisms employed by these two species to tolerate/avoid high irradiance under low temperatures during winter.

2. Materials and methods

2.1. Plant material and growth conditions

Plants from two *Rhododendron* species (*R. catawbiense* Michx. 'Catalgla' and *R. ponticum* L. 'RSBG 76/411'; RSBG is Rhododendron Species Foundation and Botanical Garden) were vegetatively propagated (semi–hardwood cuttings) and grown in the 19–L plastic pots at the David G. Leach Research Station of Holden Arboretum (Kirtland, OH, USA). About 2–year–old containerized plants were brought to the Department of Horticulture at Iowa State University (ISU) in Ames, IA, USA and maintained outdoors to be acclimated naturally from August to December 2007. All plants were grown in Fafard mix 52 (Conrad Fafard, Inc., Agawam, MA, USA) [pine bark (60%); peat, perlite and vermiculite (40%)] outside the ISU Horticulture greenhouse (latitude 42° 1' N, longitude 93° 38' W). The granular slow-release fertilizer (5% N, 2% P, 2% K, 2% Ca, 2% S, and 2% Fe; Sustâne/Natural Fertilizer of America, Inc., Cannon Falls, MN, USA) was applied to the medium surface every three weeks during the growth season from May to August 2007. Plants were watered as needed throughout the experiment.

Minimum daily air temperatures at the experiment site were recorded (Fig. 2A) from 15 August to 30 December 2007. Average daily minimum air temperatures for each of the months from August to December 2007 at this location were 16.9, 11.1, 7.7, –2.8 and –10.8°C, respectively. In the months of August, September, and late October, the air

temperature only dropped below the freezing point on one occasion. After October, the days with minimum air temperatures dropping below freezing temperatures increased dramatically. Plants were partly shaded by placing the pots randomly in the understory of a bald-cypress tree (*Taxodium distichum* L.). Diurnal changes of photosynthetically active radiation (PAR) at the surface of the uppermost leaves of the two species were monitored every two weeks on sunny days from 4 October to 25 November 2007 (Fig. 2B). Diurnal PAR ranged from ~75 μmol m^{-2} s^{-1} (0800 h) to ~1300 μmol m^{-2} s^{-1} (1400 h) with a daily average of ~ 350 μmol m^{-2} s^{-1}. All plants were watered as needed with tap water throughout the experiment.

Fully expanded leaves from the current year growth (several leaves from each of the three plants per species) were collected on sunny mornings (~ 0900 h) of each sampling date from August to December 2007 and frozen at –80ºC to be used for the analysis of chlorophyll content, malondialdehyde (MDA) content, antioxidant enzymes, antioxidant metabolites and seasonal expression profiles of ELIPs.

2.2. Leaf freezing tolerance (LFT) tests

Fully expanded leaves from the current year growth were collected to conduct LFT tests approximately every month from 15 August to 6 December 2007. Three leaves were collected from three separate plants (one leaf/plant/species). Leaf discs (diameter = 1.27 cm) were punched from the middle of the lamina (excluding the mid–vein) and one disc/leaf/plant was treated as a replication; three replications were prepared for each treatment temperature. Punched leaf discs were exposed to controlled freeze–thaw regimes followed by the assessment of injury by measuring electrolyte leakage from freeze–thaw injured tissues as

described in [27]. Tissue freezing was performed in a temperature–controlled glycol bath (Isotemp 3028; Fisher Scientific, Pittsburgh, PA, USA) from August to October or in a programmable freezer (Model 85–3.1; ScienTemp, Adrian, MI, USA) from November to December according to the detailed procedures described in [26]. LFT was defined by LT_{50}, the temperature at which 50% injury occurred and was calculated as described in [27].

2.3. Gas exchange measurements

Gas exchange was determined with a portable open gas exchange system (LI–6400; LI–COR Inc., Lincoln, NE, USA) from 20 September to 25 November 2007. In–chamber photosynthetic photon flux density (PPFD) was controlled using a 20 × 30 mm^2 leaf chamber with a light source (red + blue 6400–02B, LI–COR Inc.). Air was supplied at 500 µmol s^{-1} and the reference relative humidity was maintained at 40% for all measurements. Carbon dioxide concentration was set at 360 µl l^{-1}. P_{max} was measured at saturated PPFD (1500 µmol m^{-2} s^{-1}) on fully expanded leaves from the current year growth and all measurements were made during 1000 h to 1200 h at ambient temperatures on sunny days. Three plants from each species were chosen, and three to five fully expanded leaves from each plant per species were used to make the measurements. Hence each P_{max} data point is an average of 9 to 15 measurements per species at each sampling date.

Net photosynthesis rates (Pn) on 20 September and 25 November 2007 were measured at the same CO_2 concentration, air flow rates, and relative humidity conditions as described above except for the light intensities that ranged from 0 to 2000 µmol m^{-2} s^{-1} and 0 to 1200 µmol m^{-2} s^{-1}, respectively. Advanced regression analysis of the nonlinear curve between P_n and light intensity was fitted into an exponential function: $Pn = a\,(1 - e^{-bx}) + C$,

in which *x* is irradiance, *Pn* is net photosynthetic rate, *a* is P_{max}, *b* is apparent quantum efficiency of photosynthesis, and C is dark respiration [28]. Light saturation point (LSP) was estimated as the light level at 90% of P_{max} [29].

2.4. Chlorophyll fluorescence measurements

Modulated chlorophyll fluorescence was measured on sunny days each month with a fluorometer (PAM–2000; Walz, Effetrich, Germany) and analyzed by Data Acquisition Software DA–2000 (Walz). Intact leaves were dark–adapted with leaf clips for 30 min to measure the maximal quantum yield of photosystem II (F_v/F_m) at 1 s saturating pulse of 5000 μmol m^{-2} s^{-1}**)** according to [30]. The degree of photoinhibition was determined by the reduction in the value for F_v/F_m parameter. Seasonal data were collected on sunny mornings (1000 to 1100 h) each month. The diurnal changes in F_v/F_m were measured the same way as shown above from 0800 to 1800 on 27 August and 25 September. Three leaves from three different plants were used for all measurements (one leaf from each of the three plants per species).

2.5. Determination of chlorophyll content

For total chlorophyll content, 0.2 g frozen leaf sample was ground into fine powder. Five ml buffered 80% aqueous acetone was added to the powder, and chlorophyll concentrations were determined spectrophotometrically as described in [31].

2.6. RcELIPs expression profiles using real–time RT–PCR

In a previous study we noted that ESTs (expressed sequence tags) encoding ELIPs constituted the most abundant class of 400 ESTs (at ~10%) that were randomly identified from a cDNA library prepared from cold acclimated / winter-collected leaves of *R. catawbiense* while no ELIP cDNA was picked from the non-acclimated EST library of approximately equal size [12]. Recently, Peng et al. (2008) [32] further classified these 40 ESTs into seven unique *ELIP* genes, and named them *RcELIP1-7.* To determine the seasonal expression profiles of seven *RcELIPs* in the present study, leaf tissues were collected at approximately monthly intervals from August to December 2007 from the same *R. catawbiense* and *R. ponticum* plants that were used for LFT and photochemistry measurements and antioxidant analysis. Total leaf RNA was extracted according to the modified hot–borate method [33]. The RNA concentration and quality was determined by spectrophotometry, and its integrity was assessed by electrophoresis in 1% (w/v) formaldehyde agarose gels [34]. The residual genomic DNA in the extract was removed by several treatments with RNase–free DNase I (Invitrogen, Carlsbad, CA, USA). First–strand cDNA was synthesized using approximately 2 μg of total RNA, 1 μg Oligo$(dT)_{18}$ and M–MLV reverse transcriptase, according to the manufacturer's instructions (Fisher Scientific, Pittsburgh, PA, USA). The cDNAs were diluted to 100 μl with sterile water of which 2 μl was used for each real–time RT–PCR sample.

Real–time RT–PCR was carried out in a real–time PCR system (7900HT, ABI, Foster City, CA, USA) using real–time PCR Power Mix Kit (SYBR Green I as fluorescent dye, ABI). The reaction mixture (25 μl) contained 2 μl of first-strand cDNA, 0.3 μM of each of the forward and reverse primers and appropriate amounts of other components as recommended by the manufacturer (ABI). PCR conditions and the sequence of primers used

to amplify seven *RcELIPs* and housekeeping genes were as described in [32]. Real–time RT–PCR was carried out with three analytical replications.

2.7. MDA assay

MDA is the ultimate product of membrane lipid peroxidation, and its content is often related to the extent of oxidative damage caused by ROS [35]. Leaf MDA content from the two species was assayed according to the procedure described in [36]. Leaf sample (0.4 g frozen tissue) was ground in a pre–chilled mortar and homogenized with 5 ml of 80% cold ethanol. MDA concentration was expressed as nmol MDA per gram of fresh weight.

2.8. Extraction and assay of antioxidant metabolites

Total ascorbate (tAsA) was extracted according to [37]. Frozen leaf tissue (250 mg) was ground in a pre–chilled mortar with 5 ml of a 6% (w/v) trichloroacetic acid (TCA). The extract was then centrifuged at 4000 g for 45 min at 4°C and the supernatant was collected for analysis. The supernatant was adjusted to pH 7.0 with enough 150 mM sodium phosphate buffer (pH 7.4), combined with 10 mM dithiothreitol, and incubated at room temperature in the dark for 1 h. Samples were mixed with a solution containing 10% (w/v) TCA, 44% H_3PO_4 (v/v), 4% bipyridyl (w/v) in 70% ethanol (v/v) and 3% $FeCl_3$ (w/v) and after incubation at 37°C for 1 h, the absorbance at 525 nm was recorded. The concentration of total ascorbate was estimated using a standard calibration curve with pure ascorbate.

Total glutathione (tGSH) was extracted according to the procedure described in [38]. A 0.5 g of frozen leaf tissue was ground in a pre–chilled mortar with 5 ml of 5% (w/v) cold meta–phosphoric acid. The extract was centrifuged at 4000 g for 30 min at 4°C to pellet

debris and supernatant was neutralized with 0.5 M sodium phosphate buffer (pH 7.5) and collected for analysis. Total glutathione was measured in 1 ml reaction mixture containing 125 mM sodium phosphate buffer (pH 7.5), 6.3 mM EDTA, 6 mM DTNB, 0.3 mM NADPH, and 200 µl supernatant. Reaction was initiated by adding 1 unit of pure glutathione reductase to the reaction mixture and absorbance changes were monitored every 20 seconds at 412 nm. Total glutathione content was estimated by interpolating slope values in a calibration curve performed with pure standards.

2.9. Extraction and assay of antioxidant enzymes

Extracts for the determination of antioxidant enzymes activity were prepared according to [39]. Frozen leaf sample (0.3g) was ground with 6 ml of 100 mM sodium phosphate buffer (pH 7.5), containing 0.5 mM EDTA, 2% polyvinylpyrrolidone (PVP–40) and 0.3% Triton X–100, with the addition of 1 mM ascorbate in the case of APX assay. The homogenates were centrifuged at 12,000 g for 20 min at 4°C and the supernatants were collected as enzyme extracts for the following assays.

SOD (EC 1.15.1.1) activity was estimated by recording the decrease in the absorbance of nitroblue tetrazolium (NBT) dye by the enzyme at 560 nm [40]. Three milliliters of the reaction mixture consisted of 50 mM sodium phosphate buffer (pH 7.8), 13 mM methionine, 75 µM NBT, 20 µM riboflavin, 10 µM EDTA and 100 µl enzyme extract. One unit SOD activity was defined as the amount of enzyme required to cause 50% inhibition of the reduction of NBT.

CAT (EC 1.11.1.6) activity was determined [39] every 1 min by monitoring the decrease in absorbance at 240 nm due to decomposition of H_2O_2 in 1 ml reaction mixture

containing 50 mM sodium phosphate buffer (pH 7.0), 1 mM H_2O_2 and 10 µl enzyme extract. The reaction was initiated by adding H_2O_2.

APX (EC 1.11.1.11) activity was determined by monitoring the rate of drop in absorbance (per min) at 290 nm as a result of ascorbate oxidation [41]. One ml reaction mixture contained 50 mM sodium phosphate buffer (pH 7.4), 0.3 mM ascorbate, 0.06 mM EDTA, and 5 µl enzyme extracts and 0.2 mM H_2O_2 which was added to initiate the reaction.

POD (EC 1.11.1.7) activity was based on the determination of guaiacol oxidation at 470 nm by H_2O_2 according to [39]. The 1 ml reaction mixture contained 100 mM sodium phosphate buffer (pH 7.0), 20 mM guaiacol, 12 mM H_2O_2, and 50 µl enzyme extract.

2.10. Statistical analysis

Data were presented as mean ± standard errors. Differences among species and months / sampling time were analyzed with two-way ANOVA, and means were compared by the least significant difference (LSD) test. Means were considered to be different when $P \leq 0.05$. Statistical analysis was done with SPSS 11.0 for Windows statistical software package.

3. Results

3.1. Seasonal changes in LFT

LFT in both species increased seasonally as average minimum air temperatures dropped from August to December 2007 (Fig. 2 and Table 1). LT_{50} of *R. ponticum* decreased from – 4.8°C (August) to a maximum of –16.1°C (December), while that of *R. catawbiense* decreased from –7.1°C (August) to a maximum of –33.6°C (December). There was ~ 50%

gain in the LT_{50} between August and October for the two species while both exhibited ≥ 2-3 fold gain in LT_{50} between October and December sampling period.

3.2. Light saturation point (LSP), maximum photosynthesis (P_{max}) and chlorophyll fluorescence (F_v/F_m)

Light response curves for the two species were established on 20 September and 25 November 2007 (Fig. 3A, B). Essentially, there was no difference in LSP between the two species for September sampling (~1500 μmol $m^{-2}s^{-1}$) (Fig. 3A), however, in late November, it was much lower for *R. catawbiense* (~ 200 μmol $m^{-2}s^{-1}$) compared to *R. ponticum* (~ 600 μmol $m^{-2}s^{-1}$) (Fig. 3B). Thus LSP for September leaves was 2.5-fold and 7.5-fold higher than the November samples for *R. ponticum* and *R. catawbiense*, respectively.

Seasonal P_{max} (Fig. 3C) was measured at 1500 μmol m^{-2} s^{-1}; light response curves indicated that this saturated PPFD did not cause apparent decline in P_{max} even in November (data not shown) and produced similar photosynthetic response as 1200 μmol m^{-2} s^{-1} (Fig. 3B). P_{max} decreased during cold acclimation in both species (Fig. 3C) with a 33% and 80% reduction for *R. ponticum* and *R. catawbiense*, respectively, between September and November. *R. catawbiense* leaves exhibited significantly lower P_{max} than *R. ponticum* throughout the sampling period dropping to its lowest in late November when it was only ~ 25% of that of *R. ponticum*.

Diurnal and seasonal changes in F_v/F_m between the two species are shown in Fig. 4. Diurnal data indicated that *R. catawbiense* leaves were significantly more photoinhibited (smaller values of F_v/F_m) than *R. ponticum* in both NA (Fig. 4A) and CA (Fig. 4B) plants, particularly when the irradiance was greatest (Fig. 2B) at 1200 or 1400 h. Seasonal data (Fig.

4C) indicated no significant difference in F_v/F_m between the two species from August to October with values close to 0.8. From October onwards F_v/F_m decreased significantly in both species, particularly along with increased frequency of sub-freezing temperatures (Fig. 2A), however, CA leaves of *R. catawbiense* had significantly lower (though by small margin) F_v/F_m than *R. ponticum*.

3.3. Seasonal changes in leaf chlorophyll content

Leaf chlorophyll content decreased in both species from August (non-acclimated state) to December (cold acclimated state) (Fig. 5). *Rhododendron ponticum* had significantly higher chlorophyll content than *R. catawbiense* leaves throughout the course of this study; by ~23% and ~15% in August and December, respectively.

3.4. Relative expression profiles of RcELIPs during seasonal CA

Compared with NA (August–collected) leaves, all seven *RcELIPs* were significantly up-regulated during the seasonal CA in both species (Fig. 6). Generally, *R. ponticum* leaves accumulated more *RcELIPs* in NA state (August and September) while, November and onwards, all *RcELIPs* were significantly more expressed in *R. catawbiense*. To determine whether a general relationship between *RcELIP* expression and CA-induced freezing tolerance existed, Δ*RcELIP* expression (calculated as fold-increase averaged across seven *RcELIPs* at each sampling period compared to the NA /August levels) and ΔLT_{50} (absolute value of the difference between LT_{50} in August and other months) were calculated (Table 1). While relatively smaller increase in *RcELIPs* expression (~ 2–fold and ~ 4–fold in *R. ponticum* and *R. catawbiense,* respectively) occurred from August to October, significantly

greater increases occurred from October onwards peaking in December when it was ~ 11–fold and ~ 48–fold for *R. ponticum* and *R. catawbiense*, respectively (Table 1). These relative changes in ELIP expression paralleled similar relative increases in LT_{50} (Table 1), i.e. smaller changes between August to October followed by significantly greater increment from October onwards. Regression performed using Δ*RcELIP* expression and ΔLT_{50} values from Table 1 indicated strong positive correlation ($R^2 = 0.90$) and a regression slope for *R. catawbiense* to be about twice that for *R. ponticum* (Fig. 7).

3.5. Seasonal changes in MDA content and antioxidant metabolites / enzymes

Seasonal changes in the MDA content and antioxidant metabolites of the two species during seasonal CA are shown in Fig. 8. MDA content increased in both species from August (NA state) to December (CA state) (Fig. 8A). Whereas, in general, *R. ponticum* maintained a relatively higher level of leaf MDA throughout the sampling period, the relative increase from August to December in *R. ponticum* was ~61% compared to ~200% for *R. catawbiense* indicating a substantially higher lipid-peroxidation in the latter.

Data indicated that tAsA and tGSH accumulated during seasonal CA in both species (Fig 8B, C). While *R. ponticum* accumulated overall higher amount of tAsA and tGSH throughout the season, degree of this increase in CA leaves relative to NA (August–collected) tissues was higher in *R. catawbiense* than *R. ponticum* (~100% *versus* ~ 30% for tAsA (Fig. 8B) and ~11–fold *versus* ~10 fold for tGSH content (Fig. 8C).

Data for four antioxidant enzymes' activities are shown in Fig. 9, which indicate a general increase in activity of all enzymes during CA. *Rhododendron ponticum* showed overall higher activities than *R. catawbiense* for all but APX which was similar in both

species. SOD and APX activities in CA tissues were similar as NA leaves in both species (Fig. 9A, B) while CAT activity increased 2.7–fold and 3.6–fold in *R. ponticum* and *R. catawbiense*, respectively (Fig. 9C). Only POD activity increased more in *R. ponticum* (~3.2–fold) than in *R. catawbiense* (~1.6–fold) during seasonal CA, respectively (Fig. 9D).

4. Discussion

4.1. Leaf freezing tolerance (LFT)

Both species exhibited increase in LFT from August to December, and the thermonastic species (*R. catawbiense*) was significantly more freeze-tolerant than non-thermonastic *R. ponticum* (Table 1). Research on the relationship between LFT and thermonastic leaf movements in *Rhododendron* suggests a significantly positive association between the degree of leaf curling and magnitude of cold tolerance [42]. Our results are consistent with this observation. Differences in freezing tolerance of the two species may be a consequence of their geographical distribution; less hardy *R. ponticum* is native to central Asia and Europe (Turkey, Georgia, Armenia, Lebanon, Spain, Portugal, Bulgaria) with relatively warmer winters than eastern United States (Mountains in North Carolina and Virginia), the native range of *R. catawbiense.*

4.2. Seasonal photoinhibition

Photoinhibition is frequently determined by chlorophyll fluorescence or gas exchange measurements. While reduction in F_v/F_m parameter indicates compromised PSII efficiency [43], decrease in the maximum photosynthetic rates (P_{max}) has also been used as an indication of photoinhibtion [4]. Our data indicated that P_{max}, F_v/F_m, and chlorophyll content for both

species significantly decreased during seasonal CA (Fig. 3C, Fig. 4C and Fig. 5), suggesting that as the temperatures decreased through fall and winter (Fig. 2A) the leaves became progressively less efficient at processing the incident photon flux. Earlier reports have observed similar seasonal photoinhibition in *R. catawbiense* and *R. maximum* [25, 44] and other understory evergreens [45, 46]. Recent studies in subalpine fir (*Abies lasiocarpa*), lodgepole pine (*Pinus contorta*), and bearberry (*Arctostaphylos uva-ursi*) [47, 48] also showed a significant winter down-regulation of photosynthetic capacity and loss of PSII efficiency compared with summer–collected leaves. Harris et al. 2006 [44] noted a relatively greater reduction in F_v/F_m from October (~0.8) to November (~0.5) for *R. catawbiense* leaves than that observed in the present study (from 0.78 to 0.63) during a similar interval. Such difference may be attributed to the differences in age of plants used in the two studies and the environment (light, temperature) to which the plants were exposed; Harris et al. (2006) used ~50 year-old field plants grown as understory of *Acer rubrum* while we used ~2 year-old potted clones located at an experimental site which was only partially shaded with mid-day irradiance typically reaching up to ~1300 μmol m^{-2} s^{-1}; light saturation point (LSP) of ~ 1500 μmol m^{-2} s^{-1} in September (Fig. 3A) indicates higher light availability and light-utilization efficiency of plants used in our study.

Photoinhibition is typically associated with, but not necessarily accompanied by chlorophyll degradation and a reduction of P_{max} [49]. Consistent with this view, our data showed a general decrease of total chlorophyll content in the two species (Fig. 5) as well as photoinhibition during seasonal CA (Fig. 3C and Fig. 4C). Moreover, a significantly lower LSP for November 25 samples of *R. catawbiense* leaves (compared to *R. ponticum*) (Fig. 3B)

may, in part, be associated with relatively lower leaf chlorophyll content of *R. catawbiense* (Fig 5).

Greater photoinhibition in *R. catawbiense* [indicated by smaller P_{max} , much more so during winter, (Fig. 3C) and lower F_v/F_m (Fig. 4C)] in late November compared to the *R. ponticum* suggest a higher sensitivity of *R. catawbiense* leaves to incident light during winter. These observations together with a significantly greater decrease in LSP of *R. catawbiense* leaves during winter (1500 to 200 *vs* to 600 μmol m^{-2} s^{-1}; Fig. 3B) suggest *R. catawbiense* leaves are more likely to experience 'excess' photon-flux and, therefore, may need 'greater' arsenal of mechanisms to reduce light stress in winter; these mechanisms may include robust protection of chlorophyll from excess light, efficient antioxidant system and/or avoidance of excess light via thermonasty.

The light response curves of *R. ponticum* and *R. catawbiense* in November (Fig. 3B) mimic a typical response from 'sun' and 'shade' leaves, respectively, and may be associated with differences in their leaf anatomies. Our recent study of comparative leaf anatomy using these two species [26] noted that *R. ponticum* leaves showed some characters of 'sun' leaves such as thicker leaf lamina, higher stomatal density and two layers of upper epidermis, whereas, *R. catawbiense* leaves had one layer of upper epidermis.

One of the reasons for the reduction in PSII photochemical efficiency in higher plants is believed to be the employment of xanthophyll cycle in a photoprotective process whereby plants convert violaxanthin (V) into zeaxanthin (Z) and antheraxanthin (A) under excess light [9, 50]. Although not measured in our study, the total amount of the xanthophyll cycle pigments, especially (Z+A)/(V+Z+A), has been shown to increase in some evergreens (Douglas fir and ponderosa pine) during the winter months [51]. A recent study in *R.*

catawbiense also revealed up-regulation of leaf xanthophyll pool in winter acclimated plants compared to summer-collected leaves, suggesting a photoprotective role for these pigments [45].

4.3. RcELIP expression and photoprotection

ELIPs belong to a multigene family of proteins that are structurally related to the Light Harvesting Complexes (LHCs) and are speculated to function as pigment carrier or chlorophyll exchange proteins to protect chloroplasts from high light stress [20, 52]. In support of their photoprotective role, an *Arabidopsis* mutant defective in targeting ELIPs to thylakoids was found to be sensitive to photo-oxidation while over-expression of *ELIPs* enhanced its light-tolerance [15]. A previous study in our lab showed that cDNAs encoding *ELIP* homologs were the most abundant class in an EST library generated from winter-collected leaf tissues of *R. catawbiense* [12]. Recent studies, reporting ELIP proteins in several overwintering evergreens – subalpine firs and lodgepole pines [47] and bearberry [48], showed no accumulation of ELIPs in the summer-collected leaves but their distinct abundance in the winter-collected samples. Collectively, these studies suggest that one possible mechanism by which overwintering evergreens might prevent photooxidative damage during winter is via accumulating ELIPs. Consistent with this hypothesis, we noted a significant up-regulation of seven *RcELIPs* genes from August to December in both *Rhododendron* species (Fig. 6) at transcriptional level. Further investigation of the seasonal profiles at the protein level should be beneficial to uncover the possible role of RcELIPs in these two species. Moreover, a strong positive correlation between the degree of cold acclimation ability and corresponding increment in ELIP accumulation in the two species

divergent in their freezing tolerance (Table 1 and Fig. 7) suggests that an enhanced ability of leaves to protect chloroplasts from excess light may be one of the key components of a multi-factorial cold acclimation process in evergreen rhododendrons. The rate of seasonal increase in ELIP transcript abundance (per unit change in LT_{50}) for *R. catawbiense* was twice that for *R. ponticum*, which supports our hypothesis that *R. catawbiense* may need more efficient up-regulation of photo-protection systems than *R. ponticum*. However, other possible functional roles of ELIP up-regulation in conferring freezing tolerance can not be ruled out as *R. catawbiense* is the hardier of the two species.

4.4. Leaf antioxidant systems and photoprotection

Tissue MDA content has been used as an important bio-marker of oxidative stress-induced damage by ROS [35]. Although both species showed seasonal increase in MDA content and thus oxidative stress, a substantially greater increase in the MDA content from August to December for *R. catawbiense* leaves (triple the corresponding increase in *R. ponticum*) (Fig. 8A) suggests greater ROS damage in *R. catawbiense* leaves and is consistent with their likely greater light sensitivity and vulnerability to photo-oxidation.

Increased activity of leaf antioxidant systems in overwintering evergreens is believed to be one of the important components of winter acclimation and associated increased freezing tolerance, presumably due to their ROS scavenging capacity [53–58]. Accordingly, the present study showed that antioxidant metabolites (tAsA and tGSH; Fig. 8B, C) and enzymes (CAT and POD; Fig. 9C, D) were significantly up-regulated during seasonal CA in the two *Rhododendron* species; however, APX activity was only marginally increased (~20%) (Fig. 9B) while SOD activities (Fig. 9A) essentially remained unaltered. Others have

also shown similar little to no seasonal change in SOD and APX activities in overwintering evergreen, *Picea abies* [59] and *Taxus x media* [17]. Therefore, it is conceivable that 'constitutive' activities of SOD and APX were perhaps sufficient for ROS protection in the two rhododendron species under investigation.

Our data indicated an overall higher accumulation of antioxidants (both metabolites and enzymes) in *R. ponticum* than in *R. catawbiense* from August to December (Fig. 8B, C and Fig. 9). With no thermonastic leaf curling and marginal drooping during cold winters, *R. ponticum* leaves are likely more prone to harvest excess photon flux as temperatures drop and, therefore, greater ROS accumulation. However, P_{max} and F_v/F_m data indicated that *R. ponticum* was less photoinhibited than thermonastic *R. catawbiense* (Fig. 3C and Fig. 4C). Whether overall higher levels of antioxidant metabolites and enzymes in *R. ponticum* contributed to relatively lower photoinhibition observed during winter months in this species, is a question that can not be directly addressed in this study, however, our data point towards this possibility. Our data also indicated that the degree of increments (as percent of August levels) in tAsA and tGSH content and the CAT activity from NA to CA state were significantly greater in *R. catawbiense*, (Fig. 8B, C and Fig. 9C), which, again, supports our hypothesis for the need for more efficient up-regulation of antioxidant system in this species during overwintering.

4.5. Thermonasty and photo-protection

Evergreens have evolved several mechanisms to reduce and/or tolerate the excess light that reaches chlorophyll, particularly under winter conditions [9]. One way to achieve the former is to alter the angle or shape of the leaf to minimize the light interception. Leaf

reorientation to a pendant position is characteristic of many evergreens in temperate habits. Many rhododendrons undergo leaf curling in addition to vertical reorientation during the winter [60]. These cold-induced leaf movements (thermonasty) are believed to have an adaptive significance likely related to the combination of high-light and low temperatures [23]. Nilsen's group has shown that *R. maximum* leaves that were restricted from thermonasty (i.e. artificially forced to remain flat) in the winter exhibited lower quantum yield in the spring than those unrestricted (or naturally curled) [24], and that restricted leaves were more photoinhibited throughout the winter and slower to recover photosynthesis and PSII efficiency in spring [25]. Comparative photochemistry of restricted *versus* non-restricted leaves of the thermonastic species, *R. catawbiense* was not conducted in the present study and all gas exchange and chlorophyll fluorescence measurements were made on naturally unrolled leaves. However, *R. catawbiense* was more photoinhibited during fall and winter (Fig. 3 and Fig. 4) than the 'non-thermonastic' *R. ponticum*. Greater photoinhibition of *R. catawbiense* leaves may be related to their significantly lower LSP (by ~67%), and suggests that photoprotective mechanisms in *R. catawbiense* (in spite of an additional, presumably, beneficial feature, i.e. thermonasty) were not as effective in reducing photoinhibition as those in *R. ponticum*. It is noteworthy, however, that factors other than ELIPs, antioxidants and thermonasty, such as leaf anatomy, might also be involved in plant's response to excess light.

In conclusion, the two species respond differently to winter conditions and have evolved various strategies to reduce and / or tolerate photooxidative stress in winter. Both species have some common strategies including, accumulation of ELIPs and antioxidant systems. Whereas *R. ponticum* accumulates overall higher antioxidant metabolites and

enzymes, *R. catawbiense* employs more efficient up-regulation of ELIPs and antioxidant systems; the latter also exhibits thermonastic leaf movements. Both species undergo photoinhibition during winter with *R. ponticum* leaves being relatively less photoinhibited. Such difference may be related to differential sensitivity to excess light in winter and protection efficiencies of ELIPs and antioxidants in the two specie, among other adaptations. Although, thermonasty did not seem to provide a clear added advantage to *R. catawbiense* vis-à-vis resistance to photoinhibition (when compared to *R. ponticum*), its adaptive significance in photoprotection for *R. catawbiense* can not be ruled out. The differences in photoinhibition may also be associated with leaf anatomies in the two species. The additional layer of upper epidermis in *R. ponticum*, and extra palisade layer and waxy cuticle in *R. catawbiense* [26] might represent leaf structural adaptations for reducing light injury in winter in these species, and together with ELIPs, antioxidant system and thermonasty constitute photoprotection system in rhododendrons.

Acknowledgements

This journal paper of the Iowa Agriculture and Home Economics Experiment Station, Ames, Iowa (Project 3601) was supported by Hatch Act and State of Iowa funds. We thank Dr. Allen D. Knapp and Ms. Maria M. Hartt (Department of Agronomy, Iowa State University) for providing the fluorometer and technical assistance with F_v/F_m measurements. We also thank Arlen Patrick (greenhouse manager, Department of Horticulture, ISU) for assisting with plant care throughout this study.

References

[1] Sakai, W. Larcher, Frost survival of plants: responses and adaptation to freezing stress, Springer, New York, 1987.

[2] C.J. Weiser, Cold resistance and injury in woody plants, Science 169 (1970) 1269–1278.

[3] C.L. Guy, Cold acclimation and freezing stress tolerance: role of protein metabolism, Annu. Rev. Plant Physiol. Plant Mol. Biol. 41 (1990) 187–223.

[4] G. Öquist, N.P.A. Huner, Photosynthesis of overwintering evergreen plants, Annu. Rev. Plant Biol. 54 (2003) 329–355.

[5] M.F. Thomashow, Plant cold acclimation: freezing tolerance genes and regulatory mechanisms, Annu. Rev. Plant Physiol. Plant Mol. Biol. 50 (1999) 571–599.

[6] Z. Xin, J. Browse, Cold comfort farm: the acclimation of plants to freezing temperatures, Plant Cell Environ. 23 (2000) 893–902.

[7] A. Sakai, L. Fuchigami, C.J. Weiser, Cold hardiness in the genus *Rhododendron*, J. Amer. Soc. Hort. Sci. 111 (1986) 273–280.

[8] W.G. Hopkins, N.P.A. Huner, Introduction to Plant Physiology, Wiley, New York, 2003.

[9] W.W.III. Adams, C.R. Zarter, V. Ebbert, B. Demmig–Adams, Photoprotective strategies of overwintering evergreens, BioScience 54 (2004) 41–49.

[10] C.H. Foyer, M. Lelandais, K.J. Kunert, Photooxidative stress in plants, Physiol. Plant. 92 (1994) 696–717.

[11] S. Rossini, A.P. Casazza, E.C.M. Engelmann, M. Havaux, R.C. Jennings, C. Soave, Suppression of both ELIP1 and ELIP2 in *Arabidopsis thaliana* does not affect tolerance to photoinhibition and photooxidative stress, Plant Physiol. 141 (2006) 1264–1273.

[12] H. Wei, A.L. Dhanaraj, L.J. Rowland, Y. Fu, S.L. Krebs, R. Arora, Comparative analysis of expressed sequence tags (ESTs) from cold-acclimated and non-acclimated leaves of *Rhododendron catawbiense* Michx., Planta 221 (2005) 406–416.

[13] B. Demmig–Adams, W.W.III. Adams, The xanthophyll cycle, protein turnover, and the high light tolerance of sun-acclimated leaves, Plant Physiol. 103 (1993) 1413–1420.

[14] B. Demmig–Adams, W.W.III. Adams, Photoprotection in an ecological context: the remarkable complexity of thermal dissipation, New Phytol. 172 (2006) 11–21.

[15] C. Hutin, L. Nussaume, N. Moise, I. Moya, K. Kloppstech, M. Havaux, Early light-induced proteins protect *Arabidopsis* from photooxidative stress, Proc. Natl. Acad. Sci. USA 1008 (2003) 4921–4926.

[16] K.K. Niyogi, Photoprotection revisited: genetic and molecular approaches, Annu. Rev. Plant Physiol. Plant Mol. Biol. 50 (1999) 333–359.

[17] A.S. Verhoeven, A. Swanberg, M. Thao, J. Whiteman, Seasonal changes in leaf antioxidant systems and xanthophyll cycle characteristics in *Taxus x media* growing in sun and shade environments, Physiol. Plant. 123 (2005) 428–434.

[18] K. Asada, The water-water cycle in chloroplasts: scavenging of active oxygen and dissipation of excess photons, Annu. Rev. Plant Physiol. Plant Mol. Biol. 50 (1999) 601–639.

[19] P. Xu, Y. Guo, J. Bai, L. Shang, X. Wang, Effects of long-term chilling on ultrastructure and antioxidant activity in leaves of two cucumber cultivars under low light, Physiol. Plant. 32 (2008) 467–478.

[20] I. Adamska, The Elip family of stress proteins in the thylakoid membranes of pro- and eukaryota. In: Aro EM, Andersson B (eds) Advances in photosynthesis and respiration-regulation of photosynthesis, Kluwer Academic Publishers, Dordrecht, The Netherlands, 2001, pp 487–505.

[21] M.H. Montané, K. Kloppstech, The family of light harvesting-related proteins (LHCs, ELIPs, HLIPs): was the harvesting of light their primary function? Gene 258 (2000) 1–8.

[22] E.T. Nilsen, Influence of water relations and temperature on leaf movements of *Rhododendron* species, Plant Physiol. 83 (1987) 607–612.

[23] E.T. Nilsen, Thermonastic leaf movements: a synthesis of research with *Rhododendron*, Bot. J. Linn. Soc. 110 (1992) 205–233.

[24] Y. Bao, E.T. Nilsen, The ecophysiological significance of leaf movements in *Rhododendron maximum* L., Ecology 69 (1988) 1578–1587.

[25] R.B. Russell, T.T. Lei, E.T. Nilsen, Freezing induced leaf movements and their potential implications to early spring carbon gain: *Rhododendron maximum* as exemplar, Funct. Ecol. 23 (2009) 467–471.

[26] X. Wang, R. Arora, H.T. Horner, S.L. Krebs, Structural adaptations in overwintering leaves of thermonastic and non-thermonastic *Rhododendron* species, J. Amer. Soc. Hort. Sci. 133 (2008) 768–776.

[27] C.C. Lim, R. Arora, E.D. Townsend, Comparing Gompertz and Richards functions to estimate freezing injury in *Rhododendron* using electrolyte leakage, J. Amer. Soc. Hort. Sci. 123 (1998) 246–252.

[28] S.C. Thomas, F.A. Bazzaz, Asymptotic height as a predictor of photosynthetic characteristics in Malaysian rain forest trees, Ecology 80 (1999) 1607–1622.

[29] J. C. Watling, M.C. Press, W.P. Quick, Elevated CO_2 induces biochemical and ultrastructural changes in leaves of the C4 cereal sorghum. Plant Physiol. 123 (2000) 1143–1152.

[30] M. Heddad, H. Noren, V. Reiser, M. Dunaeva, B. Andersson, I. Adamska, Differential expression and localization of early light-induced proteins in *Arabidopsis*, Plant Physiol. 142 (2006) 75–87.

[31] R.J. Porra, W.A. Thompson, P.E. Kriedemann, Determination of accurate extinction coefficients and simultaneous equations for assaying chlorophylls *a* and *b* extracted with four different solvents: verification of the concentration of chlorophyll standards by atomic absorption spectroscopy, Biochim. Biophys. Acta 975 (1989) 384–394.

[32] Y. Peng, W. Lin, H. Wei, S.L. Krebs, R. Arora, Phylogenetic analysis and seasonal cold acclimation-associated expression of early light-induced protein genes of *Rhododendron catawbiense*, Physiol. Plant. 132 (2008) 44–52.

[33] T.A. Wilkins, L.B. Smart, Isolation of RNA from plant tissue. In: Krieg PA (ed) A laboratory guide to RNA: isolation, analysis, and synthesis, Wiley, New York, 1996, pp 21–41.

[34] J. Sambrook, E.F. Fritsch, T. Maniatis, Molecular cloning: A laboratory manual, 2nd edn. Cold Spring Harbor Laboratory Press, Plainview, New York, 1989.

[35] K. Asada, T. Endo, J. Mano, C. Miyake, Molecular mechanisms for relaxation of and protection from light stress. In: Satoh K, Murata N (eds) Stress responses of photosynthetic organisms, Elsevier Science BV, Amsterdam, 1998, pp 37–52.

[36] D. Hodges, J. DeLong, C. Forney, R. Prange, Improving the thiobarbituric acid-reactive-substances assay for estimating lipid peroxidation in plant tissues containing anthocyanin and other interfering compounds, Planta 207 (1999) 604–611.

[37] M.Y. Law, S.A. Charles, B. Halliwell, Glutathione and ascorbic acid in spinach (*Spinacia oleracea*) chloroplasts, Biochem. J. 210 (1983) 899–903.

[38] M.E. Anderson, Determination of glutathione and glutathione disulfide in biological samples, Methods Enzymol. 113 (1985) 548–555.

[39] D. Prochazkova, R.K. Sairam, G.C. Srivastava, D.V. Singh, Oxidative stress and antioxidant activity as the basis of senescence in maize leaves, Plant Sci. 161 (2001) 765–771.

[40] R.A. Dhindsa, P. Plumb–Dhindsa, T.A. Thorpe, Leaf senescence: correlated with increased permeability and lipid peroxidation, and decreased levels of superoxide dismutase and catalase, J. Exp. Bot. 126 (1981) 93–101.

[41] Y. Nakano, K. Asada, Hydrogen peroxide is scavenged by ascorbate specific peroxidases in spinach chloroplasts, Plant Cell Physiol. 22 (1981) 867–880.

[42] E.T. Nilsen, A. Tolbert, Does winter leaf curling conifer cold stress tolerance in *Rhododendron*? J. Amer. Rhododendron Soc. 47 (1993) 98–104.

[43] K. Maxwell, G.N. Johnson, Chlorophyll fluorescence – a practical guide, J. Exp. Bot. 51 (2000) 659–668.

[44] G.C. Harris, V. Antoine, M. Chan, D. Nevidomskyte, M. Königer, Seasonal changes in photosynthesis, protein composition and mineral content in *Rhododendron* leaves, Plant Sci. 170 (2006) 314–325.

[45] W. Oberhuber, H. Bauer, Photoinhibition of photosynthesis under natural conditions in ivy (*Hedera helix* L.) growing in an understory of deciduous trees, Planta 185 (1991) 545–553.

[46] A.S. Verhoeven, W.W.III. Adams, B. Demmig-Adams, The xanthophyll cycle and acclimation of *Pinus ponderosa* and *Malva neglecta* to winter stress, Oecol. 118 (1999) 277–287.

[47] C.R. Zarter, W.W.III. Adams, V. Ebbert, D.J. Cuthbertson, I. Adamska, B. Demmig–Adams, Winter down-regulation of intrinsic photosynthetic capacity coupled with up-regulation of Elip-like proteins and persistent energy dissipation in a subalpine forest, New Phytol. 172 (2006) 272–282.

[48] C.R. Zarter, W.W.III. Adams, V. Ebbert, I. Adamska, S. Jansson, B. Demmig–Adams, Winter acclimation of PsbS and related proteins in the evergreen *Arctostaphylos uva-ursi* as influenced by altitude and light environment, Plant Cell Environ. 29 (2006) 869–878.

[49] B. Demmig–Adams, D.L. Moeller, B.A. Logan, W.W.III. Adams, Positive correlation between levels of retained zeaxanthin + antheraxanthin and degree of photoinhibition in shade leaves of *Schefflera arboricola* (Hayata) Merrill., Planta 205 (1998) 367–374.

[50] O. Björkman, B. Demmig–Adams, Regulation of photosynthetic light energy capture, conversion and dissipation in leaves of higher plants. *In* ED Schulze, MM Caldwell

(eds) Ecophysiology of Photosynthesis. Ecological Studies 100, Springer Verlag, Berlin, 1994, pp 1747.

[51] W.W.III. Adams, B. Demmig–Adams, Carotenoid composition and down regulation of photosystem II in three conifer species during the winter, Physiol. Plant. 92 (1994) 451–458.

[52] I. Adamska, ELIPs-light-induced stress proteins, Physiol. Plant. 100 (1997) 794–805.

[53] J.V. Anderson, B.I. Chevone, J.L. Hess, Seasonal variation in the antioxidant system of eastern white pine needles, Plant Physiol. 98 (1992) 501–508.

[54] A.G. Doulis, A. Hausladen, B. Mondy, R.G. Alscher, B.I. Chevone, J.L. Hess, R.L. Weiser, Antioxidant response and winter hardiness in red spruce (*Picea rubens* Sarg.), New Phytol. 123 (1993) 365–374.

[55] B.A. Logan, S.C. Grace, W.W.III. Adams, B. Demmig–Adams, Seasonal differences in xanthophyll cycle characteristics and antioxidants in *Mahonia repens* growing in different light environments, Oecol. 116 (1998) 9–17.

[56] L. Luo, S. Lin, H. Zheng, Y. Lei, Q. Zhang, Z. Zang, The role of antioxidant system in freezing acclimation-induced freezing resistance of *Populus suaveolens* cuttings, Forestry Stud. Chi. 9 (2007) 107–113.

[57] J.C. Pennycooke, S. Cox, C. Stushnoff, Relationship of cold acclimation, total phenolic content and antioxidant capacity with chilling tolerance in petunia (*Petunia* × *hybrida*), Environ. Exp. Bot. 53 (2005) 225–232.

[58] A. Polle, W. Kröniger, H. Rennenberg, Seasonal fluctuations of ascorbate-related enzymes: acute and delayed effects of late frost in spring on antioxidative systems in needles of Norway spruce (*Picea abies* L.), Plant Cell Physiol. 37 (1996) 717–725.

[59] A. Polle, H. Rennenberg, Field studies on Norway spruce trees at high altitudes: II. Defense systems against oxidative stress in needles, New Phytol. 121 (1992) 635–642.

[60] E.T. Nilsen, The relationship between freezing tolerance and thermotropic leaf movement in five *Rhododendron* species. Oecol. 87 (1991) 63–71.

Table 1 Leaf freezing tolerance (LT_{50}), changes in LT_{50} (ΔLT_{50}), and relative expression of *RcELIPs* in *R. ponticum* and *R. catawbiense* during seasonal cold acclimation. LT_{50} is defined as the temperature at which 50% injury occurs. Plants were cold-acclimated outdoors from August to December 2007. Mean monthly minimum air temperatures at the experiment site from August to December were 16.9, 11.1, 7.7, –2.8 and –10.8°C, respectively (see Fig. 2 for details). Values of LT_{50} are presented as mean ± standard errors (n=3).

Sampling date	***R. ponticum***		***R. catawbiense***	
	LT_{50} (ΔLT_{50})[a] (°C)	***RcELIP* expression[b]**	**LT_{50} (ΔLT_{50}) (°C)**	***RcELIP* expression**
15 Aug	–4.8 ± 0.26 (0)	1.0	–7.1 ± 0.28 (0)	1.0
9 Sept	–4.8 ± 0.19 (0)	1.3	–10.5 ± 0.31 (3.4)	1.6
21 Oct	–7.3 ± 0.15 (2.5)	1.9	–10.5 ± 0.63 (3.4)	4.1
8 Nov	–13.8 ± 0.61 (9.0)	5.8	–29.0 ± 1.58 (21.9)	22.2
6 Dec	–16.1 ± 0.69 (11.3)	10.7	–33.6 ± 0.90 (26.5)	48.7

[a]ΔLT_{50} (in parenthesis) are the absolute values of LT_{50} difference between August and other months.

[b]*RcELIP* expression of the two species in each month was calculated relative to their expression in August (taken as 1). The values are based on the average for all seven *RcELIPs* as presented in Fig. 6.

Figure legends

Fig. 1. The photographs showing thermonastic leaf movements and lack thereof in *R. catawbiense* and *R. ponticum*, respectively. A) *R. catawbiense* plant showing thermonasty in winter (December) as marked by red arrows while *R. ponticum* plant showing no leaf curling but marginal drooping; B) Close up of *R. catawbiense* in summer (July); C) Close up of *R. ponticum* in summer; D) Close up of *R. catawbiense* in winter; arrows indicate leaf bending and curling; E) Close up of *R. ponticum* in winter. The pictures (A, D and E) were taken while the ambient temperature was –5°C.

Fig. 2. Daily minimum air temperature (A) and diurnal photosynthetically active radiation (PAR) (B) at the experiment site. Minimum air temperatures were recorded from 15 August to 30 December 2007. PAR, at the surface of the uppermost leaves, was monitored every two weeks from 4 October to 25 November 2007 at every two hours starting from 8000 h to 1800 h. Four measurements were made on clear days at each time period, and PAR at different times of day is plotted as mean ± standard errors. The specific sampling dates (for leaf freezing tolerance, analysis of malondialdehyde and antioxidant systems, and ELIPs expression) are shown with the arrows pointing upwards along the x–axis.

Fig. 3. Light response curves (net photosynthetic rate, Pn as a function of light intensity) (A and B) and maximum photosynthetic rate (P_{max}) (C) for *R. ponticum* and *R. catawbiense*. Pn was measured on 20 September (A) (ambient air temperatures was 22°C), and 25 November (B) (ambient air temperatures was 5°C), respectively. All measurements were made at 360 µl

l^{-1} CO_2 on sunny days. P_{max} was measured at 1500 μmol m^{-2} s^{-1} and the data are presented as mean ± standard errors of 9 to 15 measurements (three measurements for one leaf; three to five leaves from each of three plants per species).

Fig. 4. Diurnal (A and B) and seasonal (C) changes of maximal quantum yield of photosystem II (F_v/F_m) in *R. ponticum* and *R. catawbiense*. Dark-adapted (30 min) leaves were used for the measurement of diurnal changes in F_v/F_m at different times of day on 27 August (A) (minimum and maximum air temperatures were 17°C and 33°C) and 25 November (B) (minimum and maximum air temperatures were –2°C and 6°C) for non-acclimated and cold-acclimated plants, respectively. All measurements were made on sunny days. Data are presented as mean ± standard errors of three individual leaves (one leaf from each of three plants per species).

Fig. 5. Seasonal changes of total leaf chlorophyll content in *R. ponticum* and *R. catawbiense*. Plants were cold-acclimated outdoors from August to December 2007. Data are represented as mean ± standard errors (n=3).

Fig. 6. Seasonal changes of the relative expression profiles of seven *RcELIPs* in *R. ponticum* and *R. catawbiense*. Total RNA was extracted (at approximately monthly intervals) and used for cDNA synthesis. The transcript levels of each *RcELIP* were plotted relative to the expression of *R. ponticum* in August (taken as 1). Real–time RT–PCR was carried out with three replications and data are represented as mean ± standard errors.

Fig. 7. Regression of relative expression of *RcELIPs* on changes in leaf freezing tolerance (ΔLT_{50}) for *R. ponticum* and *R. catawbiense*. The relative expression of *RcELIPs* for each species in each month was calculated relative to their expression in August (taken as 1). The values are based on the average of seven *RcELIPs* (as in Fig. 6) and presented in Table 1. ΔLT_{50} are the absolute values of LT_{50} difference between August and other months based on the data shown in Table 1.

Fig. 8. Seasonal changes in malondialdehyde (MDA) content (A) and antioxidant metabolites, total ascorbate (B) and total glutathione (C) for *R. ponticum* and *R. catawbiense* leaf tissues. Plants were cold-acclimated outdoors from August to December 2007. Data are represented as mean ± standard errors (n=3).

Fig. 9. Seasonal changes in the activities of antioxidant enzymes for *R. ponticum* and *R. catawbiense* leaf tissues. Antioxidant enzymes include superoxide dismutase (SOD) (A), ascorbate peroxidise (APX) (B), catalase (CAT) (C), and peroxidase (POD) (D). Plants were cold-acclimated outdoors from August to December 2007. Data are represented as mean ± standard errors (n=3).

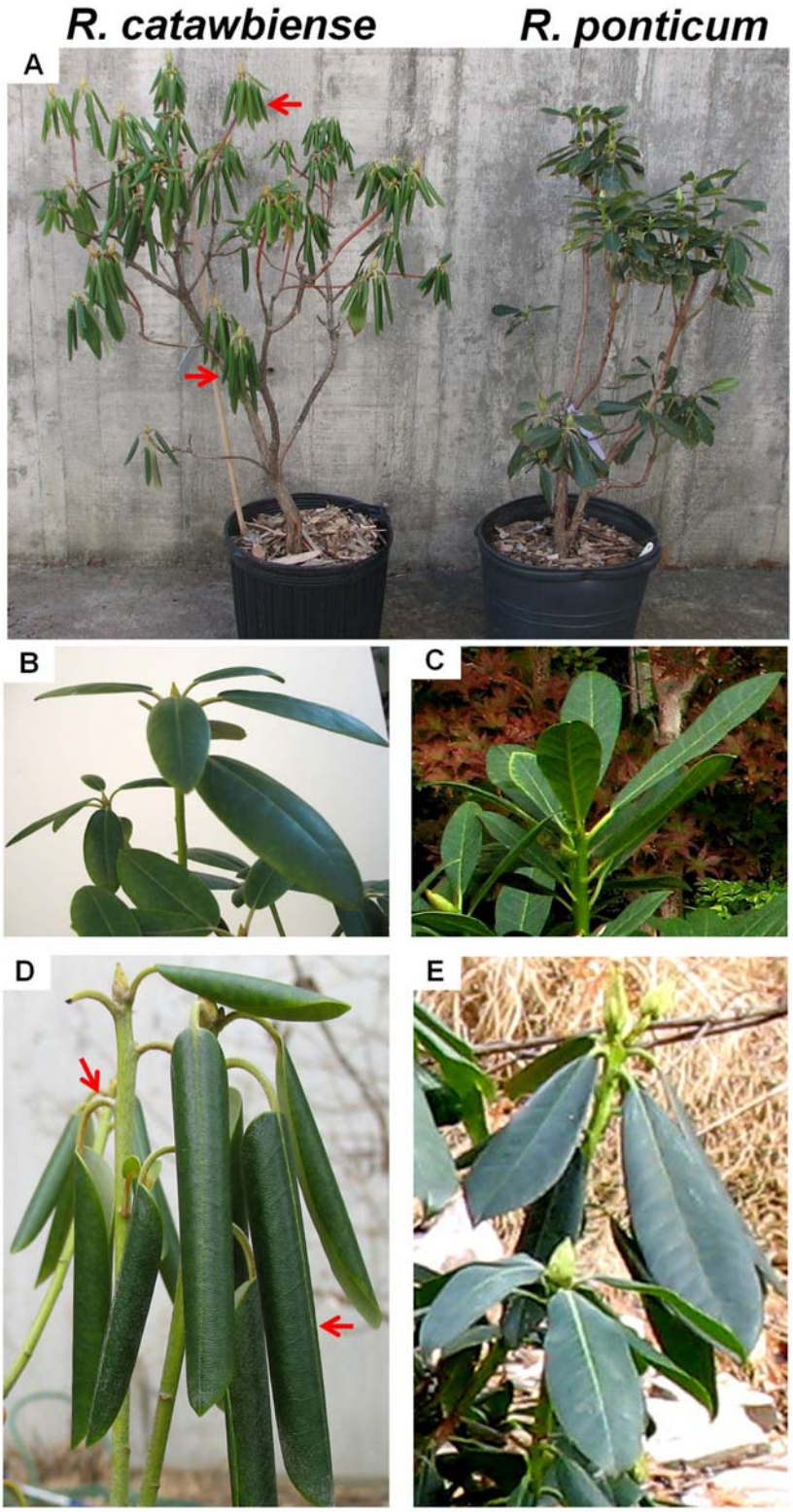

Fig. 1

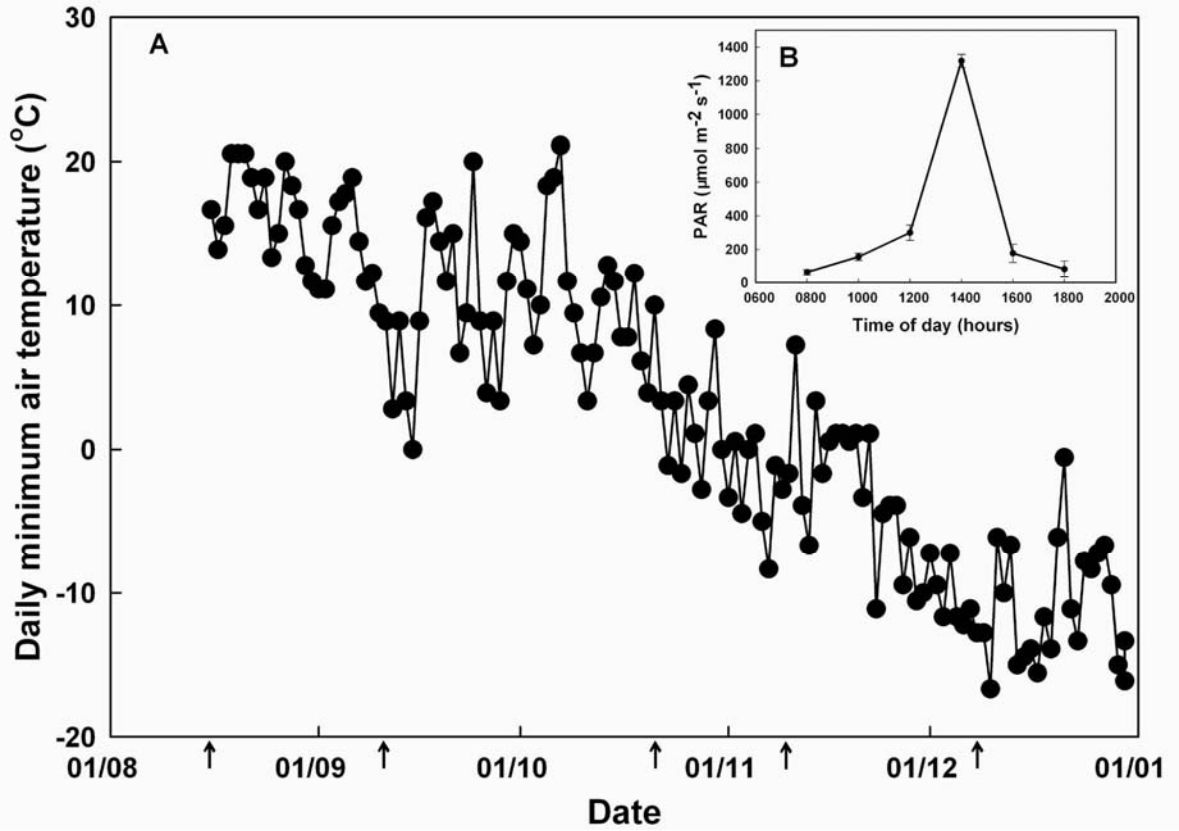
A
B
Daily minimum air temperature (°C)
30
20
10
0
-10
-20
01/08
01/09
01/10
01/11
01/12
01/01
Date
PAR (µmol m-2 s-1)
1400
1200
1000
800
600
400
200
0
0600
0800
1000
1200
1400
1600
1800
2000
Time of day (hours)

Fig. 2

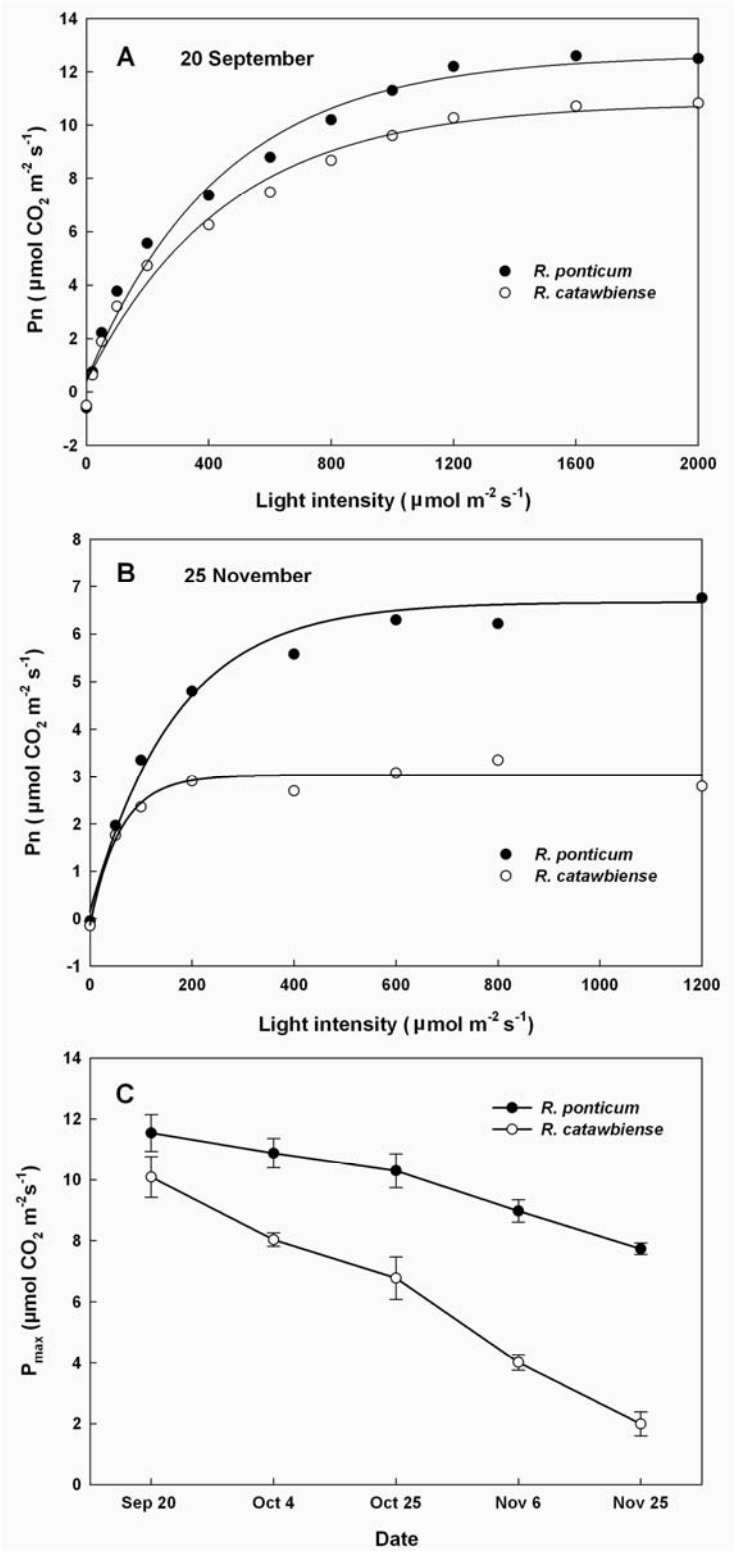
A
20 September
Pn (µmol CO2 m-2 s-1)
Light intensity (µmol m-2 s-1)
R. ponticum
R. catawbiense
B
25 November
Pn (µmol CO2 m-2 s-1)
Light intensity (µmol m-2 s-1)
R. ponticum
R. catawbiense
C
Pmax (µmol CO2 m-2s-1)
Sep 20
Oct 4
Oct 25
Nov 6
Nov 25
Date
R. ponticum
R. catawbiense

Fig. 3

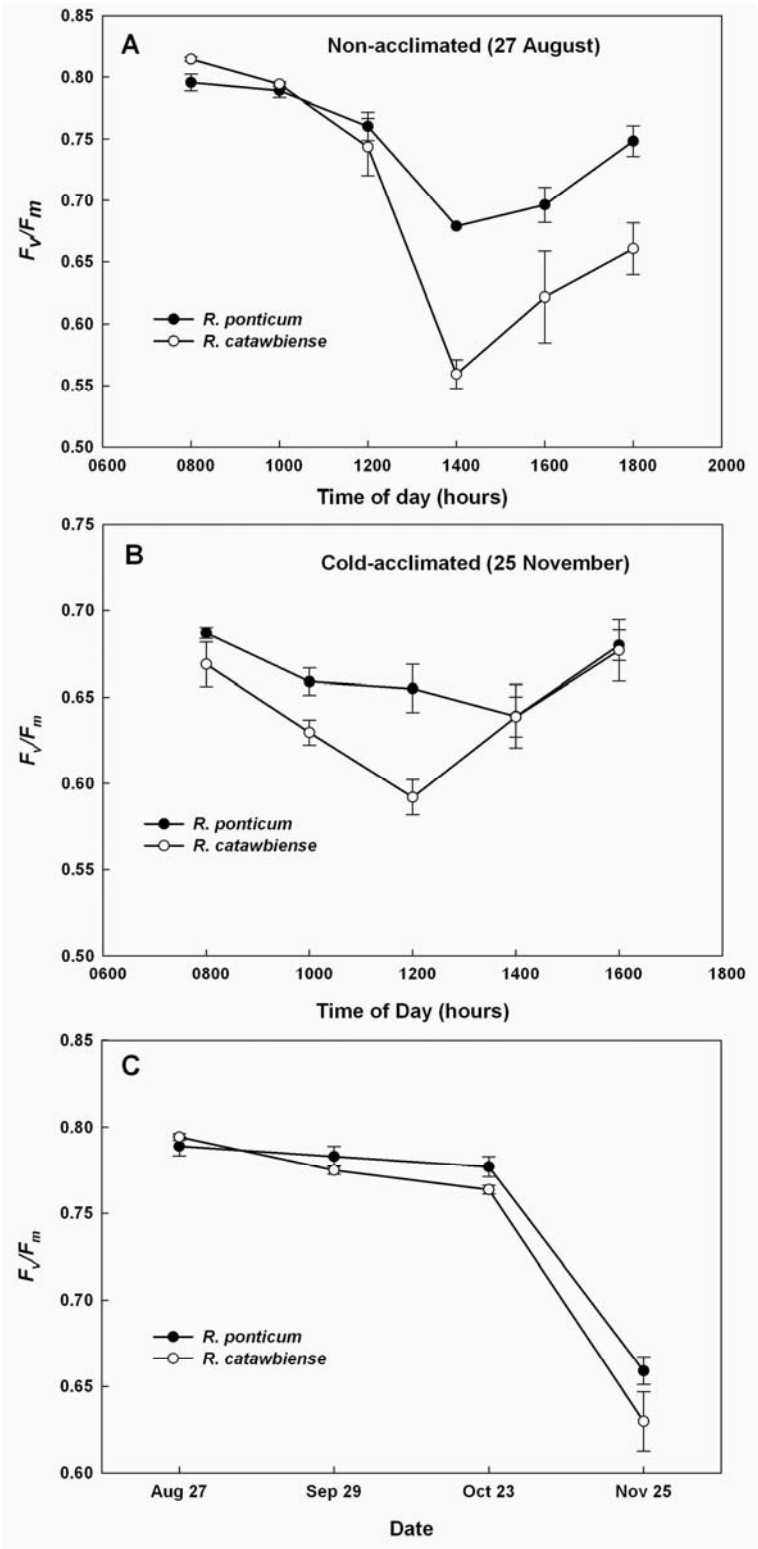
A
Non-acclimated (27 August)
F_v/F_m
R. ponticum
R. catawbiense
Time of day (hours)
B
Cold-acclimated (25 November)
F_v/F_m
R. ponticum
R. catawbiense
Time of Day (hours)
C
F_v/F_m
R. ponticum
R. catawbiense
Aug 27
Sep 29
Oct 23
Nov 25
Date

Fig. 4

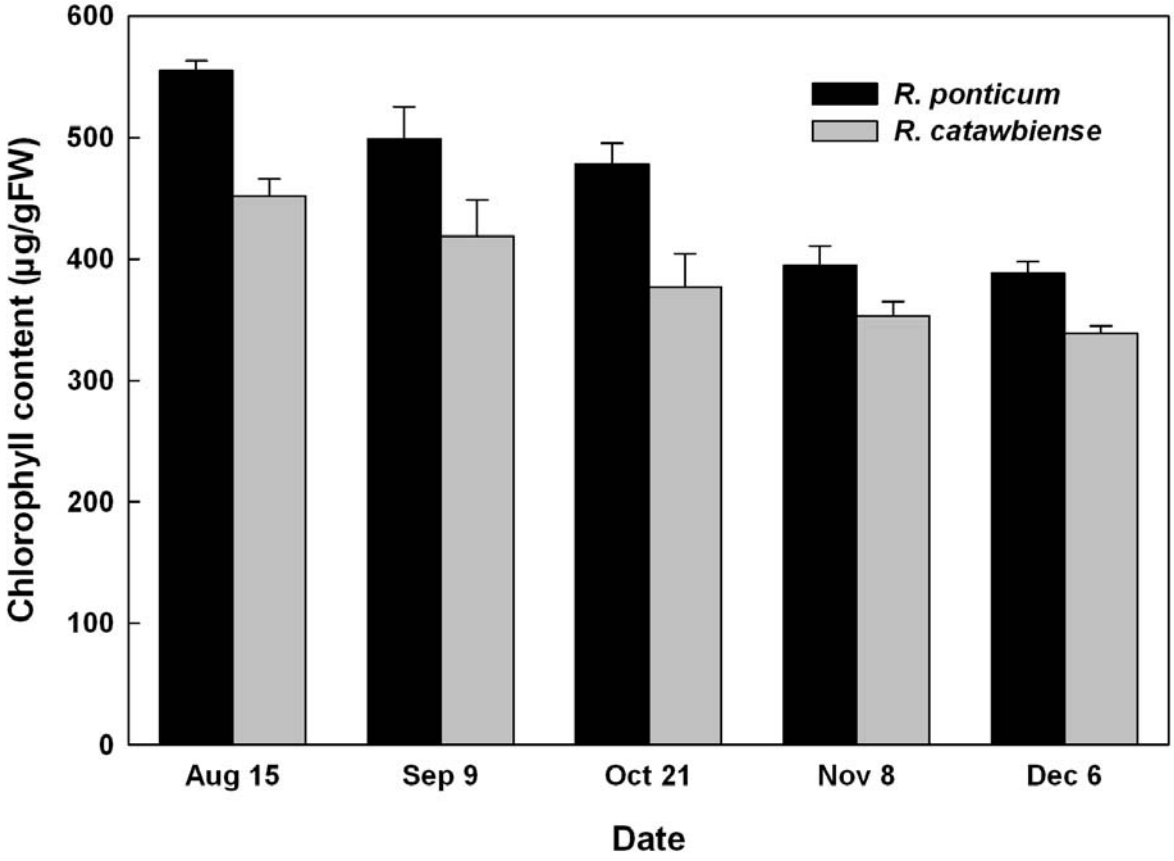
600
500
400
300
200
100
0
Chlorophyll content (µg/gFW)
R. ponticum
R. catawbiense
Aug 15
Sep 9
Oct 21
Nov 8
Dec 6
Date

Fig. 5

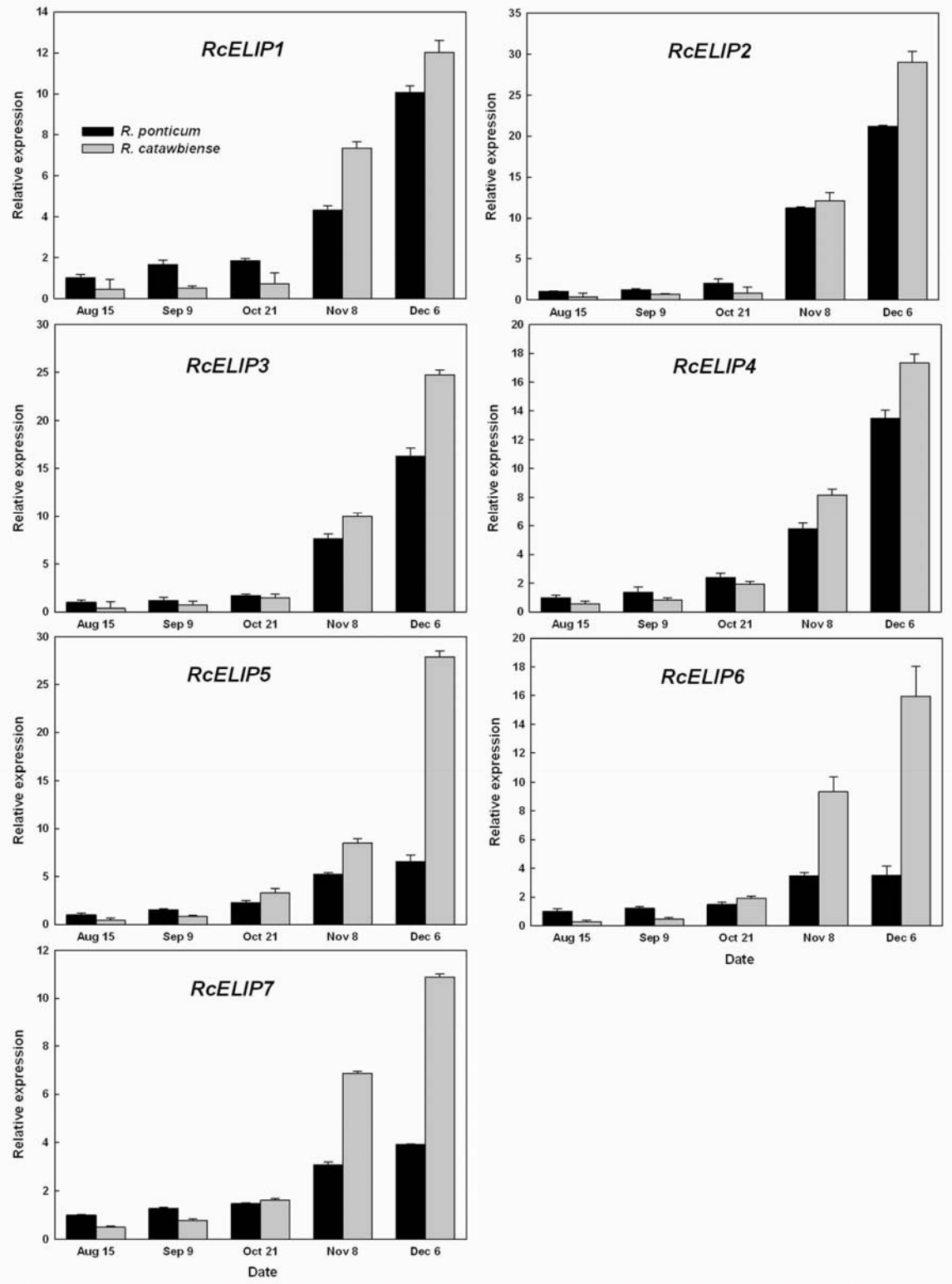
RcELIP1
R. ponticum
R. catawbiense
RcELIP2
RcELIP3
RcELIP4
RcELIP5
RcELIP6
RcELIP7
Relative expression
Aug 15
Sep 9
Oct 21
Nov 8
Dec 6
Date

Fig. 6

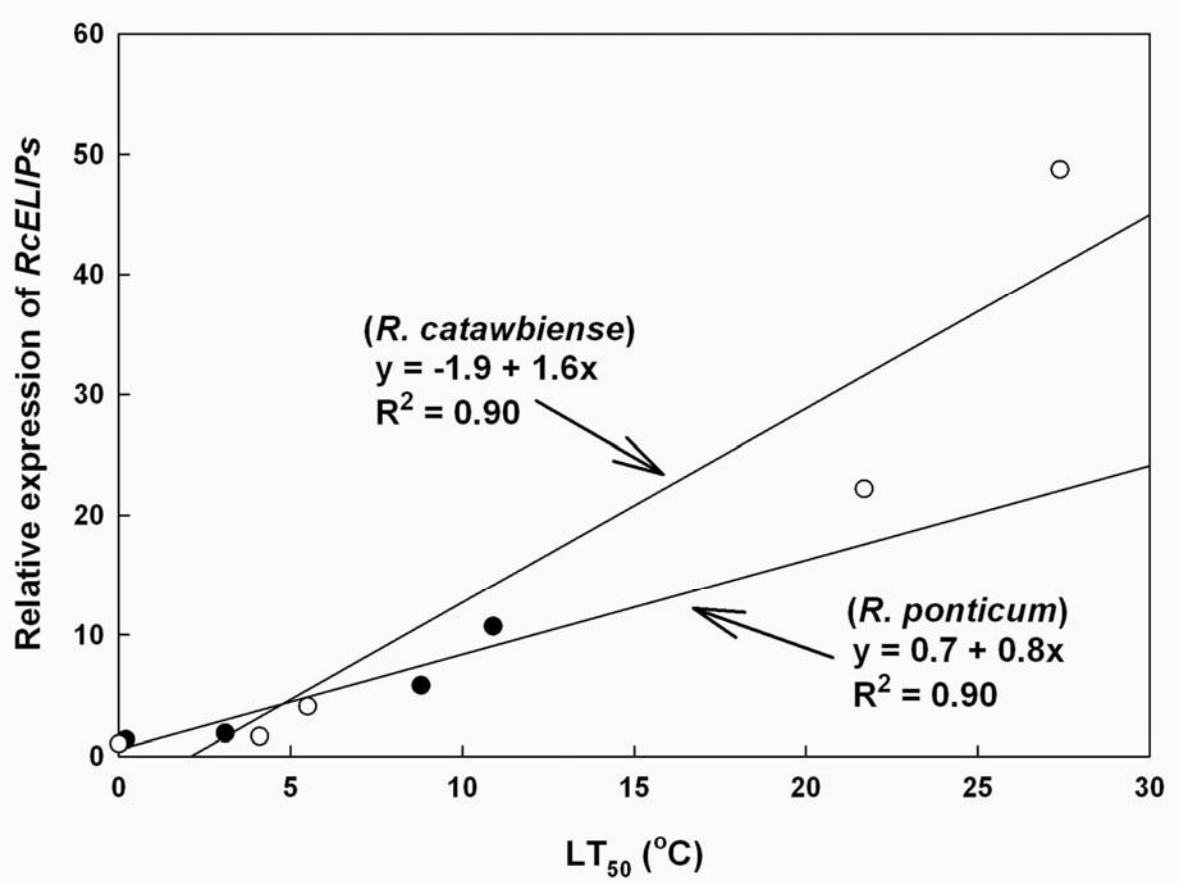
Relative expression of RcELIPs
LT50 (°C)
(R. catawbiense)
y = -1.9 + 1.6x
R2 = 0.90
(R. ponticum)
y = 0.7 + 0.8x
R2 = 0.90
0
10
20
30
40
50
60
0
5
10
15
20
25
30

Fig. 7

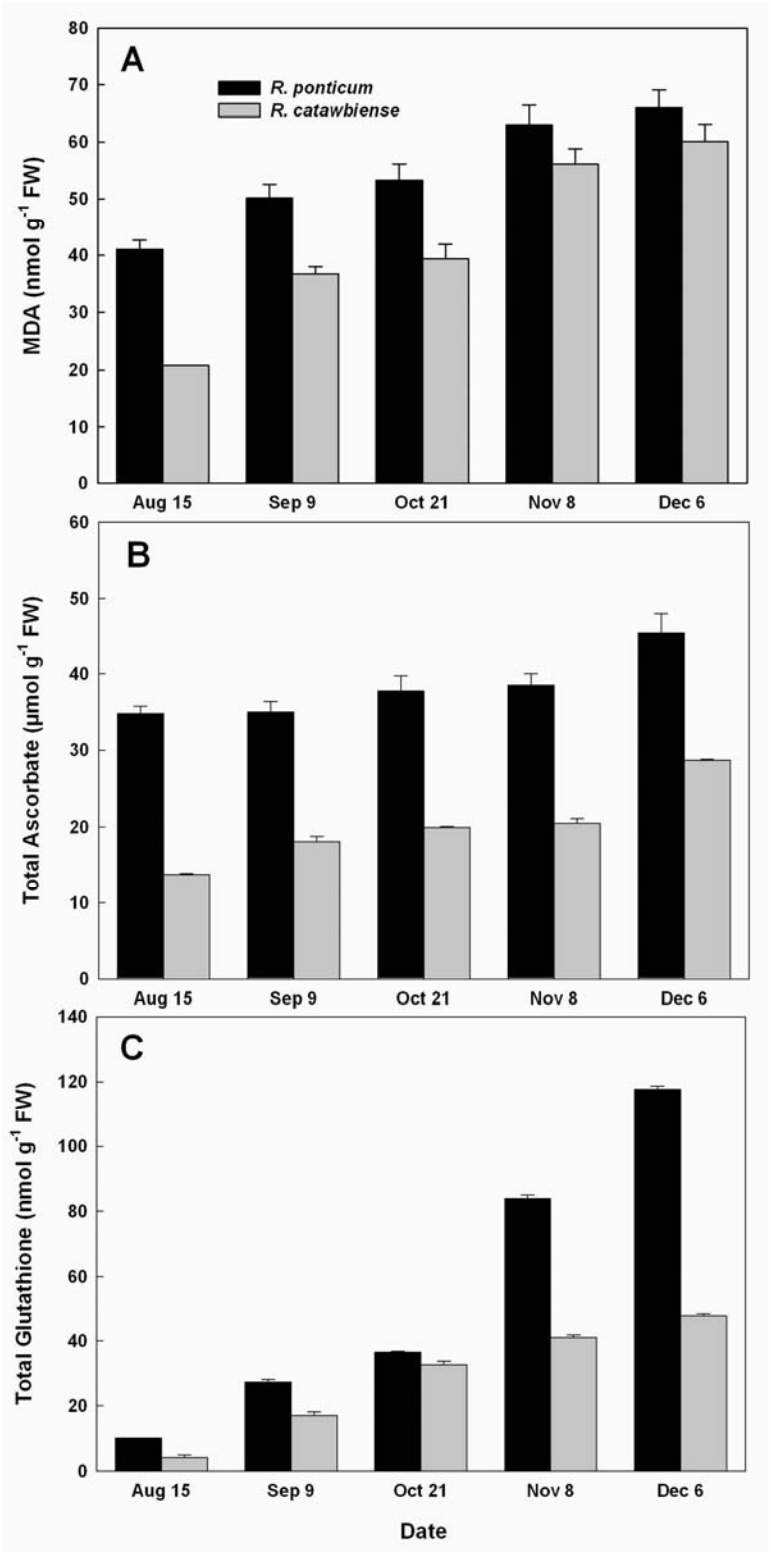
A
R. ponticum
R. catawbiense
MDA (nmol g-1 FW)
0
10
20
30
40
50
60
70
80
Aug 15
Sep 9
Oct 21
Nov 8
Dec 6
B
Total Ascorbate (µmol g-1 FW)
0
10
20
30
40
50
60
Aug 15
Sep 9
Oct 21
Nov 8
Dec 6
C
Total Glutathione (nmol g-1 FW)
0
20
40
60
80
100
120
140
Aug 15
Sep 9
Oct 21
Nov 8
Dec 6
Date

Fig. 8

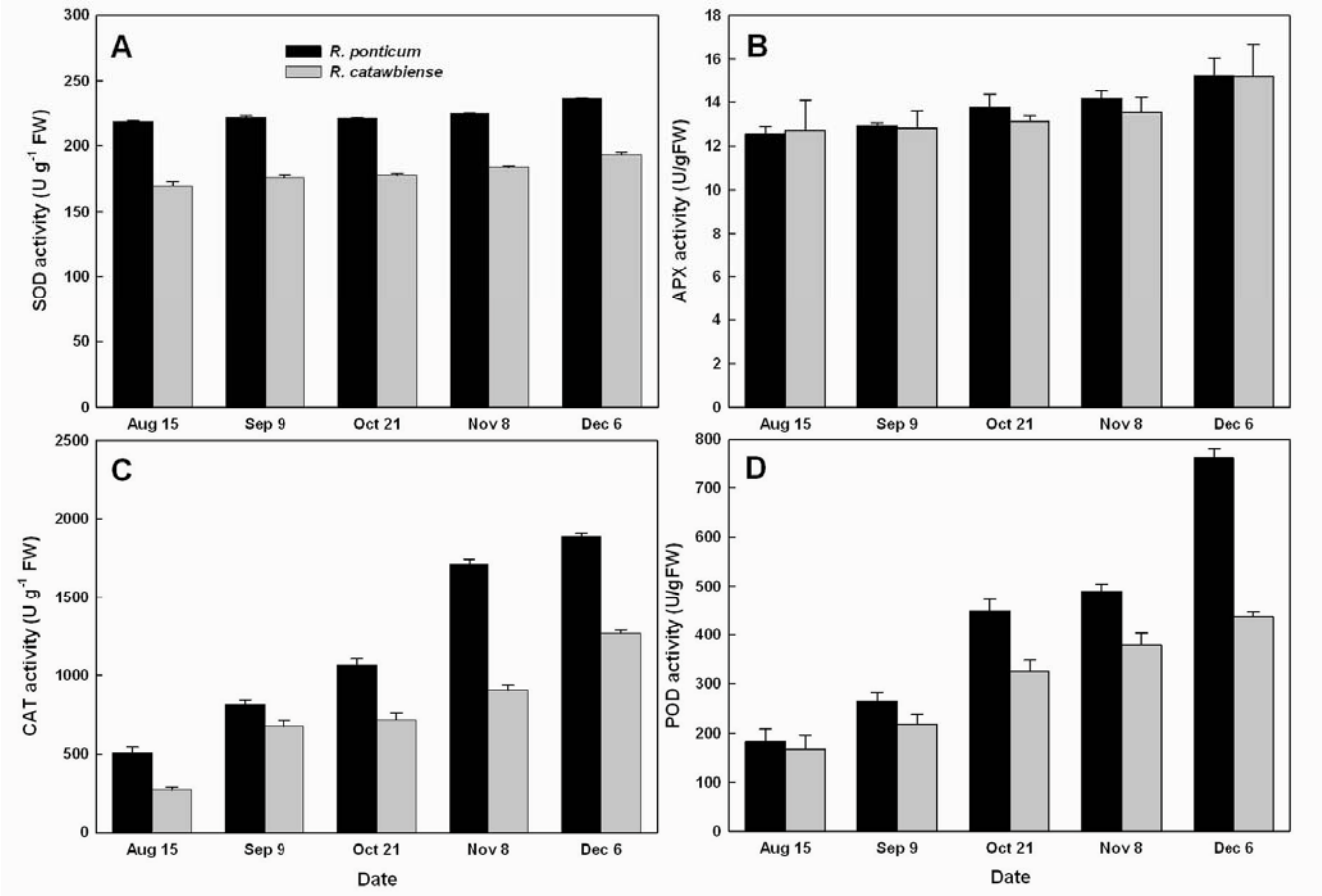
A
R. ponticum
R. catawbiense
SOD activity (U g-1 FW)
B
APX activity (U/gFW)
C
CAT activity (U g-1 FW)
D
POD activity (U/gFW)
Aug 15
Sep 9
Oct 21
Nov 8
Dec 6
Date

Fig. 9

CHAPTER 4. IS EXPRESSION OF PLASMA MEMBRANE AQUAPORINS (*Rhododendron catawbiense* PIP2s) ASSOCIATED WITH THERMONASTY IN *RHODODENDRON*?

To be submitted for refereed publication as a "short communication"

Xiang Wang [a], Anania Fessehaie [b], Stephen L. Krebs [c], and Rajeev Arora [a,*]

[a] *Department of Horticulture, Iowa State University, Ames, IA 50011, USA*

[b] *Seed Science Center, Iowa State University, Ames, IA 50011, USA*

[c] *The Holden Arboretum, 9500 Sperry Road, Kirtland, OH 44094, USA*

***Corresponding author:**

Rajeev Arora

Department of Horticulture

Iowa State University

Ames, IA 50011, USA

E-mail: rarora@iastate.edu

Tel.: +1 515-294-0031

Fax: +1 515-294-0730

ABSTRACT

Some *Rhododendron* species show thermonastic leaf movements (drooping and curling) upon exposure to subfreezing temperatures. It is hypothesized that thermonastic leaf curling and uncurling result from water redistribution across the cell membranes leading to loss or gain of turgor in epidermal cells. Aquaporins are involved in facilitating transport of water molecules across cell membranes. To study whether the leaf curling in rhododendrons is associated with the altered expression of previously identified aquaporins (*RcPIP2s*) in *Rhododendron catawbiense*, we investigated the changes of *RcPIP2s* transcripts while the leaves of a thermonastic and nonthermonastic species (*Rhododendron catawbiense* and *Rhododendron ponticum*, respectively) were exposed to a series of temperature regimes in controlled conditions. Progressively cooler subfreezing temperatures induced thermonastic leaf curling in *R. catawbiense* (and uncurling upon warming), whereas *R. ponticum* leaves showed no leaf curling. Gene expression analysis using real-time RT-PCR indicated that there was no apparent association between the *RcPIP2s* expression and thermonastic leaf curling in the two *Rhododendron* species under investigation.

Keywords: Aquaporins, *Rhododendron*, Thermonasty

Abbreviations: AQPs, aquaporins; MIP, major intrinsic protein; PIPs, plasma membrane intrinsic proteins

1. Introduction

Plant leaf movements can be mediated in two ways: irreversible (growth) or reversible (swelling) changes in cell volume [1]. In some plant species, e.g. tobacco, the diurnal and circadian leaf folding and unfolding (described as epinastic) are the results of different growth rates of the upper and lower leaf surfaces. In contrast, leaf movement can also be mediated in many species (e.g. *Mimosa*, *Phaseolus* and *Samanea*) by turgor-regulated reversible cell volume changes of motor organs called pulvini (described as nyctinasty). Pulvini can co-ordinate rapid water exchange across the cell membrane and induce swelling and shrinking of cells located on opposite sides of the tissue, resulting in the movement of leaves and leaflets. As important woody plants grown widely in public gardens with great horticultural interest, some evergreen *Rhododendron* species exhibit thermonasty, a phenomenon of leaf movements (drooping and curling) induced by subfreezing temperatures [2]. Although the physiological cause of thermonasty is not yet well understood, it is believed that the thermonastic response (especially leaf curling) to subfreezing temperatures may be a result of changes in redistribution of tissue water content [3, 4].

In the present study, we only focused on leaf curling in *Rhododendron* and not on leaf drooping component of thermonasty. *Rhododendron* leaf curling has been shown to occur in the field after 10-20 minutes exposure to ambient temperature below –2 to –5°C [2, 5-7]. Water movement across the leaf cell membranes is important for water homeostasis in maintaining turgor and cell volume, and thus in controlling leaf movement. Although the physiological cause of thermonasty is not yet well understood, it is believed that the leaf curling caused by subfreezing temperatures is a result of changes / redistribution of tissue

water, which in turn could cause certain cells to selectively lose turgor leading to the leaf curling [4].

This redistribution of water is likely regulated by water channels, named aquaporins (AQPs) [8]. AQPs, which facilitate transport of water molecules across cell membranes, belong to the major intrinsic protein (MIP), and regulate hydraulic conductivity in response to changing environmental conditions [9, 10]. Evidence is accumulating that AQPs play an important role in plant hydraulic relations at the cell, tissue, organ, and whole-plant level. They facilitate the rapid, passive exchange of water across cell membranes and are responsible for up to 95% of the water permeability of cell membranes [11, 12]. Previous reports also concluded that AQPs are important components involved in leaf movement in different species, e.g. *Nicotiana tabacum*, *Mimosa pudica* and *Samanea saman* [12].

As the largest number of AQP members in higher plants, plasma membrane intrinsic proteins (PIPs) can be divided into two phylogenetic groups, named PIP1 and PIP2. Previous reports showed that aquaporins of the PIP2 subfamily exhibited more efficient water channel activity than members of the PIP1 clusters [10, 13, 14]. We have previously constructed the cDNA libraries prepared from summer- and winter-collected leaves of *Rhododendron catawbiense* to identify the cold-acclimation responsive genes in this species [15]. Two cDNAs encoding AQP homologs (*RcPIP2;1* and *RcPIP2;2*) were identified [16], and it was later demonstrated that *RcPIP2s* were indeed bonafide AQPs with significant water channel activity [8]. In the present study, the leaves from two *Rhododendron* species (*R. catawbiense* and *R. ponticum*) which differ in their thermonastic behavior (former shows leaf curling in winter while the latter does not) were used to investigate whether or not *RcPIP2s* expression patterns were associated with leaf curling. We hypothesize that *RcPIP2s* expression would be

significantly downregulated concomitant to subfreezing temperature-induced leaf curling in *R. catawbiense*, whereas similar temperature regimes would result in relatively minor, if any, changes of *RcPIP2s* expression in the nonthermonastic *R. ponticum*.

2. Materials and methods

The cultivars from *R. catawbiense* 'Catalgla' and *R. ponticum* 'RSBG 76/411' were grown and maintained outdoors from summer 2008 to March 2009. Plant materials and growth conditions were as previously described [17]. Fully expanded leaves from the previous year's growth were collected outdoors (set as the control treatment) on March 11, 2009 (at ~ 0900 HR) when the air temperature was 12ºC, and immediately frozen at –80ºC until the analysis of gene expression profiles; plants from both species maintained their cold-acclimated status on March 11 as indicated by their leaf freezing tolerance (–32.4ºC and –20.4ºC for *R. catawbiense* and *R. ponticum*, respectively) compared to their non-acclimated tolerance in August (–7.1ºC and –4.8ºC for *R. catawbiense* and *R. ponticum*, respectively). Three twigs (one twig from each of three plants per species) were then cut and immediately put into a growth chamber (used for sample collection) already maintained at 0ºC. In order to minimize the effect of opening of the chamber door for photography, and consequent transient warming, on leaf uncurling, another chamber was programmed to identical temperature regimes as the one in sample collection chamber and used to take pictures of thermonastic or non-thermonastic behavior at each treatment temperature. Three representative leaves from each species were cut from the twigs; two were placed in the sample collection chamber while one in the chamber used for photography. Thermocouples were attached to the leaves to monitor the leaf temperatures. When leaf temperature reached

0ºC, the twigs were exposed for another 30 min, and samples were collected immediately after the photography and stored at –80ºC for the RNA extraction. The same procedure was applied to a series of cooling (0 to -2, -2 to -4, -4 to -6ºC) and re-warming temperatures (-6 to -3, -3 to 0, 0 to 21ºC). At each step, the leaves were exposed for another 30 min after they reached the desired treatment temperature except for -2ºC treatment at which leaves were exposed for 60 min.

Total RNA extraction and first-strand cDNAs were synthesized according to [17]. Real-time PCR was carried out in a PCR system (7900HT, ABI, Foster City, CA, USA) using real-time PCR Power Mix Kit (SYBR Green as fluorescent dye, Fisher). Absolute copy number of the genes per nanogram total RNA was determined by the standard curves (copy number as a function of CT value) generated using a 2X dilution series of reverse transcriptase (RT)-PCR products. The copy number was determined based on the size and the mass of the RT-PCR products. The reaction mixture (25 μl) contained 2 μl of first-strand cDNA, 0.45 μM of each of the forward and reverse primers and appropriate amounts of other components as recommended by the manufacturer. The PCR system was programmed as follows: 15 min at 95°C for pre-denature; 40 cycles of 20 s at 95°C, 20 s at 60°C and 30 s at 72°C for each gene. Data were collected during the extension step. Real-time PCR was carried out with three replications.

Housekeeping gene for *Rhododendron* – *RhUBQ*–ubiquitin – was selected as reference gene. The forward and reverse primer pairs to amplify *RhUBQ*, *RcPIP2;1* and *RcPIP2;2*, respectively, were as follows: *RhUBQ* – F/R: 5'–TGGCTGGGTGCAGCAAT–3' and 5'–TGGTATGTTCAAGTGTGCGGTAA–3'; *RcPIP2;1* – F/R: 5'–TTCGCCGTATTCATGGTTCA–3' and 5'–TGATTCCGGTGCCTGTGAT–3'; *RcPIP2;2* –

F/R: 5'–GGGCCATATGCGGTGTTG–3' and 5'–CGGTCGTAGTGCGACTTCTG–3'. The accession numbers for *RhUBQ*, *RcPIP2;1* and *RcPIP2;2* genes are CV015651, DQ341104, EU287448, respectively.

Data were presented as mean ± standard errors. Differences among species and temperatures were analyzed with two-way ANOVA, and means were compared by the least significant difference (LSD) test. Means were considered to be different when $P \leq 0.05$.

3. Results and discussion

The performance of leaves from the two species showing curling or no curling is presented in Fig. 1. *R. ponticum* did not show any curling throughout the experiment (Fig. 1). Complete leaf curling occurred in *R. catawbiense* only when the leaf temperature reached –6°C (Fig. 1E); no curling (Fig. 1A-D) in *R. catawbiense* was observed before this treatment. Partial (Fig. 1F) or complete uncurling (Fig. 1G-F) was observed in *R. catawbiense* when the leaf temperature was progressively re-warmed to –3, to 0, and finally to 21°C. The temperature at which curling in excised leaves occurred was likely between –4°C and –6°C for *R. catawbiense*, which is somewhat lower than a previous report [2] where it occurred between –1°C and –4°C under field conditions. Our observations based on the thermocouple readings gave no indication of any exothermic event (flash warming) in the leaves while they were cooled up to –6°C in growth chamber. Therefore, based on the lack of exothermic event, it might be safe to claim that ice nucleation did not occur and that ice was not formed in the leaves of the two species during the course of this study. And therefore, redistribution of cellular water, if causally associated with thermonasty, was not due to an extracellular freezing event. This suggestion appears to be consistent with Nilsen's observation that the

freezing point for leaves of *R. catawbiense* was between –7°C and –8°C while leaf curling was completed by a leaf temperature of –4°C [7].

The gene expression levels of *RcPIP2s* are shown in Fig. 2. In general, *RcPIP2;1* (Fig. 2A) and *RcPIP2;2* (Fig. 2B) had similar expression patterns across the two species. Specifically, the two genes were significantly downregulated in both species when leaves were brought from outdoors (12°C) to 0°C, which may reflect a 'cold-shock' response; however, upregulation of the two genes was observed from 0°C to –4°C in *R. ponticum* and from 0°C –2°C in *R. catawbiense*. The two genes showed significant downregulation from –4°C to –6°C in *R. ponticum* and from –2°C to –4°C in *R. catawbiense*. During stepwise warming from –6°C to 21°C, *R. ponticum* exhibited a relatively greater upregulation of these two genes than *R. catawbiense* (Fig. 2). Fluctuations in *RcPIP2s* expression would indicate changes in water fluxes across membranes assuming that water channel activity followed the expression kinetics of these genes. However, the overall similar expression patterns of *RcPIP2s* between these two species indicate that the expression of *RcPIP2s* is likely not associated with the species performance with respect to thermonasty since *R. catawbiense* exhibited leaf curling / uncurling while *R. ponticum* did not. However, other studies on leaf movement in tobacco (*Nicotiana tabacum*) [18] and mimosa (*Mimosa pudica*) [19] indicated that AQP activity / expression was an important component of leaf movement phenomenon.

Interestingly, *RcPIP2s* expression, in general, was substantially higher (about 5~7-fold) in *R. ponticum* than that in *R. catawbiense* (Fig. 2), which presents a basis for the following speculation in the favor of *RcPIP2s* expression being potentially associated with thermonasty. The 'constitutive' higher expression of *RcPIP2s* in *R. ponticum* (Fig. 2) may be sufficient for this species to 'buffer' any changes in the water movement across plasma

membrane such that a relatively smaller reduction in their expression is not enough to cause loss of turgor and, therefore, leaf curling; on the contrary, even a small reduction in *RcPIP2s* expression in *R. catawbiense* leaves might be sufficiently large enough to result in changes of turgor due to overall much lower 'constitutive' expression of these genes in this species.

The overall relatively lower expression of *RcPIP2s* in *R. catawbiense* leaves (Fig. 2) might also be associated with the vulnerability of this species to winter desiccation. Evidence is accumulating in favor of a correlation between upregulation of AQPs and drought tolerance [20-23]. Our anatomical findings from an earlier study [24] where the overall opening of stomatal pores per unit leaf area (an integrated value of stomatal density and pore size) was ~ 2-fold higher in *R. catawbiense* than *R. ponticum*, suggested that thermonasty may be a particularly beneficial trait in this species by serving as a desiccation-avoidance strategy.

Nilsen has proposed two other possible causes for leaf curling in rhododendrons [4]. One has to do with the movement of ions from the abaxial to the adaxial side of the leaf causing the adaxial leaf cells to expand while the abaxial leaf cells to contract without a change in whole organ tissue hydration; the other possible cause putatively resides in the cell wall structure whereby some components may undergo conformational changes at critical temperatures. In summary, our data from the comparative study of a pair of thermonastic and nonthermonastic species indicate no apparent association between *RcPIP2s* expression and leaf curling / no curling in the two *Rhododendron* species. More detailed investigation involving AQP studies at the protein level as well as at the transcriptional level corresponding to the adaxial and abaxial sides of the leaf in several thermonastic and nonthermonastic *Rhododendron* species may provide further insights into the role of AQPs in

leaf curling in *Rhododendron*.

Acknowledgements

This journal paper of the Iowa Agriculture and Home Economics Experiment Station, Ames, Iowa (Project 3601) was supported by Hatch Act and State of Iowa funds. We thank Arlen Patrick and Peter Lawlor (greenhouse managers, Department of Horticulture, Iowa State University) for assisting with plant care throughout this study.

References

[1] N. Uehlein, R. Kaldenhoff, Aquaporins and plant leaf movements, Ann. Bot. 101 (2008) 1–4.

[2] E.T. Nilsen, Influence of water relations and temperature on leaf movements of *Rhododendron* species, Plant Physiol. 83 (1987) 607–612.

[3] W. Haupt, M.E. Feileib, The physiology of movements. New York: Springer Verlag, (1979).

[4] E.T. Nilsen, Thermonastic leaf movements: a synthesis of research with *Rhododendron*, Bot. J. Linnean Soc. 110 (1992) 205–233.

[5] Y. Fukuda, Hygronastic leaf curling and uncurling movement of the leaves of *Rhododendron micranthum* Turcz. with respect to temperature and resistance to cold, Jap. J. Bot. 6 (1933) 191–224.

[6] E.T. Nilsen, Seasonal and diurnal leaf movements of *Rhododendron maximum* L. in contrasting irradiance environments, Oecologia 65 (1985) 296–302.

[7] E.T. Nilsen, The relationship between freezing tolerance and thermotropic leaf movements in five *Rhododendron* species, Oecologia 87 (1991) 63–71.

[8] Y. Peng, R. Arora, G. Li, X. Wang, A. Fessehaie, *Rhododendron catawbiense* plasma membrane intrinsic proteins are aquaporins, and their over-expression compromises constitutive freezing tolerance and cold acclimation ability of transgenic *Arabidopsis* plants, Plant Cell Environ. 31 (2008) 1275–1289.

[9] P. Agre, M. Bonhivers, M.J. Borgnia, The aquaporins, blueprints for cellular plumbing systems, J. Biol. Chem. 273 (1998) 14659–14662.

[10] R. Kaldenhoff, M. Fischer, Aquaporins in plants, Acta Physiol. 187 (2006) 169–176.

[11] T. Henzler, Q. Ye, E. Steudle, Oxidative gating of water channels (aquaporins) in *Chara* by hydroxyl radicals, Plant Cell Environ. 27 (2004) 1184–1195.

[12] R.B. Heinen, Q. Ye, F. Chaumont, Role of aquaporins in leaf physiology, J. Exp. Bot. 60 (2009) 2971–2985.

[13] M.J. Daniels, T.E. Mirkov, M.J. Chrispeels, The plasma membrane of *Arabidopsis thaliana* contains a mercury-insensitive aquaporin that is a homolog of the tonoplast water channel protein TIP, Plant Physiol. 106 (1994) 1325–1333.

[14] I. Johansson, M. Karlsson, V.K. Shukla, M.J. Chrispeels, C. Larsson, P. Kjellbom, Water transport activity of the plasma membrane aquaporin PM28A is regulated by phosphorylation, Plant Cell 10 (1998) 451–459.

[15] H. Wei, A. L. Dhanaraj, L.J. Rowland, Y. Fu, S.L. Krebs, R. Arora, Comparative analysis of expressed sequence tags (ESTs) from cold-acclimated and non-acclimated leaves of *Rhododendron catawbiense* Michx., Planta 221 (2005) 406–416.

[16] H. Wei, A.J. Dhanaraj, R. Arora, L.J. Rowland, Y. Fu, L. Sun, Identification of cold acclimation-responsive *Rhododendron* genes for lipid metabolism, membrane transport and lignin biosynthesis: importance of moderately abundant ESTs in genomic studies, Plant Cell Environ. 29 (2006) 558–570.

[17] X. Wang, Y. Peng, J.W. Singer, A. Fessehaie, S.L. Krebs, R. Arora, Seasonal changes in photosynthesis, antioxidant systems and *ELIP* expression in a thermonastic and non-thermonastic *Rhododendron* species: a comparison of photoprotective strategies in overwintering plants, Plant Sci. 177 (2009) 607–177.

[18] F. Siefritz, B. Otto, G.P. Bienert, A. van der Krol, R. Kaldenhoff, The plasma membrane aquaporin NtAQP1 is a key component of the leaf unfolding mechanism in tobacco, Plant J. 37 (2004) 147–155.

[19] P. Fleurat-Lessard, N. Frangne, M. Maeshima, R. Ratajczak, J.L. Bonnemain, E. Martinoia, Increased expression of vacuolar aquaporin and H^+-ATPase related to motor cell function in *Mimosa pudica* L., Plant Physiol. 114 (1997) 827–834.

[20] X.H. Cui, F.S. Hao, H. Chen, J. Chen, X.C. Wang, Expression of the *Vicia faba* VfPIP1 gene in *Arabidopsis thaliana* plants improves their drought resistance, J. Plant Res. 121 (2008) 207–214.

[21] H.L. Lian, X. Yu, D. Lane, W.N. Sun, Z.C. Tang, W.A. Su, Upland rice and lowland rice exhibited different PIP expression under water deficit and ABA treatment, Cell Res. 16 (2006) 651–660.

[22] P. Martre, R. Morillon, F. Barrieu, G.B. North, P.S. Nobel, M.J. Chrispeels, Plasma membrane aquaporins play a significant role during recovery from water deficit, Plant Physiol. 130 (2002) 2101–2110.

[23] Y. Zhang, Z. Wang, T. Chai, Z. Wen, H. Zhang, Indian mustard aquaporin improves drought and heavy-metal resistance in tobacco, Mol. Biotech. 40 (2008) 280–292.

[24] X. Wang, R. Arora, H.T. Horner, S.L. Krebs, Structural adaptations in overwintering leaves of thermonastic and nonthermonastic *Rhododendron* species, J. Amer. Soc. Hort. Sci. 133 (2008) 768–776.

Figure legends

Fig. 1. The photographs showing thermonastic leaf curling or lack thereof in response to different treatment temperatures in *R. ponticum* (left) and *R. catawbiense* (right), respectively. Same leaf (for respective species) was used for the photography across all temperature treatments through curling and uncurling. (A) Pictures showing no leaf curling while the leaves were sampled outside on March 11, 2009 when the air temperature was 12ºC (control) and immediately placed in the growth chamber at 0°C; (B) Pictures showing no leaf curling while the leaves were exposed to 0°C for 30 min; (C) Pictures showing no leaf curling while the leaves were exposed to –2°C for 60 min; (D) Pictures showing no leaf curling while exposed to –4°C for 30 min; (E) Pictures showing no leaf curling for *R. ponticum* but complete curling for *R. catawbiense* while the leaves were exposed to –6°C for 30 min; (F) Pictures showing no leaf curling for *R. ponticum* and partial uncurling for *R. catawbiense* while the leaves were re-warmed and exposed to –3°C for 30 min; (G) Pictures showing no leaf curling for *R. ponticum* and complete uncurling for *R. catawbiense* while the leaves were re-warmed and exposed to 0°C for 30 min; (H) Pictures showing no leaf curling while the leaves were re-warmed at 21°C for 30 min.

Fig. 2. Quantitative expression (as absolute copy number) of *RcPIP2;1* (A) and *RcPIP2;2* (B) genes in the leaves of *R. ponticum* and *R. catawbiense* exposed to different temperature treatments (as in Fig. 1). The transcript level of each gene is given as molecular copy numbers in 1 ng of total RNA. Real–time RT–PCR was carried out with three replications and data are represented as mean ± standard errors.

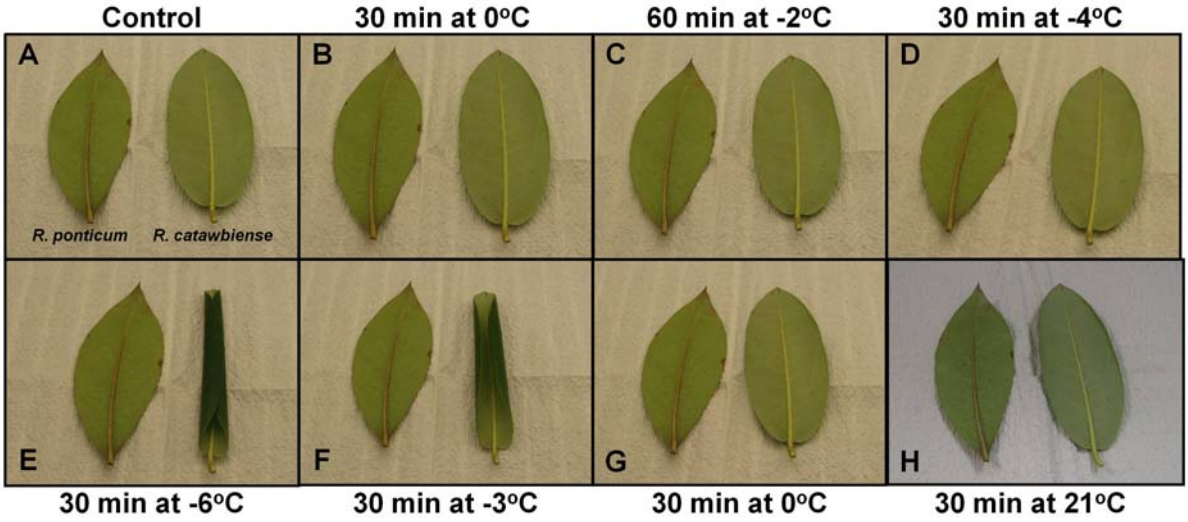
Control
30 min at 0°C
60 min at -2°C
30 min at -4°C
A
B
C
D
R. ponticum
R. catawbiense
E
F
G
H
30 min at -6°C
30 min at -3°C
30 min at 0°C
30 min at 21°C

Fig. 1

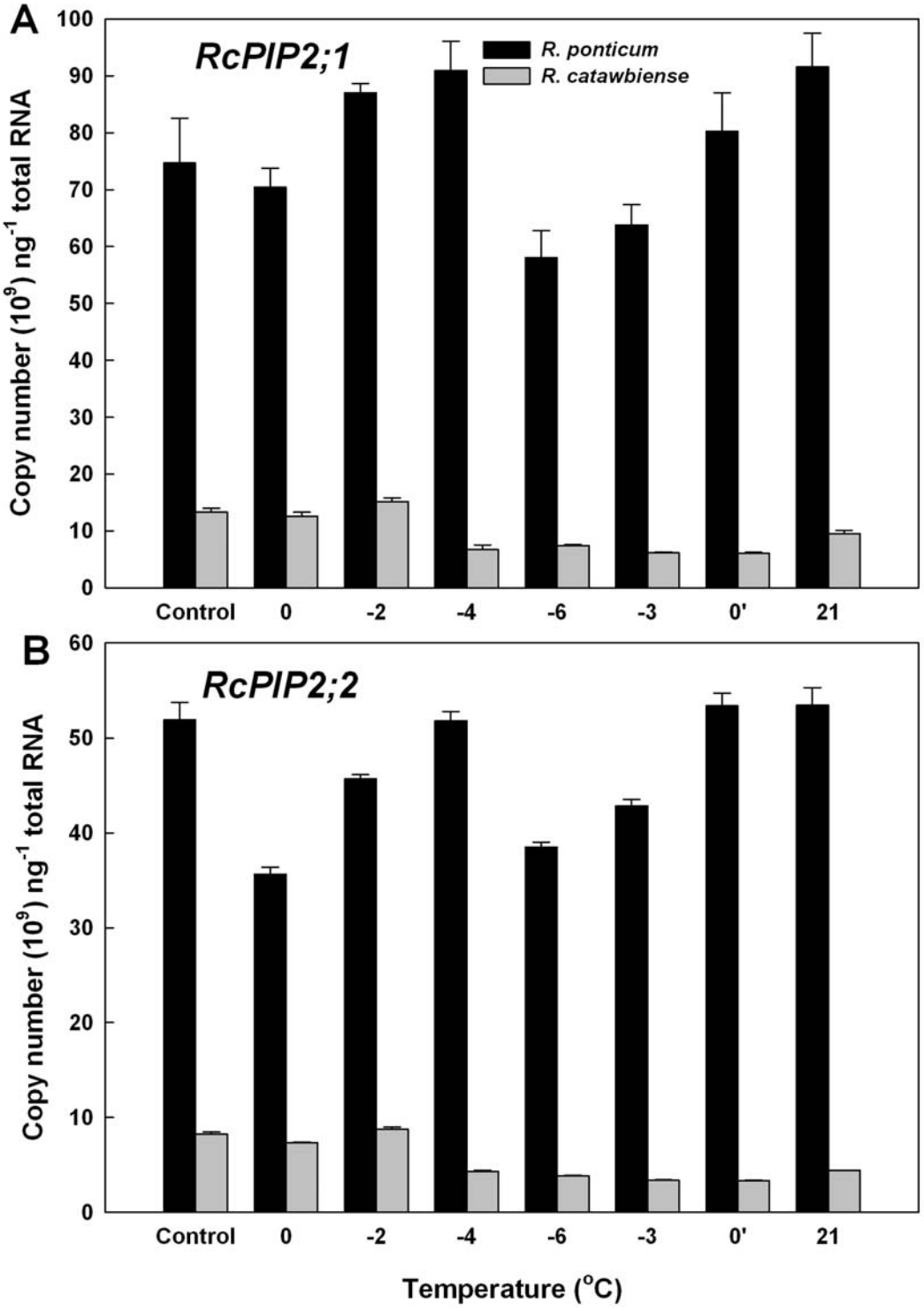
A
RcPIP2;1
R. ponticum
R. catawbiense
Copy number (10^9) ng^-1 total RNA
100
90
80
70
60
50
40
30
20
10
0
Control
0
-2
-4
-6
-3
0'
21
B
RcPIP2;2
Copy number (10^9) ng^-1 total RNA
60
50
40
30
20
10
0
Control
0
-2
-4
-6
-3
0'
21
Temperature (°C)

Fig. 2

CHAPTER 5. GENERAL CONCLUSION

Previous chapters represent published work and work that has just been submitted for publication. In this chapter, I provide an overview of key results and conclusions from the entire dissertation. I used two *Rhododendron* species (*R. catawbiense* and *R. ponticum*) to study their different photoprotective strategies during seasonal cold acclimation at morphological, anatomical, physiological, biochemical and molecular levels; I also studied whether or not *RcPIP2s* (*R. catawbiense* PIP2s) expression patterns were associated with thermonastic leaf curling in rhododendrons.

Microscopic data revealed that the two *Rhododendron* species evolved distinct leaf anatomy which could have potential adaptive significance to high light at subfreezing temperatures (chapter 2). Compared with *R. catawbiense*, *R. ponticum* has significantly thicker leaf blades but thinner cuticles. There is one layer of upper epidermis and three layers of palisade mesophyll in *R. catawbiense*, whereas *R. ponticum* has two distinct layers of upper epidermis and two layers of palisade mesophyll. I suggest that the additional layer of upper epidermis in *R. ponticum* and thicker cuticle and extra palisade layer in *R. catawbiense* represent structural adaptations for reducing light injury in leaves and could serve a photoprotective function in winter when leaf photochemistry is generally sluggish. The overall higher opening of stomatal pores per unit leaf area in *R. catawbiense* indicates that *R. catawbiense* may be more prone to winter desiccation and that thermonasty may be a particularly beneficial trait in this species by serving as desiccation-avoidance strategy in addition to a photoprotection role.

Comparative study of photoprotection strategies at biochemical and molecular levels during seasonal cold acclimation between the two *Rhododendron* species suggests that the two species respond differently to winter conditions and have evolved various strategies to reduce and / or tolerate photooxidative stress in winter (chapter 3). In particular, both species have evolved some common strategies including downregulation of photosynthesis capacity, accumulation of early light-induced proteins (ELIPs) and antioxidant systems. *R. ponticum* accumulates overall higher antioxidant metabolites and enzyme activities, whereas, *R. catawbiense* has more efficient upregulation of ELIPs and antioxidant systems during seasonal cold acclimation; *R. catawbiense* also exhibits thermonastic leaf movements. Both species undergo photoinhibition during winter with *R. ponticum* leaves being relatively less photoinhibited. Such difference may be related to differential sensitivity to excess light in winter and protection efficiencies of ELIPs and antioxidants in the two species, among other adaptations. Although, thermonasty did not seem to provide a clear added advantage to resist photoinhibition in *R. catawbiense*, its adaptive significance in photoprotection cannot be ruled out. The differences in photoinhibition may also be associated with the distinct leaf anatomies (as shown in chapter 2) in the two species. The additional layer of upper epidermis in *R. ponticum*, and extra palisade layer and waxy cuticle in *R. catawbiense* might represent leaf structural adaptations for reducing light injury in winter in these species, and together with ELIPs, antioxidant system and thermonasty constitute photoprotection system in rhododendrons.

To investigate whether or not *RcPIP2s* expression patterns were associated with leaf curling, the leaves of the thermonastic and nonthermonastic species (*R. catawbiense* and *R. ponticum*, respectively) were exposed to a series of temperature regimes in controlled

conditions (chapter 4). Progressively cooler temperatures in the subfreezing range employed in this study induced thermonastic leaf curling in *R. catawbiense* (and uncurling upon warming), whereas *R. ponticum* leaves showed no curling. Data of gene expression at the transcriptional level using real-time RT-PCR showed similar expression patterns of *RcPIP2s* across the two species, suggesting that there is no apparent association between *RcPIP2s* expression and leaf curling / no curling in the two *Rhododendron* species. However, further investigations involving AQP studies at the protein level as well as at the transcriptional level corresponding to the adaxial and abaxial sides of the leaf with more thermonastic and nonthermonastic *Rhododendron* species may provide further insights into the role of AQPs in leaf curling in *Rhododendron*.

Appendix A

P-values for the Tables and Figures in the Dissertation

This appendix provides the p-values for the statistical analyses of the data presented in the chapters 2, 3 and 4 of this dissertation. In each table, p-values are presented for both the mean comparisons between species as well as mean differences within each species. Table 1 shows the p-values for the data from chapter 2 (JASHS paper). Tables 2-11 describe the p-values for the data in chapter 3 (Plant Science paper). Tables 12 and 13 show the p-values for the data in Figure 2 of chapter 4.

Table 1. P-values for the data from chapter 2 (JASHS paper). NA, non-acclimated; CA, cold-acclimated.

	Difference across the species in NA leaves	Difference across the species in CA leaves	Difference within the species (*R. ponticum*) in NA and CA leaves	Difference within the species (*R. catawbiense*) in NA and CA leaves
LT_{50}[a]	< 0.001	< 0.001	< 0.001	< 0.001
Fv/Fm[a]	0.539	0.041	0.005	< 0.001
Thickness of leaf blades[b]	< 0.001	< 0.001	< 0.001	< 0.001
Thickness of adaxial epidermis[b]	< 0.001	< 0.001	0.003	0.989
Depth of palisade parenchyma[b]	< 0.001	0.183	< 0.001	0.284
Thickness of adaxial cuticles[c]	0.67	< 0.001	0.404	< 0.001
Stomatal density[d]	< 0.001	< 0.001	0.163	< 0.001
Length of stomatal pores[e]	< 0.001	< 0.001	0.072	0.502
Width of stomatal pores[e]	< 0.001	< 0.001	0.625	0.332
Opening area of stomatal pores[e]	< 0.001	0.002	0.898	0.001

[a]Data are from Table 1 of chapter 2; [b]Data are from Figure 4 of chapter 2; [c]Data are from Figure 5E of chapter 2; [d]Data are from Figure 6E of chapter 2; [e]Data are from Figure 7E-G of chapter 2.

Table 2. P-values for the seasonal changes of maximum photosynthetic rate (P_{max}) in Figure 3C of chapter 3.

	Sep 20	Oct 4	Oct 25	Nov 6	Nov 25
Difference between species	**0.125**	**0.001**	**< 0.001**	**< 0.001**	**< 0.001**
Difference within species					
R. ponticum (Sep 20)		0.445	0.159	0.004	< 0.001
R. ponticum (Oct 4)			0.474	0.018	< 0.001
R. ponticum (Oct 25)				0.091	0.002
R. ponticum (Nov 6)					0.092
R. catawbiense (Sep 20)		0.023	< 0.001	< 0.001	< 0.001
R. catawbiense (Oct 4)			0.126	< 0.001	< 0.001
R. catawbiense (Oct 25)				0.001	< 0.001
R. catawbiense (Nov 6)					0.007

Table 3. P-values for the diurnal changes of maximal quantum yield of photosystem II (Fv/Fm) in Figure 4A of chapter 3.

	8	10	12	14	16	18
Difference between species	**0.745**	**0.927**	**0.766**	**0.049**	**0.208**	**0.142**
Difference within species						
R. ponticum (8)		0.909	0.546	0.054	0.098	0.42
R. ponticum (10)			0.624	0.069	0.121	0.488
R. ponticum (12)				0.171	0.278	0.837
R. ponticum (14)					0.766	0.241
R. ponticum (16)						0.376
R. catawbiense (8)		0.728	0.226	< 0.001	0.003	0.013
R. catawbiense (10)			0.382	< 0.001	0.006	0.029
R. catawbiense (12)				0.004	0.046	0.166
R. catawbiense (14)					0.291	0.092
R. catawbiense (16)						0.505

Table 4. P-values for the seasonal changes of maximal quantum yield of photosystem II (Fv/Fm) in Figure 4C of chapter 3.

	Aug 27	Sep 29	Oct 23	Nov 25
Difference between species	**0.8**	**0.716**	**0.528**	**0.175**
Difference within species				
R. ponticum (Aug 27)		1	0.57	< 0.001
R. ponticum (Sep 29)			0.57	< 0.001
R. ponticum (Oct 23)				< 0.001
R. catawbiense (Aug 27)		0.912	0.158	< 0.001
R. catawbiense (Sep 29)			0.13	< 0.001
R. catawbiense (Oct 23)				< 0.001

Table 5. P-values for the seasonal changes of total leaf chlorophyll content in Figure 5 of chapter 3.

	Aug 15	Sep 9	Oct 21	Nov 8	Dec 6
Difference between species	**0.002**	**0.013**	**0.003**	**0.0171**	**0.106**
Difference within species					
R. ponticum (Aug 15)		0.07	0.016	< 0.001	< 0.001
R. ponticum (Sep 9)			0.49	0.002	0.001
R. ponticum (Oct 21)				0.01	0.006
R. ponticum (Nov 8)					0.83
R. catawbiense (Aug 15)		0.275	0.019	0.003	< 0.001
R. catawbiense (Sep 9)			0.168	0.036	0.013
R. catawbiense (Oct 21)				0.421	0.205
R. catawbiense (Nov 8)					0.631

Table 6. P-values for the seasonal changes of leaf malondialdehyde (MDA) content in Figure 8A of chapter 3.

	Aug 15	Sep 9	Oct 21	Nov 8	Dec 6
Difference between species	**< 0.001**	**0.003**	**0.002**	**0.096**	**0.148**
Difference within species					
R. ponticum (Aug 15)		0.032	0.006	< 0.001	< 0.001
R. ponticum (Sep 9)			0.442	0.004	< 0.001
R. ponticum (Oct 21)				0.023	0.004
R. ponticum (Nov 8)					0.463
R. catawbiense (Aug 15)		< 0.001	< 0.001	< 0.001	< 0.001
R. catawbiense (Sep 9)			0.517	< 0.001	< 0.001
R. catawbiense (Oct 21)				< 0.001	< 0.001
R. catawbiense (Nov 8)					0.333

Table 7. P-values for seasonal changes of total ascorbate content in Figure 8B of chapter 3.

	Aug 15	Sep 9	Oct 21	Nov 8	Dec 6
Difference between species	**< 0.001**	**< 0.001**	**< 0.001**	**< 0.001**	**0.005**
Difference within species					
R. ponticum (Aug 15)		0.921	0.182	0.094	< 0.001
R. ponticum (Sep 9)			0.214	0.113	< 0.001
R. ponticum (Oct 21)				0.712	0.002
R. ponticum (Nov 8)					0.004
R. catawbiense (Aug 15)		0.056	0.009	0.005	< 0.001
R. catawbiense (Sep 9)			0.392	0.277	< 0.001
R. catawbiense (Oct 21)				0.811	< 0.001
R. catawbiense (Nov 8)					< 0.001

Table 8. P-values for the seasonal changes of total glutathione content in Figure 8C of chapter 3.

	Aug 15	Sep 9	Oct 21	Nov 8	Dec 6
Difference between species	**< 0.001**	**< 0.001**	**0.003**	**< 0.001**	**< 0.001**
Difference within species					
R. ponticum (Aug 15)		< 0.001	< 0.001	< 0.001	< 0.001
R. ponticum (Sep 9)			< 0.001	< 0.001	< 0.001
R. ponticum (Oct 21)				< 0.001	< 0.001
R. ponticum (Nov 8)					< 0.001
R. catawbiense (Aug 15)		< 0.001	< 0.001	< 0.001	< 0.001
R. catawbiense (Sep 9)			< 0.001	< 0.001	< 0.001
R. catawbiense (Oct 21)				< 0.001	< 0.001
R. catawbiense (Nov 8)					< 0.001

Table 9. P-values for the seasonal changes of superoxide dismutase (SOD) in Figure 9A of chapter 3.

	Aug 15	Sep 9	Oct 21	Nov 8	Dec 6
Difference between species	**< 0.001**	**< 0.001**	**< 0.001**	**< 0.001**	**< 0.001**
Difference within species					
R. ponticum (Aug 15)		0.19	0.114	0.009	< 0.001
R. ponticum (Sep 9)			0.772	0.146	< 0.001
R. ponticum (Oct 21)				0.236	< 0.001
R. ponticum (Nov 8)					< 0.001
R. catawbiense (Aug 15)		0.008	0.001	< 0.001	< 0.001
R. catawbiense (Sep 9)			0.466	0.001	< 0.001
R. catawbiense (Oct 21)				0.008	< 0.001
R. catawbiense (Nov 8)					< 0.001

Table 10. P-values for the seasonal changes of catalase (CAT) in Figure 9C of chapter 3.

	Aug 15	Sep 9	Oct 21	Nov 8	Dec 6
Difference between species	**0.205**	**0.592**	**0.045**	**< 0.001**	**0.003**
Difference within species					
R. ponticum (Aug 15)		0.112	0.007	< 0.001	< 0.001
R. ponticum (Sep 9)			0.185	< 0.001	< 0.001
R. ponticum (Oct 21)				0.002	< 0.001
R. ponticum (Nov 8)					0.338
R. catawbiense (Aug 15)		0.039	0.025	0.002	< 0.001
R. catawbiense (Sep 9)			0.831	0.224	0.004
R. catawbiense (Oct 21)				0.312	0.007
R. catawbiense (Nov 8)					0.062

Table 11. P-values for the seasonal changes of peroxidase (POD) in Figure 9D of chapter 3.

	Aug 15	Sep 9	Oct 21	Nov 8	Dec 6
Difference between species	**0.683**	**0.199**	**0.002**	**0.005**	**< 0.001**
Difference within species					
R. ponticum (Aug 15)		0.029	< 0.001	< 0.001	< 0.001
R. ponticum (Sep 9)			< 0.001	< 0.001	< 0.001
R. ponticum (Oct 21)				0.254	< 0.001
R. ponticum (Nov 8)					< 0.001
R. catawbiense (Aug 15)		0.167	< 0.001	< 0.001	< 0.001
R. catawbiense (Sep 9)			0.007	< 0.001	< 0.001
R. catawbiense (Oct 21)				0.143	0.004
R. catawbiense (Nov 8)					0.104

Table 12. P-values for quantitative expression of *RcPIP2;1* gene in Figure 2A of chapter 4.

	Control	0	-2	-4	-6	-3	0	21
Difference between species	**< 0.001**	**< 0.001**	**< 0.001**	**< 0.001**	**< 0.001**	**< 0.001**	**< 0.001**	**< 0.001**
Difference within species								
R. ponticum (Control)		0.424	0.025	0.004	0.003	0.046	0.003	0.292
R. ponticum (0°C)			0.003	< 0.001	0.025	0.216	< 0.001	0.069
R. ponticum (-2°C)				0.458	< 0.001	< 0.001	0.39	0.21
R. ponticum (-4°C)					< 0.001	< 0.001	0.906	0.051
R. ponticum (-6°C)						0.286	< 0.001	< 0.001
R. ponticum (-3°C)							< 0.001	0.004
R. ponticum (0°C)								0.039
R. catawbiense (Control)		0.889	0.726	0.217	0.271	0.18	0.179	0.472
R. catawbiense (0°C)			0.625	0.271	0.335	0.227	0.226	0.561
R. catawbiense (-2°C)				0.117	0.151	0.094	0.094	0.288
R. catawbiense (-4°C)					0.889	0.912	0.91	0.599
R. catawbiense (-6°C)						0.803	0.801	0.698
R. catawbiense (-3°C)							0.998	0.525
R. catawbiense (0°C)								0.523

Table 13. P-values for quantitative expression of *RcPIP2;2* gene in Figure 2B of chapter 4.

	Control	0	-2	-4	-6	-3	0	21
Difference between species	**< 0.001**	**< 0.001**	**< 0.001**	**< 0.001**	**< 0.001**	**< 0.001**	**< 0.001**	**< 0.001**
Difference within species								
R. ponticum (Control)		< 0.001	< 0.001	0.94	< 0.001	< 0.001	0.224	0.21
R. ponticum (0°C)			< 0.001	< 0.001	0.022	< 0.001	< 0.001	< 0.001
R. ponticum (-2°C)				< 0.001	< 0.001	0.023	< 0.001	< 0.001
R. ponticum (-4°C)					< 0.001	< 0.001	0.198	0.185
R. ponticum (-6°C)						< 0.001	< 0.001	< 0.001
R. ponticum (-3°C)							< 0.001	< 0.001
R. ponticum (0°C)								0.969
R. catawbiense (Control)		0.444	0.66	0.002	< 0.001	< 0.001	< 0.001	0.003
R. catawbiense (0°C)			0.232	0.016	0.006	0.002	0.002	0.021
R. catawbiense (-2°C)				< 0.001	< 0.001	< 0.001	< 0.001	< 0.001
R. catawbiense (-4°C)					0.677	0.421	0.408	0.921
R. catawbiense (-6°C)						0.696	0.678	0.606
R. catawbiense (-3°C)							0.981	0.367
R. catawbiense (0°C)								0.355

APPENDIX B

Freezing Tolerance Tests and Calculation of LT_{50} for *Rhododendron* Leaves

Arora Lab

Department of Horticulture, Iowa State University, Ames, IA 50011, USA

This protocol describes the tests of leaf freezing tolerance in overwintering rhododendrons. Tissues are subjected to a controlled freeze-thaw regime followed by the assessment of injury by measuring electrolyte leakage from freeze-thaw injured tissues as described by Lim et al. (1998). Due to the high freezing tolerance of rhododendron leaves (up to –50 °C or colder), freezing tests are conducted in a temperature-controlled glycol bath (Isotemp 3028; Fisher Scientific, Pittsburgh, PA) for the leaves collected from June to middle October, and in a programmable freezer (model 85-3.1; ScienTemp, Adrian, MI) for the leaves collected from middle October to January; glycol bath can be cooled only up to –20 °C while programmable freezer can go up to –70°C.

Tests in the glycol bath

1. Turn on the glycol bath before preparing samples since it takes around 1.5 h for the bath to cool the glycol from room temperature to ~ –1 °C. Make sure that the glycol level is between the “high” and “low” marks at all times. Add more glycol if needed.
2. Prepare the non-acclimated samples at room temperature. Label test tubes (25x200mm) and add 80 µl ddH_2O to each tube including three controls (controls should stay at 0 °C without freezing throughout the freezing test). Wash the leaves and blot up the water

before punching leaf discs (diameter = 1.27 cm) with a borer. Put the discs at the bottom of the tubes, making sure that discs are in contact with water. Three to four replications are made at each treatment temperature from individual leaves (one leaf from each of the plants per species). The temperatures chosen to cool the samples depend on the possible freezing tolerance of the tissues.

3. Cover the tubes with bolts (to avoid the tubes from floating over) and put the tubes in the bath (the bath temperature should already be –1 °C). The tubes are incubated in the bath for 1 hr, at which point ice chips (*not too big or small*) are added to initiate ice-nucleation. After an additional hour at –1 °C, the temperature is cooled at a rate of 1 °C per hour until the lowest treatment temperature. Samples at each treatment temperature are removed from the glycol bath and thawed on ice overnight.
4. Measure the ion leakage. The next day samples are removed from ice and incubated at 4 °C for 1 hr and then at room temperature for another hour. Add 20 ml demineralised water to each tube and vacuum infiltrate (three times for 3 min each at ~100 kPa) with caps off. Cap the tubes and shake them for 3 h at 250 rpm. Then measure the initial electrical conductivity with a conductivity meter (model 3100; YSI Inc, Yellow Spring, OH). With the caps back on, secure the tubes with aluminum foil firmly taped over and around them. Autoclave the samples at 121 °C for 20 min (program 2). Cool down the samples to room temperature (usually takes 3-4 h) and measure the final electrical conductivity after a quick vortex.

Tests in the programmable freezer

1. Pre-set a ramp / soak program applicable to your freezing protocol (cooling rate and treatment temperatures, etc). For example, for rhododendron leaves, we use ~ 1 °C per hour cooling rate during the first 4 hours (up to –3 °C) and thereafter ~ 4 °C per hour cooling rate until the lowest treatment temperature is reached.
2. Prepare cold-acclimated samples in the cold room. This step is almost the same as for non-acclimated samples above expect preparing the samples in the cold room to avoid potential deacclimation. Also prepare three extra samples to monitor tissues temperatures using thermocouples.
3. Place the samples in the freezer and start the program. Ice chips are not added to initiate ice nucleation; however, ice nucleation does occur (typically between –2 and –4 °C) due to water in the tubes when the tissues are cooled relatively slowly (~ 1 °C per hour). Remove the samples when the tissue temperature reaches the treatment temperature.
4. Measure the ion leakage as described earlier.

Leaf freezing tolerance calculated by LT_{50}

IEC: initial electrical conductivity FEC: final electrical conductivity

% IL_t and % IL_c represent percentage ion leakage at treatment and control temperatures.

- percentage ion leakage (% IL) = IEC / FEC
- percentage injury (% $injury_t$) = (% IL_t – % IL_c) / (100 – % IL_c) * 100
- percentage adjusted injury (% adjusted $injury_t$) = (% $injury_t$ / % $injury_{max}$) * 100; here % $injury_{max}$ is the injury at –80^{o}C.

- Adjusted Injury (Adjusted_Inj): adjust the values from % adjusted injury such that if values are negative, adjust them to 0; while if values are greater than 100, adjust them to 100.
- The leaf freezing tolerance is represented by LT_{50}, the temperature at which 50% tissue is killed.

Below is an example data set to illustrate the calculation described above. Please note that the two temperature series (control and –80 ^{o}C) in the first column are not treatment temperatures.

Temp	**IEC**	**FEC**	**% IL**	**% Injury**	**% Adjusted Injury**	**Adjusted_Inj**
CTR	2.7	26.8	9.9	10.1		
CTR	2.4	20.7	11.6			
CTR	2.2	24.5	8.9			
-10	3.3	32.9	10.1	0.0	-0.1	0.0
-10	2.3	19.1	12.2	2.4	8.8	8.8
-10	2.7	23.3	11.7	1.8	6.7	6.7
-14	3.6	32.2	11.3	1.3	4.7	4.7
-14	2.5	22.3	11.2	1.2	4.3	4.3
-14	2.9	25.2	11.4	1.5	5.4	5.4
-18	3.5	30.3	11.6	1.6	6.2	6.2
-18	2.9	22.1	13.0	3.2	12.0	12.0

-18	2.9	23.4	12.3	2.4	9.2	9.2
-22	5.2	34.0	15.2	5.6	21.1	21.1
-22	3.4	24.7	13.9	4.2	15.8	15.8
-22	3.5	25.9	13.4	3.6	13.6	13.6
-26	5.5	31.0	17.6	8.3	31.1	31.1
-26	3.8	26.4	14.3	4.6	17.3	17.3
-26	4.3	25.4	16.8	7.4	27.8	27.8
-30	6.0	32.1	18.6	9.4	35.3	35.3
-30	5.8	26.5	21.8	13.0	48.6	48.6
-30	3.7	22.1	16.6	7.2	26.9	26.9
-35	6.6	30.3	21.8	13.0	48.8	48.8
-35	5.7	26.7	21.2	12.4	46.3	46.3
-35	6.3	24.6	25.6	17.2	64.2	64.2
-40	8.4	32.5	25.8	17.5	65.3	65.3
-40	5.7	24.9	22.8	14.1	52.8	52.8
-40	5.3	21.3	24.6	16.1	60.3	60.3
-45	8.1	31.2	26.0	17.7	66.3	66.3
-45	6.7	25.7	26.2	17.9	66.8	66.8
-45	9.1	27.1	33.7	26.3	98.3	98.3
-50	9.7	20.9	46.2	40.1	150.1	100.0
-50	17.3	29.3	59.1	54.5	203.8	100.0

-50	15.1	29.3	51.7	46.3	173.1	100.0
-80	9.8	31.5	31.1	23.4	26.7	
-80	8.1	24.8	32.6	25.0		
-80	11.1	28.7	38.7	31.8		

Use SAS code to calculate LT_{50} and standard error of LT_{50}. Since repeating the entire freezing test to obtain variable LT_{50} is not efficient and often impractical, this SAS code was developed to estimate mean LT_{50} and the standard errors of LT_{50} based on the Jackknife method (Efron, 1982). The Jackknife method involves taking out one data point at a time and estimating the LT_{50}. The removed data point was replaced by another data point and LT_{50} was re-estimated. This process was repeated until all data points were removed and reincorporated. By the end of this process, there should at least be 30 estimates (if nine treatment temperatures plus control with three replications) of LT_{50} for a data set as above, thus giving a mean and standard error. Before running the SAS code, first copy and paste the data from the first and last columns to a new Excel sheet (name as sheet1 here). The contents with bold and blue are the codes and detailed explanations of the codes are described in parentheses.

proc import (proc import allows us to import data from an xls file)

datafile="F:\1.8.2008.xls" out=xw replace; (out=. is how the sas data set is named)

sheet="sheet1";

range= 'A1:B31'; (Range is the range on the excel sheet that you want to be read into SAS)

getnames=yes; (getnames = yes tells SAS that the first row shows column names)

run;

(This is the start of the macro that gives the jackknife estimates the first line simply names a function which I called jackknife. The do command needs to be adjusted for each data set. Start at one but '30' needs to change to how many observations you have)

%macro jacknife;

%do i = 1 %to 30;

data datanew;

set wx; (change gp to the name that you give the data set that you read in)

if _N_ = &i then delete;

run;

proc nlin data=datanew method=marquardt best=1 iter=1000; (proc nlin estimates Gompertz curve using nonlinear least squares)

parms B=1 to 100 by 1 K=-0.30 TO -0.01 BY 0.01;

EF = exp(-K*temp);

EEF = exp(-B*EF);

model Adjusted_Inj = 100*EEF; (Adjusted_inj is what I called the adjusted injury percentage. Put whatever you named it there)

DER.B = -100*EF*EEF;

DER.K = 100*B*temp*EF*EEF;

output out=est p=gompertz;

ods output ParameterEstimates=parms; (This provides a sas data set with the estimates of B and K to get LT_{50})

run;

proc transpose data=parms out=tparms; (To get at the B and K, transpose data and rename something)

run;

(Create a sas data set containing an estimate of LT_{50} for each jackknife data set - leave one observation out)

data gest&i;

set tparms;

if _NAME_ = 'Estimate' then B = Col1;

if _NAME_ = 'Estimate' then K = Col2;

if _NAME_ ^= 'Estimate' then delete;

drop _LABEL_ Col1 Col2;

LT50 = -log((log(100)-log(50))/B)/K;

run;

```
%end;
%mend;

options mlogic symbolgen;
%jacknife;
```

(From the above code 30 data sets were created containing estimates of LT_{50} labeled gest1 - gest 30. If one has more than 30 observations or less, add or subtract gesti data sets after the set statement in the below data step accordingly)

```
data LT50;
set gest1 gest2 gest3 gest4 gest5 gest6 gest7 gest8 gest9 gest10 gest11 gest12 gest13 gest14
gest15 gest16 gest17 gest18 gest19 gest20 gest21 gest22 gest23 gest24 gest25 gest26
gest27 gest28 gest29 gest30;
run;
```

(This gives an estimate of standard deviation)

```
proc univariate data=LT50 ;
var LT50;
ods output  BasicMeasures=sd;
```
(sd is a data set that contains mean standard deviation from jackknife estimates of LT_{50})

```
run;
```

```
data sd;
set sd;
if VarMeasure ^= 'Std Deviation' then delete;
SEjk = sqrt((VarValue)**2*(29)*(29/30));
```
(This gives jackknife standard error but where 30 is the number of observations you have)

```
run;

proc print data=sd;
run;
```

Temp	Adjusted_Inj
-10	0.0
-10	8.8
-10	6.7
-14	4.7
-14	4.3
-14	5.4
-18	6.2
-18	12.0
-18	9.2
-22	21.1
-22	15.8
-22	13.6
-26	31.1
-26	17.3
-26	27.8
-30	35.3
-30	48.6
-30	26.9
-35	48.8
-35	46.3
-35	64.2
-40	65.3
-40	52.8
-40	60.3
-45	66.3
-45	66.8
-45	98.3
-50	100.0
-50	100.0
-50	100.0

References

- Efron, B. 1982. The Jackknife, the Bootstrap and other resampling plans. CBMS-NSF Reg. Conf. Ser. Appl. Mathematics 38. Soc. Ind. Appl. Mathematics, Philadelphia.
- Lim C.C., Arora R., and Townsend E.C. (1998) Comparing Gompertz and Richards functions to estimate freezing injury in *Rhododendron* using electrolyte leakage. *Journal of the American Society for Horticultural Science* 123: 246–252.

APPENDIX C

Microscale Hot Borate Method for RNA Extraction from *Rhododendron* Leaves

Arora Lab

Department of Horticulture, Iowa State University, Ames, IA 50011, USA

Prior to Extractions

- Bake all necessary glassware, metal spatulas, mortars, and pestles overnight in a 200 °C oven after wrapping them in aluminum foil. For each sample, prepare one mortar and pestle, one homogenizer and one spatula.
- DEPC-treat a sufficient volume of water for all solutions (500 ml is usually plenty).
- Prepare all reagents and solutions using autoclaved or baked glassware.

Reagents and Solutions

1. DEPC-Treated Water

   Perform all these steps under a fume hood with gloves since DEPC is a carcinogen. Add 0.05% (v/v) DEPC to the required volume of ddH_2O (for example, 250 µl DEPC to 500 ml H_2O). Mix by vigorous stirring overnight and then autoclave to break down the DEPC.

2. Hot Borate Extraction Buffer (XT Buffer) 500 ml

0.2 M Borax (Sodium-borate decahydrate) [MW=381.4]	38.14 g
30 mM EGTA [MW=380.4]	5.71 g
1% (w/v) SDS	5 g

1% sodium deoxycholic acid (deoxycholate, sodium salt)	5 g
*10 mM DTT	0.77 g
*1% Nonidet P-40, (NP-40)	5 ml
*2% (w/v) PVP-40	10 g

Dissolve Borax, EGTA, SDS, and sodium deoxycholic acid with ddH_2O in a beaker which is placed on a stirrer/heat plate (add stir bar and adjust the heat knob to 5). Cool the solution to room temperature and then adjust pH to 9.0 with NaOH. Make the solution to final volume of 500 ml. Add 250 µl DEPC to this solution, stir overnight, and autoclave next day.

The chemicals marked with * are added just before the actual extraction is conducted.

3. Proteinase K (10 mg/ml in DEPC-treated ddH_2O; aliquot and store stock at –20 °C)

The following solutions (items 4–7) are prepared with dissolving chemicals in DEPC-treated H_2O. After making them, add appropriate amount of DEPC (for example, 50 µl DEPC to 100 ml solution) and stir overnight. Autoclave next day, cool them down to room temperature, and then store at 4 °C.

4. 10 mM Tris-HCl with 1 mM EDTA (dissolve Tris-base with ddH_2O and adjust pH to 7.5 with HCl)
5. 2 M potassium chloride (KCl)
6. 2 M potassium acetate (KAc, adjust pH to 5.5 with glacial acetic acid)
7. 2 M and 8 M lithium chloride (LiCl, store at 4 °C)
8. Ethanol, 70% and 100% (store at –20 °C)

Day 1

1. Set water bath to 80 °C. Put the 14-ml Falcon plastic tubes containing 3.5ml XT buffer (for 1 g tissue) with caps on in the bath to pre-warm. Pre-chill mortars and pestles to be used with liquid nitrogen.
2. Weigh 1 g of fresh tissue quickly and flash freeze in liquid nitrogen.
3. Grind tissue in liquid nitrogen until it is fine powder.
4. Transfer the powder to the tubes with XT buffer and vortex gently for 1 min. Add 105 µl proteinase K solution (~2.2 mg) to the tissues and briefly vortex.
5. Shake the homogenate (130 rpm) at 42 °C for 1.5 h in the Incubator Shaker 4200 under the oven.
6. Remove the tubes from the shaker. Add 280 µl of 2 M KCl for a final concentration of 160 mM (*This step will precipitate proteins from the extract*). Gently vortex to mix. Incubate on ice for 1 h.
7. Centrifuge at 12,000 g for 20 min at 4°C (pre-chill the centrifuge and rotor at 4 °C for 20 min.
8. Transfer the supernatants to new labeled 14-ml Falcon tubes.
9. Add 1/3 volume of 8 M LiCl (making a final concentration of 2 M) to each sample. Incubate on ice overnight.

Day 2

1. Place tubes in the pre-chilled centrifuge and chilled rotor. Spin at 12,000 g for 20 min at 4 °C. Decant and discard supernatant.

2. Wash pellets in 4 ml of ice-cold 2 M LiCl. Disperse pellets with sterile disposable pipettes (as needed) after adding LiCl. This will minimize the retention of unwanted substances.
3. Centrifuge tubes at 12,000 g for 12 min at 4 °C. Decant and discard supernatant.
4. Repeat steps 2 & 3 at least three times or more if needed (*The supernatant should become quite clear after hand swirling when pellets have been well washed*).
5. Suspend pellets in 3 ml of 10 mM Tris-HCl (pH 7.5) and gently vortex at room temperature (*The sample may be warmed to room temperature to facilitate dissolving of pellets*).
6. Remove the insoluble material by centrifuging tubes at 12,000 g for 10 min at 4 °C.
7. Save the supernatant and transfer it to new pre-labeled 14-ml Falcon tubes. Add 300 µl (1/10 vol) of 2 M KAc (pH 5.5). Incubate on ice for 15 min. (*This will remove positively-charged polysaccharides, residual proteins, and other salt-insoluble material*)
8. Centrifuge tubes at 12,000 g for 10 min at 4 °C. Discard pellet by transferring supernatant to a new tube.
9. Precipitate RNA with 2.5X volume (~ 7.5 ml) of cold 100% ethanol. Store at –80 °C for 1-2 h or –20 °C overnight.
10. Centrifuge at ~10,000 g for 30 min at 4 °C to collect RNA. Remove ethanol and discard.
11. Wash pellets with 2 ml of 70% ethanol. Centrifuge at ~10,000 g for 5 min at 4 °C. Aspirate or pipette off the ethanol.

12. Re-suspend RNA in 100 µl of DEPC-treated water and you should see RNA pellet "dance" in solution and dissolve almost instantaneously.
13. Quantify the RNA concentration with the spectrophotometer (A_{260} and A_{280}).
14. Assess the quality of the RNA in an agarose gel (see the details below).
15. Aliquot RNA in several tubes for each sample to avoid possible degradation due to future freeze/thaw cycles. Store samples at –80 °C.

Check RNA quality in the agarose gel

Prepare the following buffers and solutions prior to running gels.

(1) 50X TAE buffer (1 L)

To make 1 L 50X TAE buffer, weigh 242 g Tris base, 136 g Na-Acetate and 18.6 g Na_2EDTA, and dissolve them with DEPC-treated H_2O. Adjust pH to 8.2 with glacial acetic acid and bring final volume to 1 L (store at RT). We use 1X TAE buffer for dissolving agarose and running gels, therefore, dilute 50X buffer to 1X buffer (for example, to make 1 L 1X buffer, take 20 ml 50X buffer and add DEPC-treated H_2O to 1 L).

(2) Ethidium Bromide (EB) (10 ml)

EB is a mutagen and must be handled with care. To make a 10 mg / ml stock, weigh 0.1 g EB and dissolve it with 10 ml DEPC-treated H_2O. Add a stir bar and let it dissolve several hours to overnight. Store in a brown bottle or cover it with aluminum foil.

(3) Gel loading buffer (10 ml)

To make 10 ml gel loading buffer, dissolve 25 mg bromophenol blue and 4 g sucrose with DEPC-treated H_2O to the final volume of 10 ml. The general rule is to use 1µl of gel loading buffer per 5µl of sample.

Making the gel

1. To make 1% agarose gel, weigh 0.3 g agarose into a 250 ml flask. Add 35 ml 1X TAE buffer. Swirl and microwave for about 1 minute to dissolve the agarose.
2. Cool the gel solution for about three minutes and then add 1µl EB and swirl.
3. Seal the gel casting plate with tape. Insert a comb in the end slot of the casting plate and the distance between the plate bottom and the teeth ends of the comb should be ~ 3 mm. Pour the gel slowly and push any bubbles away to the side using a disposable tip.
4. Leave the gel to be polymerized for at least 30 min.
5. Pour 1X TAE buffer into the gel tank to submerge the gel to 2–5 mm depth.

Preparing the samples and running the gel

1. Mix 8 µl RNA sample (~0.5 µg RNA) with 2µl gel loading buffer into a microfuge tube.
2. Load the sample into the well and close the gel tank.
3. Switch on the power and run the gel at a constant voltage (80 V) for ~ 45 min.

4. Switch off and unplug the gel tank. Visualize the gel under an ultraviolet light source in a dark-room. The good quality RNA should show two main bright bands (28S and 18S rRNA). The degraded RNA shows visible diffusion or smear underneath the two main bands.

More Information

- This protocol was adapted from Wilkins, T. A. and L. B. Smart (1996). Isolation of RNA from plant tissues *in* Krieg, P. A. (ed.) A Laboratory Guide to RNA: Isolation, Analysis, and Synthesis. Wiley-Liss, Inc.: 21-40.
- This procedure has also produced decent yields of RNA from cotton tissues, a genus that does not easily yield nucleic acids due to polysaccharides, phenolics, etc.
- Yield is approximately 30-100 µg / g leaf tissue in rhododendrons.

APPENDIX D

Light and Electron Microscopy (EM) for *Rhododendron* Leaves

Arora Lab

Department of Horticulture, Iowa State University, Ames, IA 50011, USA

Light and transmission electron microscopy (LM and TEM)

1. Punch leaf discs (diameter = 1 mm) from the mid-length along midribs in the cold room (cold-acclimated leaves) or room temperature (non-acclimated leaves). Put leaf discs into the vials containing the fixative (2% paraformaldehyde/2% glutaraldehyde in 100 mM cacodylate buffer at pH 7.2 with the addition of 1% caffeine). (*Caffeine is used to prevent phenolics from leaking out the vacuole, causing penetration problem after step 7*)
2. Put the vials with loosened caps in vacuum for 2 h until all discs sink to the bottom of the vials. Put the vials at 4 °C overnight. (*It is also safe to store the samples at 4 °C for at least one week before going to the next washing steps*)
3. Wash the discs with 100 mM cacodylate buffer (pH 7.2) at room temperature for three times/20 min each.
4. Wash the discs with ddH_2O briefly.
5. Wash the samples with 25%, 50%, 70%, 95%, and 100% ethanol, respectively, for 30 min at each step. (*This process helps to dehydrate the samples*).
6. Wash with pure acetone twice/30 min each.
7. Penetrate samples with acetone : spurr's resin (3:1) for 24 h.

8. Penetrate samples with acetone : spurr's resin (1:1) for 24 h in vacuum.
9. Penetrate samples with acetone : spurr's resin (1:3) for 48 h in vacuum.
10. Treat samples with pure spurr's resin for 24 h with caps off.
11. Treat samples again with fresh pure spurr's resin for 24 h with caps loosing.
12. Embed samples at 60 °C in an oven for 48 h.
13. Take out the fixed samples and make thick sections (1 μm for light microscopy) or thin sections (80 nm for TEM) with an ultramicrotome using glass or diamond knives.
14. The samples are now ready to be viewed with a light microscope. See the instruction to use a light microscope (Olympus BH10; Olympus Imaging America Inc.) with bright-field optics in the package.

Scanning electron microscopy (SEM)

Most parts of this protocol are the same as those for TEM except few steps.

1. Punch leaf discs (diameter = 10 mm) from the mid-length along midribs in the cold room (cold-acclimated leaves) or room temperature (non-acclimated leaves). Put leaf discs into the vials containing the fixative (2% paraformaldehyde/2% glutaraldehyde in 100 mM cacodylate buffer at pH 7.2).
2. Put the vials with loosened caps in vacuum for 2 h until all discs sink to the bottom of the vials. Put the vials at 4 °C overnight. (*It is also safe to store the samples at 4 °C for at least one week before going to the next washing steps*)
3. Wash the discs with 100 mM cacodylate buffer (pH 7.2) at room temperature for three times/20 min each).

4. Wash the discs with ddH_2O briefly.
5. Postfix samples with 1% osmium tetroxide (OsO_4). (*OsO_4 is very toxic so perform this step carefully under the hood*)
6. Wash the samples with 25%, 50%, 70%, 95%, and 100% ethanol, respectively, for 30 min at each step. (*This process helps to dehydrate the samples*).
7. Do the critical point dry using liquid CO_2 (DCP-1; Denton Vacuum). (See the instruction of this system in the package; this is a high pressure system, and perform it very carefully)
8. Attach the samples to aluminium stubs using adhesive tabs and silver painted around their edges. (*Samples can be stored in a jar with desiccatives for a long time use*)
9. Sputter-coat the samples with gold/palladium (20:80) for 2 min.
10. Samples are now ready to be viewed with a scanning electron microscope. See the instruction to use JEOL JSM-5800 LV scanning electron microscope (JEOL Ltd., Tokyo, Japan) in the package.

APPENDIX E

Malondialdehyde (MDA) Assay in *Rhododendron* Leaves

Arora Lab

Department of Horticulture, Iowa State University, Ames, IA 50011, USA

The production of MDA, a secondary end product of the oxidation of poly-unsaturated fatty acids, is considered a useful index of general lipid peroxidation. A common method for measuring MDA, referred as the thiobarbituric acid-reactive-substances (TBARS) assay, is to react it with thiobarbituric acid (TBA) and record the absorbance at 532 nm. This protocol is modified from Hodges *et al.* (1999).

Reagents

- **80% ethanol**

  80 ml ethanol is dissolved in ddH_2O (volume making up to 100 ml). Store @ 4 °C.

- **20% trichloroacetic acid (TCA)**

  20 g TCA is dissolved in ddH_2O (volume making up to 100 ml). Store @ 4 °C in dark.

- **20% trichloroacetic acid (TCA) containing 0.5% thiobarbituric acid (TBA)**

  20 g TCA and 0.5 g TBA are dissolved in ddH_2O (volume making up to 100 ml). Store @ 4 °C in dark.

Protocol

1. Pre-warm the water bath (90 °C) and pre-chill the centrifuge for 15 min at 2000 g/4 ºC.
2. Weigh 400 mg leaf tissue quickly and grind it into fine powder in liquid N_2.
3. Transfer the powder into a 14-ml plastic Falcon tube containing 5 ml 80% cold ethanol (on ice) and vortex vigorously.
4. Centrifuge at 3000 g for 15 min at 4 °C.
5. Discard pellet debris, save the supernatant into 500 µl aliquots for assay and keep on ice.
6. Mix 200 µl supernatant with 1 ml 20% TCA (−TBA); and 200 µl supernatant mixed with 1 ml 20% TCA containing 0.5% TBA (+TBA).
7. Vortex the mixture and incubate tubes at 90 °C for 1 h in the water bath. (*use 2 ml tubes; floaters*)
8. Turn on the spectrophotometer to warm up for 30 min before next step.
9. Cool down samples on ice and centrifuge at 3000 g for 10 min at 4 °C.
10. Read absorbance at 440, 532 and 600 nm of the mixture in each of the two tubes against a blank (everything but no supernatant).

Calculation of MDA content

- $[(A532_{+TBA}) - (A600_{+TBA}) - (A532_{-TBA} - A600_{-TBA})] = A$
- $[(A440_{+TBA} - A600_{+TBA}) \times 0.0571] = B$
- MDA concentration (nmol g^{-1}FW) = $2.5 \times$ **dilution** $\times [(A - B)/157000] \times 10^6$

MDA concentration is expressed as nmol MDA per gram of fresh weight. For example, if four ml supernatant is collected in step 5 for 400 mg tissue and 200 µl (step 6) is used, the **dilution** constant should be 20 (4ml/200µl). And then if you get 0.2 for (A – B), the MDA concentration should be calculated as: MDA concentration = 2.5 x 20 x (0.2/157000) × 10^6 = 63.5 nmol g^{-1}FW.

Reference

Hodges D, DeLong J, Forney C, Prange R. 1999. Improving the thiobarbituric acid-reactive-substances assay for estimating lipid peroxidation in plant tissues containing anthocyanin and other interfering compounds. Planta 207: 604–611.

APPENDIX F

Ascorbate Assay in *Rhododendron* Leaves

Arora Lab

Department of Horticulture, Iowa State University, Ames, IA 50011, USA

Ascorbate content is determined according to Law *et al.* (1983). The assay is based on the reduction of Fe^{3+} to Fe^{2+} by ascorbate in acidic solution. The Fe^{2+} forms a red chelate with bipyridyl absorbing at 525 nm.

Reagents

- **6% trichloroacetic acid (TCA)**

  6 g TCA dissolved in ddH_2O (volume making up to 100 ml). Store @ 4 °C in dark.

- **150 mM phosphate buffer (pH 7.4)**

  Prepare 1 M NaH_2PO_4 and Na_2HPO_4 solutions. Take 11.98 ml of 1 M NaH_2PO_4 and mix with 138.02 ml of 1 M Na_2HPO_4, then make up to 900 ml and adjust pH by adding more NaH_2PO_4 (pH down) or Na_2HPO_4 (pH up). Make volume to 1000 ml. Store @ 4 ºC.

- **10 mM dithiothreitol (DTT)**

  Dissolve 7.7 mg of DTT in 5 ml H_2O and then make 200 µl aliquots. Store @ −20 ºC.

- **Ascorbate determination reagent** *(every chemical below should be dissolved in 70% ethanol)*

The reagent contains 10% (w/v) trichloroacetic acid, 44% H_3PO_4 (w/v), 4% bipyridyl (w/v) in 70% ethanol (v/v) and 3% $FeCl_3$ (w/v). Prepare fresh on the day of use. Do not store.

For 100 ml reagent, prepare 70% ethanol first, then dissolve [44 g H_3PO_4, 20 ml 20% bipyridyl solution (dissolved in 70% ethanol), 10 g TCA and 3 g $FeCl_3$] in 70% ethanol to make up to 100 ml.

Extraction

1. Weigh 250 mg fresh or frozen tissue (*do it quickly to avoid rapid thaw*) and grind it into fine powder in liquid N_2.
2. Transfer the powder to 14-ml plastic Falcon tubes. The tube contains 5 ml of 6% TCA (already cold on ice before transferring the powder). Vortex the tubes vigorously.
3. Centrifuge at 4000 g for 45 min at 4 ºC (*pre-chill the centrifuge for 15 min at 2000 g/4 ºC*) and save the supernatant for assay.
4. Mix the supernatant with enough (*adjust the pH value to 6.7~7.0 with pH paper*) 150 mM phosphate buffer to neutralize extract (*4.25 ml supernatant needs ~25ml buffer making it a total of ~ 30 ml*).
5. Split extracts into two identical aliquots (~ 15 ml each).
6. Add 50 µl of 10 mM DTT to one 15 ml aliquot and vortex gently, and this will reduce all oxidized ascorbate (for assaying total ascorbate). Keep the other 15 ml aliquot for reduced ascorbate assay.

Ascorbate Assay

1. For total ascorbate, combine 100 µl of 15 ml aliquot (with DTT) with 2 ml of the ascorbate determination reagent and vortex gently.
2. Incubate the mixture at 37 ºC for 1 h with caps on to prevent evaporation of samples (Turn on the spectrophotometer to warm up for 30 min before next step).
3. Cool down the reaction mixtures on ice for 5 min and read the absorbance (525 nm) at room temperature (take 1 ml sample in the cuvette).

Preparing a standard curve

The actual amount of ascorbate is determined by extrapolation using a standard calibration curve of Na-ascorbate content (see the standard curve below which shows the regression between absorbance at 525 nm and ascorbate content of the standards). Weigh appropriate amount of Na-ascorbate and dissolve it in the ascorbate determination reagent to make a 100 nmol/ml stock solution. Then dilute it with this determination reagent to a series of Na-ascorbate contents (5, 10, 20, 30, 40, 50, 60 and 80 nmol/ml). Always prepare blank samples (ascorbate determination reagent without ascorbate added) and use them as references for spectrophotometric measurements.

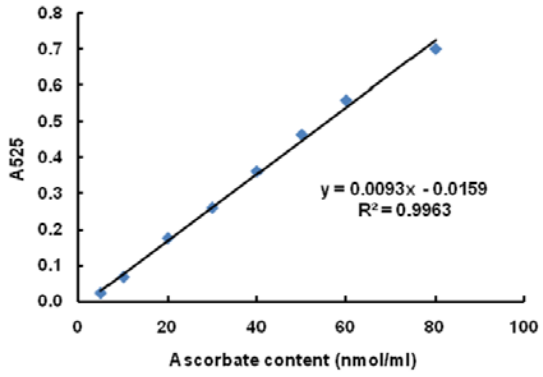

Ascorbate content calculations

Calculate total ascorbate content in a given sample using the regression equation above between ascorbate standards and A_{525} (y = 0.0093x – 0.0159). Total ascorbate content (nmol/ml) in 100 µl of 15 ml aliquot can be calculated as follows: (A_{525} + 0.0159) / 0.0093. For example, in step 3 of ascorbate assay, we get the sample A_{525} of 0.42, the ascorbate content in this sample should be (0.42 + 0.0159) / 0.0093 = 46.8 nmol/ml. To calculate the ascorbate content on per unit of fresh weight basis, the starting tissue weight and volume of original extract should be taken into account. The final ascorbate content on a fresh weight basis should be 46.8 nmol/ml x 4.25 ml x 4* g^{-1}FW = 795.6 nmol g^{-1}FW.

* factor of 4 is used to calculate on per gram FW; we used 0.25 g tissue for this extraction.

References

- Law MY, Charles SA, Halliwell B. 1983. Glutathione and ascorbic acid in spinach *(Spinacia oleracea)* chloroplasts. Biochem. J. 210: 899−903.
- Arbona V, Hossain Z, Lopez-Climent MF, Perez-Clemente RM, Gomez-Cadenas A. 2008. Antioxidant enzymatic activity is linked to waterlogging stress tolerance in citrus. Physiol. Plant. 132: 452−466.

APPENDIX G

Glutathione Assay in *Rhododendron* Leaves

Arora Lab

Department of Horticulture, Iowa State University, Ames, IA 50011, USA

Total glutathione (tGSH) was extracted according to the procedure described by Anderson (1985). Reduced glutathione (GSH) is the most abundant thiol (SH) compound in animal tissues, plant tissues, bacteria and yeast. GSH plays many different roles such as protection against reactive oxygen species and maintenance of protein SH groups. During these reactions, GSH is converted into glutathione disulfide (GSSG: oxidized form of GSH). Since GSSG is enzymatically reduced by glutathione reductase (GR), GSH is the dominant form in organisms. DTNB (5, 5'-Dithiobis (2-nitrobenzoic acid)), known as Ellman's Reagent, was developed for the detection of thiol compounds. DTNB and GSH react to generate 2-nitro-5-thiobenzoic acid and glutathione disulfide (GSSG). Since 2-nitro-5- thiobenzoic acid is a yellow colored product, GSH concentration in a sample solution can be determined by the measurement at 412 nm absorbance. GSH is generated from GSSG by GR, and reacts with DTNB again to produce 2-nitro-5-thiobenzoic acid. Therefore, this recycling reaction improves the sensitivity of total glutathione detection.

Reagents

- **5% meta-phosphoric acid**

  Dissolve 5 g meta-phosphoric acid in ddH_2O and make up volume to 100 ml. Store@4°C.

- **0.5 M phosphate buffer (pH 7.5)**

Na_2HPO_4	11.552 g
NaH_2PO_4	2.571 g

Volume made up to 200 ml – Check the final pH (should be 7.5)

- **125 mM phosphate buffer containing 6.3 mM Na-EDTA**

Na_2HPO_4	3.610 g
NaH_2PO_4	0.803 g
Na-EDTA	0.586 g

Volume made up to 250 ml – Check the final pH (should be 7.5)……**Solution A**

The following three solutions are stored at 4°C and need to be brought to room temperature before use.

- 0.3 mM NADPH ---- 11.18 mg NADPH in 50 ml of solution A
- 6 mM DTNB [5-5′’-Dithio-*bis*(2-nitrobenzoic acid)] --- 47.556 mg in 20 ml of solution A
- Glutathione reductase (GR) (10U/ ml) ------ see the product description and dissolve suitable amount of GR in solution A.

All the chemicals can be stored at 0 °C for two weeks.

- 2-vinylpyridine and triethanolamine are liquid chemicals bought from Fisher Scientific Inc. and they do not need to be made to solutions.

Extraction

- Pre-chill the centrifuge for 15 min at 2000 g / 4 ºC.
- Weigh 500 mg fresh or frozen tissue and grind it to fine powder with liquid N_2.
- Transfer the powder to a Falcon tube containing 5 ml of 5% of meta-phosphoric acid on ice.
- Vortex vigorously and centrifuge at 4000 g for 30 min at 4 °C.
- Collect the supernatant and make 400 µl aliquots (the supernatant can be stored for more than six months at –20 °C).
- Take 400 µl supernatant and add 600 µl of 0.5 M phosphate buffer (pH 7.5). The final pH should be 7- 7.5 (check with pH paper).……**Solution B**

For 54 reactions:

NADPH (0.3 mM)	……..… 21 ml
DTNB (6 mM)	……..……. 3 ml
ddH_2O	…….……. 3 ml
Total Reaction Mixture (**RM**)	….……27 ml

Incubate the **RM** at 25 °C for 1 h (use water bath) prior to assay.

For total glutathione (GSH + GSSH):

- Add 50 µl dH_2O to 1 ml of solution B……**Solution C**
- Keep solution C at room temperature for 1 h.

For oxidised glutathione (GSSH):

- Add 20 µl of 2-vinylpyridine (approx. 2 drops) + 30 µl triethanolamine (approx. 3 drops) to 1 ml of solution B.
- Vortex this mixture for 1 min.
- Incubate the mixture at 25 °C for 1 h (use water bath)……**Solution D**

Prepare a GSH standard curve

- Prepare stock solution of 20 mM GSH (30.73 mg in 5 ml 5% metaphosphoric acid)
- Dilute 50 µl of this stock to 10 ml with 5% metaphosphoric acid giving 100 µM solution.
- Dilute above solution with 5% metaphosphoric acid to obtain 30, 24, 18, 12 and 6 µM standards.
- Take 400 µl of each solution and add 600 µl 0.5 M phosphate buffer (pH 7.5) + 50 µl ddH_2O……. **Solution E**

Prepare the standard curve by conducting the following assay with each standard solution (30, 24, 18, 12 and 6 µM).

- Take 500 µl RM in cuvette
- Add 200 µl solution E (standards)
- Add 136 µl GR
- Mix quickly
- Read absorbance from 0 up to 3 min (10 seconds interval) at 412 nm
- Blank: no sample (500 µl RM + 200 µl 0.5M buffer + 136 µl GR)

The following figure shows how absorbance for individual standards changes at different time-points (10 seconds interval). Based on this figure, the slopes for each standard are calculated as rates (A_{412nm} / min). The rate is the function of standard concentration and is plotted against GSH concentration (see the insert).

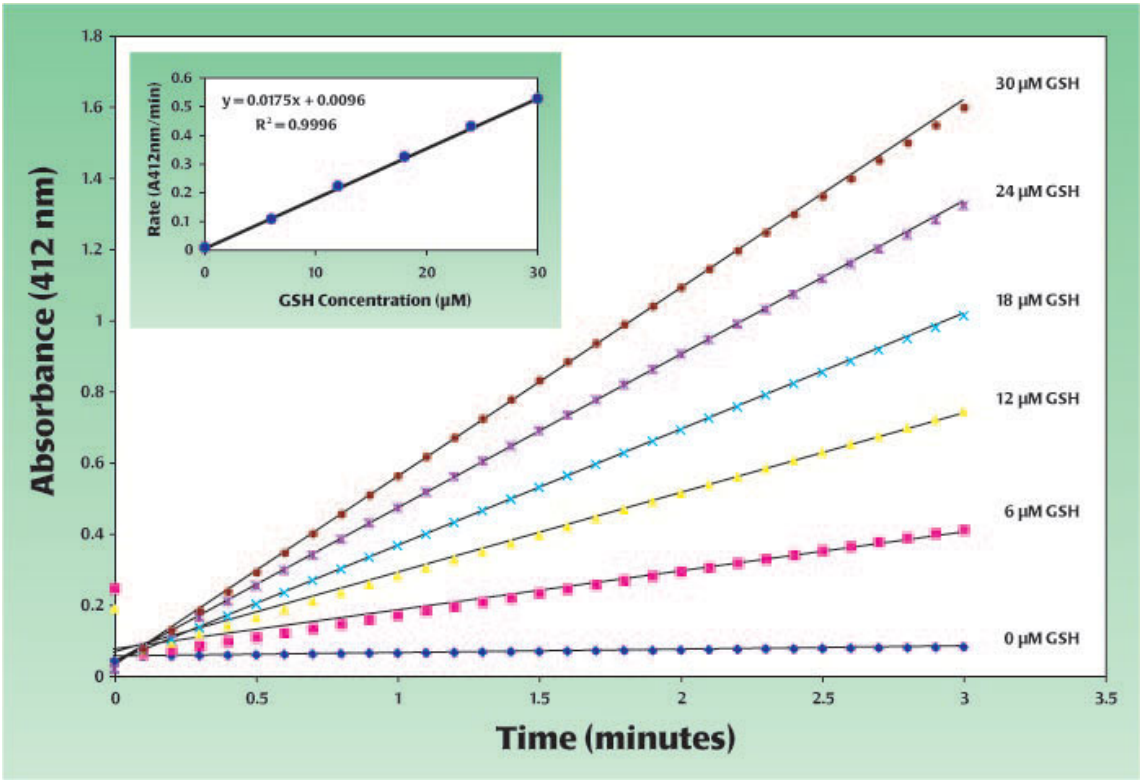

Assay

- Take 500 µl **RM** in the cuvette
- Add 200 µl sample (solution C)
- Add 136 µl GR
- Mix quickly (use the parafilm to cover the upper portion of cuvette for better mixing)
- Blank: no sample (500 µl RM + 200 µl 0.5M buffer + 136 µl GR)

- Read the absorbance from 0 up to 2 min at 412 nm every 20 seconds

For each sample, the change of absorbance at 412 nm is plotted against time and then the slope (rate) is calculated. Then GSH concentration in the sample is calculated according the standard curve above (the insert). For example, if the rate / slope of a sample is 0.4, the GSH concentration should be (0.4 – 0.0096) / 0.0175 = 22.3 μM, using the equation (in the insert) y = 0.0175x + 0.0096. Therefore, x = (y – 0.0096) / 0.0175

Reference

Anderson ME. 1985. Determination of glutathione and glutathione disulfide in biological samples. Methods Enzymol 113: 548–555.

VITA

NAME OF AUTHOR: Xiang Wang

DATE AND PLACE OF BIRTH: January 9, 1980, Wuhan, China

EDUCATION

Ph.D. in Horticulture, Iowa State University, December 2009
M.S. in Ecology, Chengdu Institute of Biology, Chinese Academy of Sciences, June 2005
B.S. in Agronomy, Huazhong Agricultural University, China, June 2002

PUBLICATIONS

1. **Wang X**, Fessehaie A, Krebs SL, Arora R. Is expression of plasma membrane aquaporins (*Rhododendron catawbiense* PIP2s) associated with thermonasty in *Rhododendron*? (To be submitted as a refereed "short communication")
2. **Wang X**, Peng Y, Singer JW, Fessehaie A, Krebs SL, Arora R. 2009. Seasonal changes in photosynthesis, antioxidant systems and *ELIP* expression in a thermonastic and non-thermonastic *Rhododendron* species: a comparison of photoprotective strategies in overwintering plants. *Plant Science* 177: 607–617.
3. **Wang X**, Arora R, Horner HT, Krebs SL. 2008. Structural adaptations in overwintering leaves of thermonastic and nonthermonastic *Rhododendron* species. *Journal of the American Society for Horticultural Science* 133: 768–776. (Journal Cover)
4. Peng Y, Arora R, Li G, **Wang X**, Fessehaie A. 2008. *Rhododendron catawbiense* plasma membrane intrinsic proteins are aquaporins, and their over-expression compromises constitutive freezing tolerance and cold acclimation ability of transgenic *Arabidopsis* plants. *Plant, Cell and Environment* 31: 1275–1289.
5. **Wang X**, Yin C, Li C. 2005. Population differences in adaptive responses to drought stress in *Populus przewalskii* Maxim. *Chinese Journal of Applied and Environmental Biology* 12: 496–499.
6. Yin C, **Wang X**, Duan B, Luo J, Li C. 2005. Early growth, dry matter allocation and water use efficiency of two sympatric *Populus* species as affected by water stress. *Environmental and Experimental Botany* 53: 315–322.
7. Yin C, Duan B, **Wang X**, Li, C. 2004. Morphological and physiological responses of two contrasting poplar species to drought stress and exogenous abscisic acid application. *Plant Science* 167: 1091–1097.